This pdf file contains all figure pages in the dissertation:

LATE HOLOCENE HYDROLOGIC AND CLIMATIC VARIABILITY IN THE WALKER LAKE BASIN, NEVADA AND CALIFORNIA

By

Fasong Yuan

A Dissertation

Submitted to the University at Albany, State University of New York

in Partial Fulfillment of

the Requirements for the Degree of

Doctor of Philosophy

College of Arts & Sciences

Department of Earth & Atmospheric Sciences

2003

scale variability of ENSO and currently the paleoclimatic records that have been generated are insufficient in achieving detailed histories for different climate variables at a regional scale (JONES et al., 2001).

In an attempt to refine our understanding of climatic and hydrologic variability in the western United States, this research has focused on extracting paleoclimatic information for sediments in Walker Lake (Nevada, USA). In spite of the fact that Walker Lake is geographically situated on a correlation hinge point with respect to the interannual mode of ENSO climate today, it is not clear how the low-frequency modes (>10 years) of ENSO behave in this critical region. The paleo-record of past changes in Walker Lake basin hydrologic conditions developed as part of this research is high-resolution (near triennial) for the last millennium.

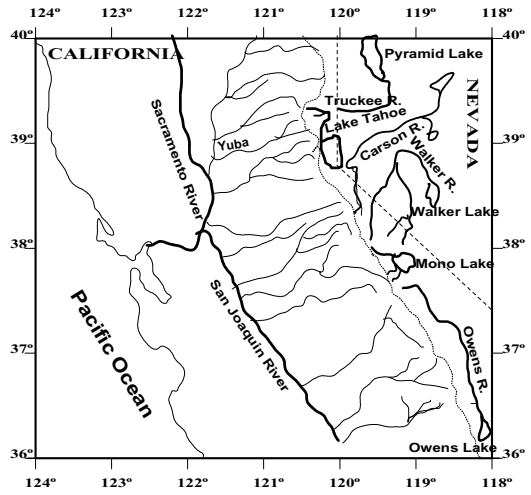

Figure 1-1. Drainage of streams emanating from the Sierra Nevada, California and Nevada (After *Benson et al.*, 2002).

1.1 Lakes in the western Great Basin

There are primarily five major lakes in the western Great Basin (Pyramid Lake, Lake Tahoe, Walker Lake, Mono Lake, and Owens Lake) (Figure 1-1). These lakes, located on the leeside of the Sierra Nevada, are fed by rivers and streams that have headwaters in the Sierra Nevada. Lake Tahoe is the

associated with the noted Pacific-wide climatic regime shift in 1976 (GRAHAM, 1994; MANTUA et al., 1997; TRENBERTH and HURRELL, 1994).

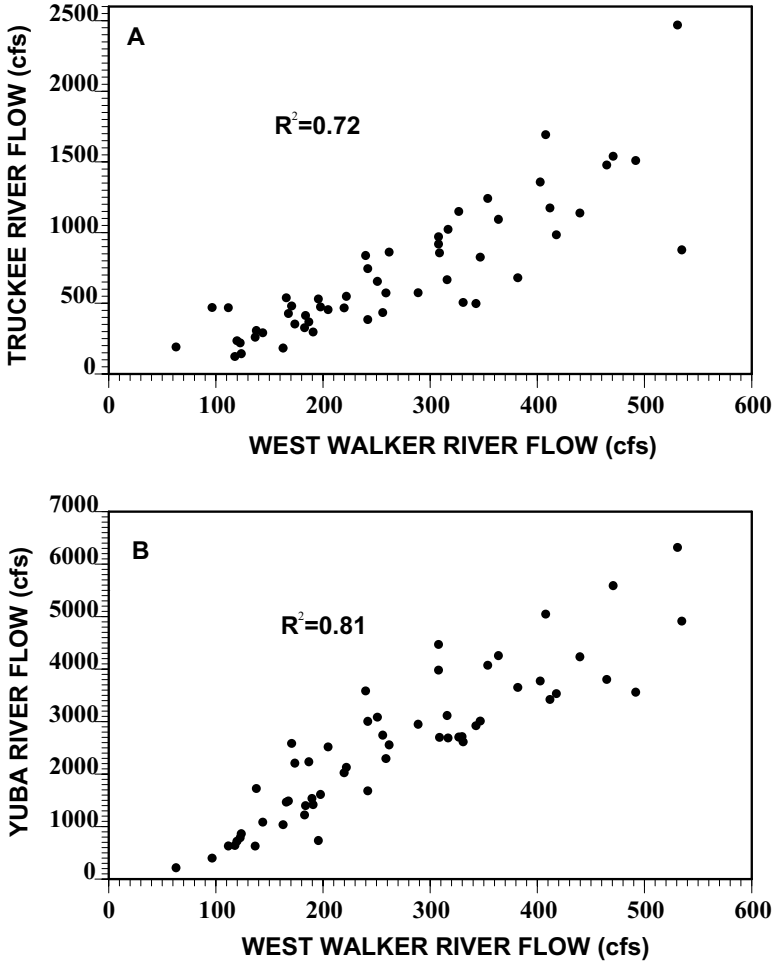

Figure 1-2. Correlation analyses of historical (1940-2000) river flow data in drainages on both sides of the Sierra Nevada. A: Stream flow correlation between the West Walker River (WWR) near Coleville, California and the Truckee River (TR) at Reno, Nevada. B: Stream flow correlation between WWR and the Yuba River (YR) near Marysville, California. Note that river flow data were taken from USGS water resources website, http://water.usgs.gov and calendar yearly average values were calculated. The English unit of cfs denotes cubic feet per second. Gage sites selected are considered to be only minimally effected by water diversions.

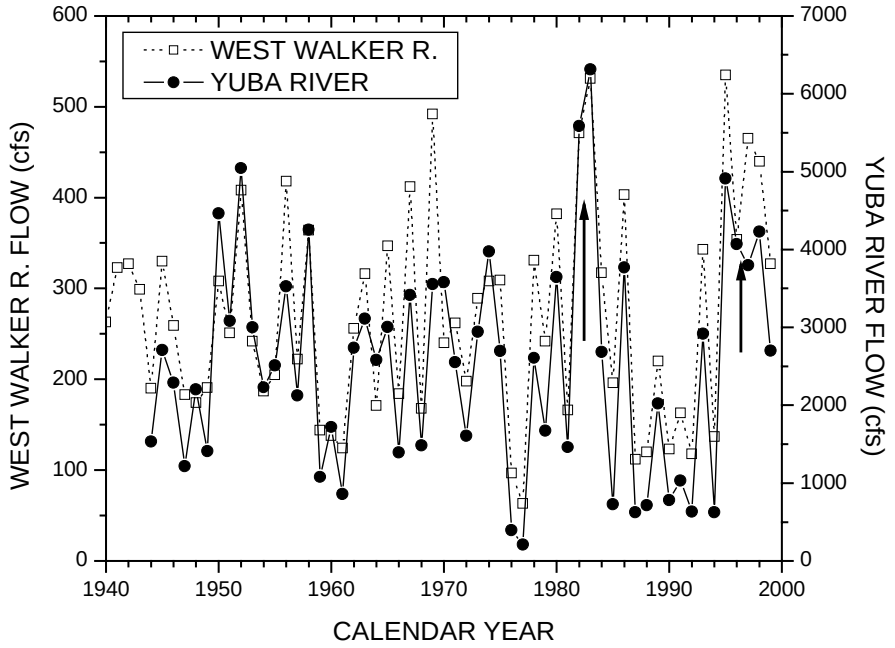

Figure 1-3. Comparison of instrumental river flow of the West Walker River (WWR) near Coleville, California and the Yuba River (YR) near Marysville, California. Solid arrows indicate the two exceptionally strong ENSO events of 1982/83 and 1997/98 (original data from USGS website, http://water.usgs.gov).

Decadal and interdecadal climate modes of coupled atmosphere-ocean variability have recently been recognized in instrumental records (GHIL and VAUTARD, 1991; MANTUA et al., 1997; ZHANG et al., 1997). Moreover, the 15- and 25-year periodicities detected in a 135-year-long historic instrumental temperature record (JONES et al., 1986) have been confirmed in much longer annual resolution proxy records of coral cores and varve sediments (BIONDI et al., 1997; QUINN et al., 1996). Mantua et al. (1997) defined a Pacific Decadal Oscillation (PDO) index based on North Pacific Sea Surface Temperature (SST) back to 1900. During the positive phase of PDO index, the SST of the Central North Pacific is cooler than average while SST in the Gulf of Alaska and along the Pacific coast of North America is warmer than average. In general, there is not a robust correlation on year-to-year scale between variations in WWR flow and the PDO (Figure 1-4A). However, comparison of low-frequency variations of the WWR flow and PDO index records back to 1940 reveals an intricate pattern

of associations. During intervals when the PDO index is positive, the WWR flow tends to be positively correlated with the PDO while during times when the PDO index is negative the WWR flow tends to be negatively correlated with the PDO (Figure 1-4B). This indicates that the low-frequency mode of SST variability on interdecadal time-scales over the Pacific Ocean is associated with fluctuations in winter precipitation of the Sierra Nevada and consequently affected the stream flow like the WWR in the Walker River Drainage Basin.

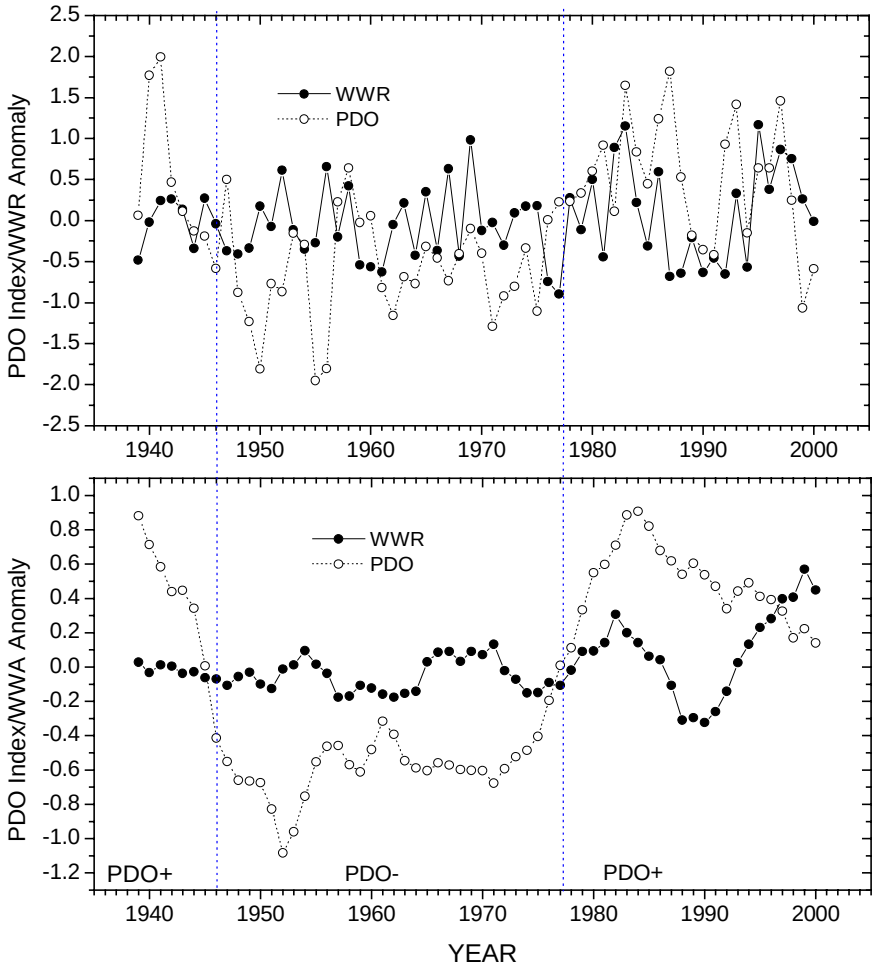

Figure 1-4. Comparison of the PDO index (open circles; Mantua et al., 1997) and the West Walker River (WWR) flow anomaly near Coleville, California (solid dots; USGS). PDO index used is the annual mean value and WWR anomaly is calculated through expression: $(Q_i - Q_e)/(2\delta)$. Upper Panel: Year to year comparison. Lower Panel: 9-point running average comparison. Two vertical dashed lines denote two climate regime shifts that occurred in 1946 and 1977, respectively.

in this region, such as the intervals centered on 1400 and 900 years B.P. The Sacramento River flow record suggested a transition from high to low flow near 1350AD (MEKO et al., 2001) while other paleoclimatic evidence indicated an abrupt switch from extreme drought to very wet conditions at more southerly latitudes in the Sierra Nevada and the neighboring White Mountains (GRAUMLICH, 1993; HUGHES and FUNKHOUSER, 1996; HUGHES and GRAUMLICH, 1996; MEKO et al., 2001). Hughes and Funkhouser (1996) suggested that the hydrologic variability of recent centuries would differ from that of earlier centuries as decadal and multi-decadal droughts occurred more frequently before 1500AD than since. However, questions still remain about the spatial and temporal late-Holocene hydrologic variability in this region.

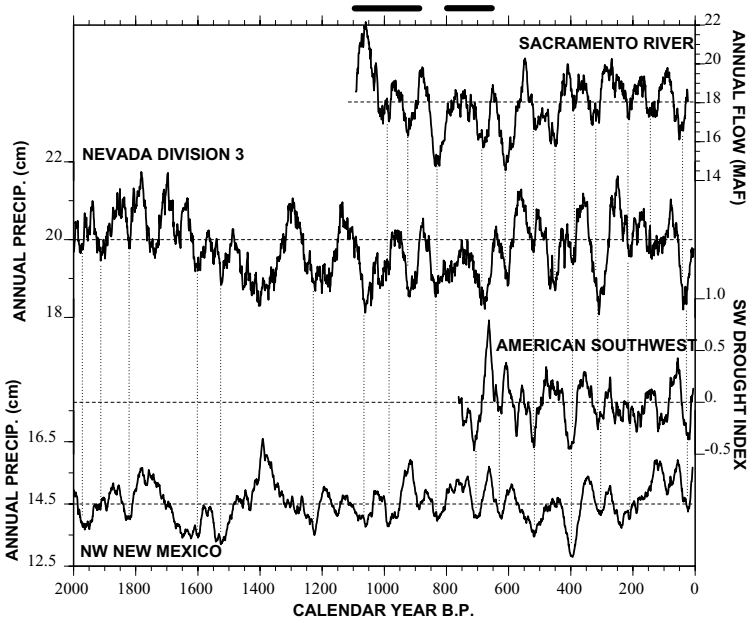

Figure 1-5. Comparison of 40-year moving averages of tree-ring based paleoclimatic records of the western U.S. (1) Sacramento River flow record (MEKO et al., 2001), MAF stands for million acre feet; (2) Nevada Division 3 precipitation record (HUGHES and GRAUMLICH, 1996); (3) American Southwest drought index (COOK et al., 1999); (4) Northwestern New Mexico precipitation record. Horizontal dashed lines denote mean values of each record while vertical dashed lines represent pervasive droughts in the regions (GRISSINO-MAYER, 1996). Two black bars denote two Medieval severe droughts that were previously proposed through dated tree stumps (STINE, 1994).

It has long been recognized that fluctuations in lake level are an indicator of climate (HALLEY, 1715) and closed basin lakes are thought to potentially preserve detailed paleoclimatic records due to

their sensitivity to changes in hydrologic balance. In Walker Lake, Benson et al. (1991) produced a series of proxy records derived from cored sediments. They suggested that wet intervals (high lake levels) occurred between 4.8 and 2.7ka, approximately at 1.25ka, and over last 300 years up until the anthropogenic lowering that began in 1922. They also concluded that droughts occurred around 2ka and 1ka BP. Based on a high-resolution $\delta^{18}O$ record derived from cored sediments in Pyramid Lake, Nevada, Benson et al. (2002) identified 18 multi-decadal to centennial droughts that occurred from 2740 to 110 years BP in this region. Most of these droughts, such as those that terminated at ~1120, ~860, ~760, ~640, ~540, and ~280 years BP (BENSON et al., 2002), were associated with droughts recorded in tree-ring based river flow data in the northern Sierra Nevada (MEKO et al., 2001) and other paleoclimatic records from dated tree stumps (STINE, 1994).

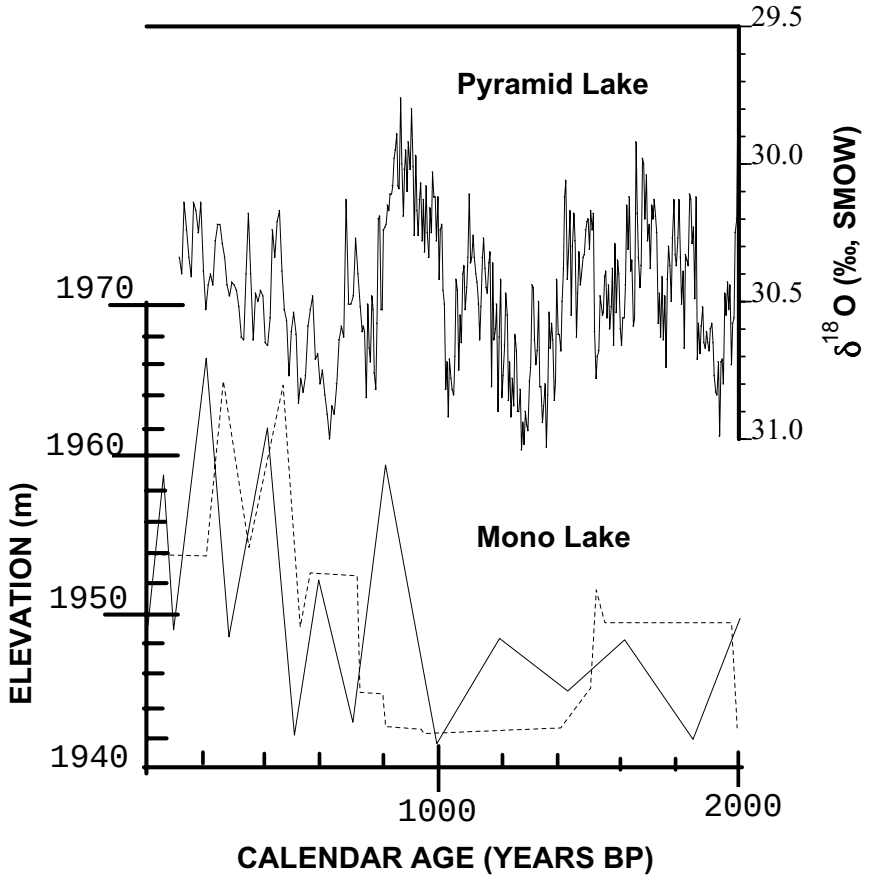

suggested that monohydrocalcite appears to be the dominant carbonate mineral present in sediments deposited during the past 2000 years. High Mg/Ca molar ratios (> 2) inhibit the formation of other carbonate minerals and allow monohydrocalcite to precipitate (SPENCER, 1977).

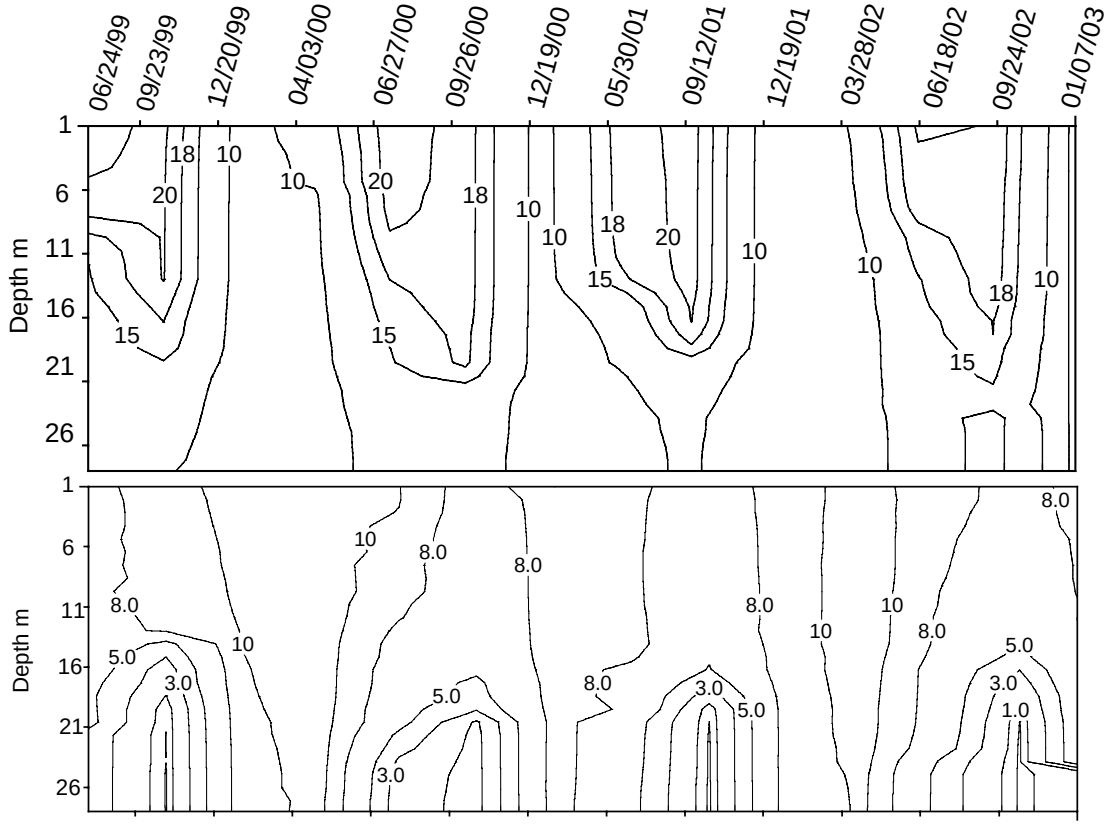

Figure 1-7. Temperature in ºC (upper panel) and dissolved oxygen (DO) in mg L^{-1} (lower panel). Original data from NDEP (2003).

1.5 Objective of this dissertation research

The central objective of this dissertation research is focused on the reconstruction of the last ~1000 years of climatic and hydrologic variability in the Walker Lake drainage basin through elemental and isotopic analyses of cored lake sediments. Because the Walker Lake basin is situated in a climatically critical region, the hydrographic history in this region during the past thousand years has the potential

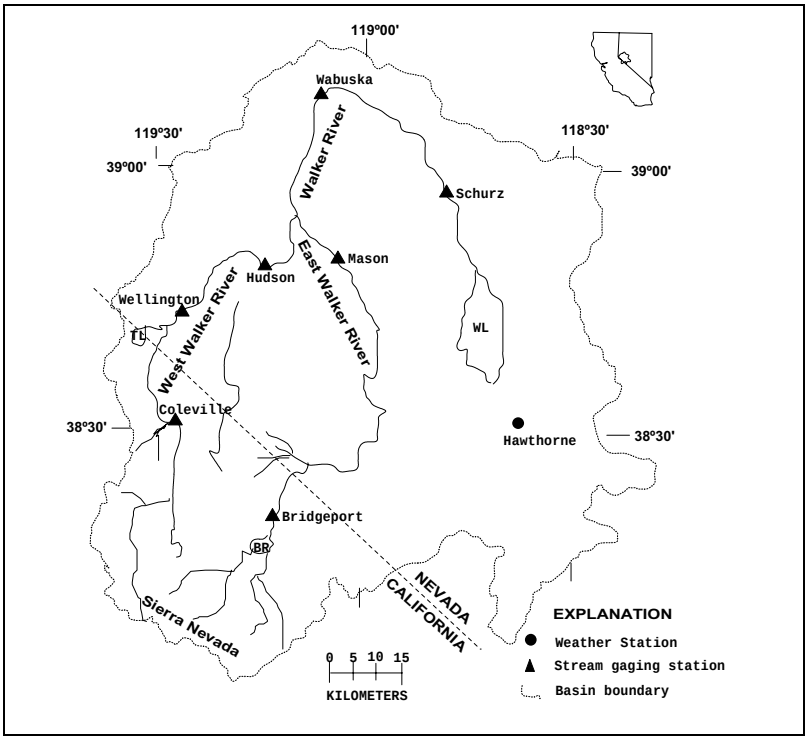

Figure 2-1. Walker Lake drainage basin, Nevada and California showing location of the Walker River and Walker Lake (BENSON and LEACH, 1979).

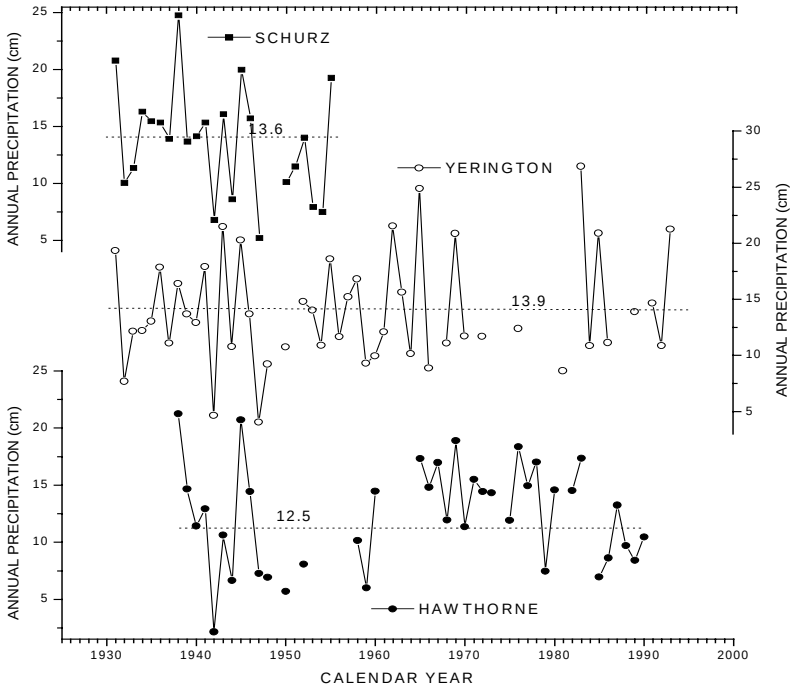

Figure 2-2. Historic instrumental precipitation records of Walker Lake and its adjacent areas (original data from National Climate Data Center). Horizontal dashed lines represent long-term averages of annual precipitation at each weather station indicated.

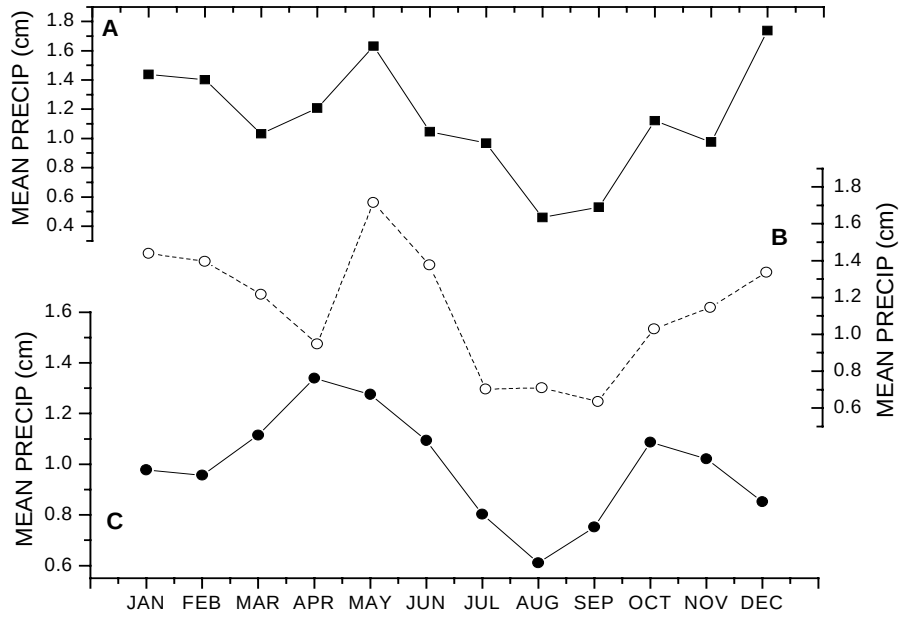

Figure 2-3. Precipitations climatologies near Walker Lake and its adjacent areas. A) Schurz Weather Station (1931-1945). B) Yellington Weather Station (1931-1993). C) Hawthorne Weather Station (1938-1990) (original data from NCDC).

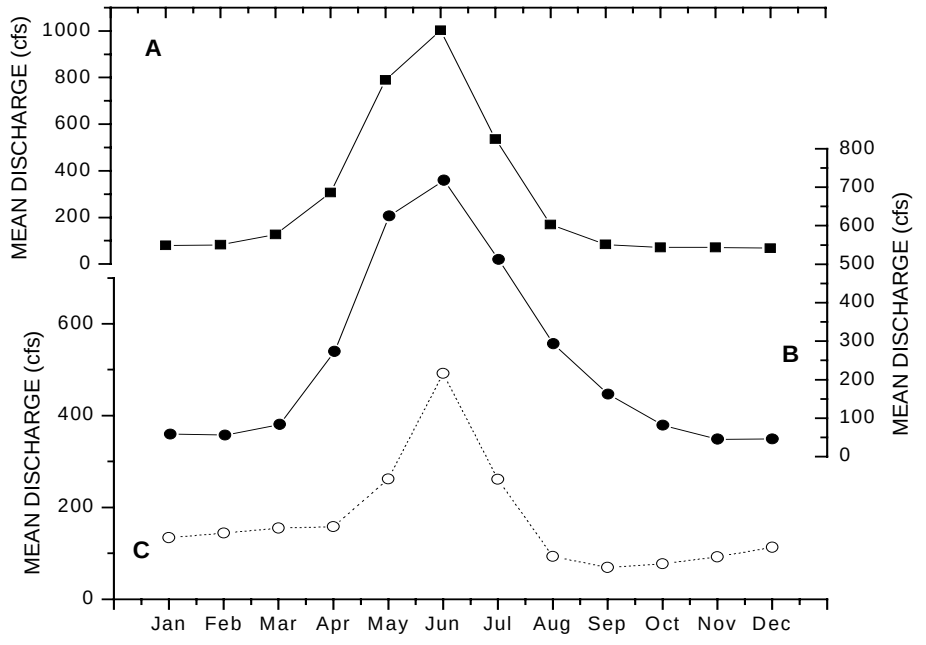

Figure 2-4 Average monthly river discharge of the Walker River at gauging stations near Coleville (A), Wellington (B), and Wabuska (C) (original data from US Geological Survey website http://water.usgs.gov).

The confluence of the WWR and the East Walker River (EWR) is located approximately 20 miles upstream from the Wabuska gauging station (Figure 2-1). The gauging station at Wabuska (operated by the USGS) has a continuous stream flow record back to 1944 and records an annual mean stream discharge of 0.16 km^3. However, only about 88% of water passing Wabuska eventually enters Walker Lake according to annual discharge records from Schurz and Wabuska gauging stations spanning 1978 to 1995 (Figure 2-5). The amount of the stream flow near Schurz is highly correlated with the Wabuska gage record (Figure 2-6). This linear correlation will be used to correct the amount of the Walker River flow (near Wabuska) that eventually enters Walker Lake.

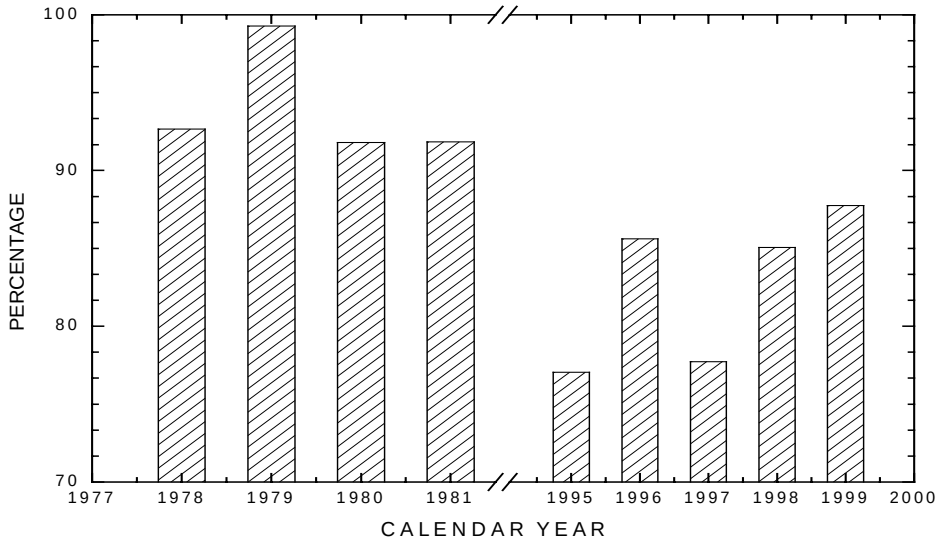

Figure 2-5 Histogram showing variations in the percentage of river discharge at the Wabuska gauging station passing through the Schurz gauging station (original data from USGS).

Since groundwater inflow and /or outflow are negligible (MILNE, 1987) and on-lake precipitation (P) is a minor component (<10 %) of the total water input to the lake, variations in lake level are primarily affected by stream flow (Q) and evaporation (E) according to the hydrologic mass balance. In fact, changes in lake volume (ΔV) vary linearly with the amount of Walker River flow (Figure 2-7). This also suggests that variations in the Walker River discharge are the primary contributor to lake volume changes over the past five decades or more.

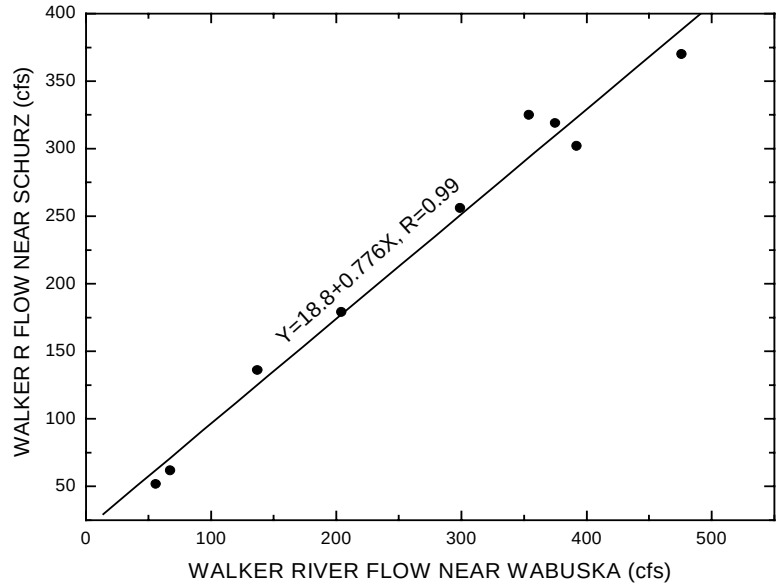

Figure 2-6 Linear correlation of river discharge of the Walker River near the Wabuska and Schurz based on the annual mean river discharge data spanning 1978 to 1999 (original data from USGS).

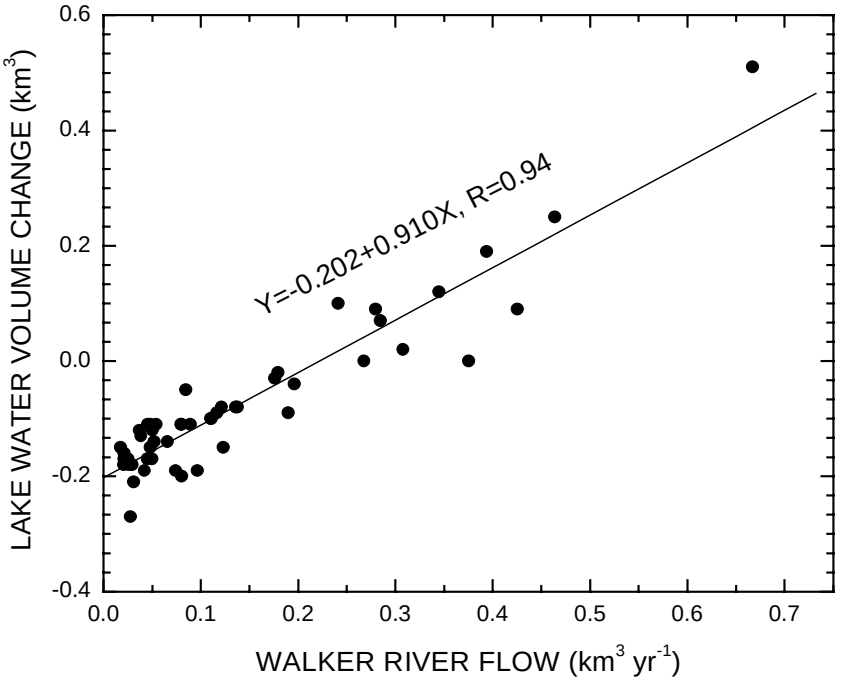

Figure 2-7 Positive linear stream correlation of river discharge between the Walker River and lake volume change of Walker Lake from 1945 to 1995 (original data from USGS).

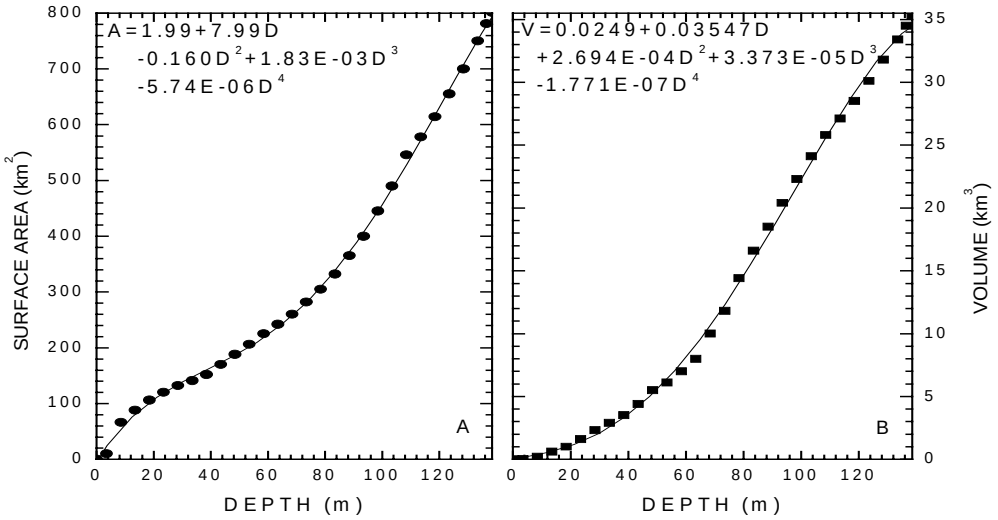

Figure 2-8 Plots of Walker Lake hypsometric data. A) Surface area vs. depth. B) Volume vs. depth (original data from *Dr. L. Benson, personal communication*, 2001).

Based on a straightforward water balance equation, $\frac{\Delta V}{\Delta t} = Q + P - E$, change in lake volume is determined by the Walker Lake hypsometric settings (Figure 2-8A,B), and the amounts of the Walker River flow, on-lake precipitation, and evaporation. The long-term annual on-lake precipitation rate is 0.125 m. On the basis of the historical lake level record and the annual Walker River flow record (documented USGS), the long-term annual mean evaporation rate of Walker Lake can be estimated through the least root mean square error (BENSON et al., 2002), $\xi = \sqrt{\frac{\sum_{i=1}^{n}(L_i^c - L_i^m)^2}{n}}$, where L_i^m is the measured lake level and L_i^c is the lake level computed through the water mass balance equation. The calendar-year stream flow record (1944 to 1999) of the Walker River near Wabuska is used and corrected through the stream flow correlation between the Wabuska and Schurz gauging stations (Figure 2-6). Computations indicate that long-term mean annual evaporation rate (1944-1995) is about 1.39 m (see Figure 2-9), which is close to *Milne*'s (1987) estimate (1.35 m).

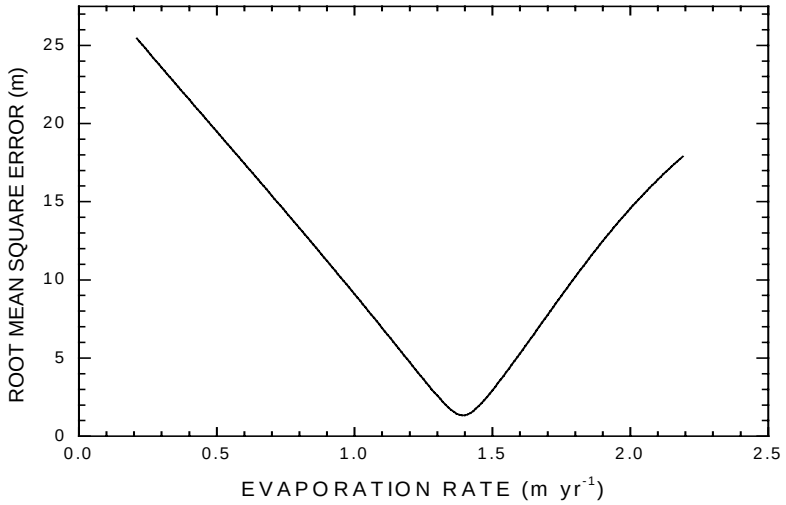

Figure 2-9 Walker Lake long-term mean annual evaporation rate estimated using corrected calendar-year inflow, fixed-rate (0.127 m yr^{-1}) of on-lake precipitation, and measured lake levels for the period 1944-1995. A long-term (1944-1995) average value of 1.39 m yr^{-1} was obtained through the least root-mean-square error (difference) between measured and computed lake levels over the period 1944-1995 (original data from USGS).

2.4 Surface Water $\delta^{18}O$

In Walker Lake basin, there are three types of surface-water with distinct $\delta^{18}O$ ratios, $\delta^{18}O_L$ of lake water > $\delta^{18}O$ of on-lake precipitation ($\delta^{18}O_{PP}$) > $\delta^{18}O$ of stream water ($\delta^{18}O_R$) (Table 2-1). Because of the vast majority (>90%) of water in the Walker River is derived from Sierra Nevada snowmelt, the $\delta^{18}O_R$ is usually lower than any other components. The $\delta^{18}O_{PP}$ is related with the source of water vapor and ambient temperature when the water vapor condensation occurs. The $\delta^{18}O_{PP}$ at Sutcliffe, a weather station near Pyramid Lake, is –9.8 ± 4.4 (‰, VSMOW) (BENSON, 1994). In Walker Lake, direct measurement of the $\delta^{18}O_{PP}$ is not available. Since the evaporation/precipitation ratio is greater than 10, the contribution of on-lake precipitation to the $\delta^{18}O_L$ is relatively small. Thus, the $\delta^{18}O_{PP}$ value of precipitation at the Sutcliffe weather station was adopted for the isotopic simulation of Walker Lake.

Table 2-1 Surface waters and their oxygen isotopic signatures

Surface Water	Stream Water	Rainfall	Lake Water	Subtotal
Quantity [2] (km^3)	0.155	0.019	2.50	2.67
%	5.8	0.71	93	100
$\delta^{18}O$ (‰, SMOW)	-13.6±0.6	-9.8±4.4	0±2	

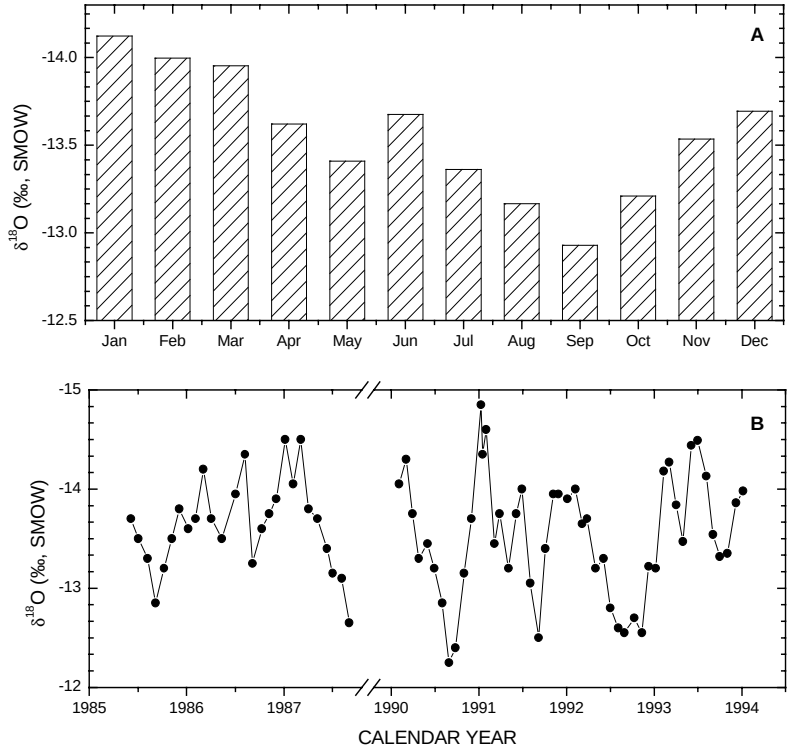

Figure 2-10 Variations in $\delta^{18}O$ of stream water near the Wabuska gauging station. A) Monthly mean $\delta^{18}O$. B) A time series of $\delta^{18}O$ record of stream water near the Wabuska gauging station (original data from *Dr. L. Benson, personal communication*, 2001).

The $\delta^{18}O_R$ of the Walker River flow at the Wabuska gauging station in the interval from 1985 to 1994 was measured by Dr. L. Benson of the USGS. The $\delta^{18}O_R$ tends to be higher in late summer than other seasons (Figure 2-10A), indicating that irrigation return-flow may alter the isotopic signature of the Walker River. The average $\delta^{18}O_R$ is –13.6 (‰, SMOW) with standard deviation of ± 0.6 (‰,

SMOW). Variations in the $\delta^{18}O_R$ observed are relatively small as the coefficient of variance (CV) is 4.4% (Figure 2-10B). Direct measurements of the $\delta^{18}O_L$ of Walker Lake back to 1977 have been previous published. Newton and Grossman (1988) reported an average $\delta^{18}O_L$ of Walker Lake of 2.8 ‰ (SMOW) based on the analysis of 13 samples collected from the lake in September 1977. Benson et al. (1996; 1991) reported 78 measurements of $\delta^{18}O_L$ that spanned 1981 to 1994. The results from 1977 to 1994 are shown in Figure 2-11. There was a negative correlation between the $\delta^{18}O_L$ and the lake surface elevation (r^2= 0.94, n=56) in the dry intervals from 1985 to 1994 when only a small amount of the Walker River flow entered the lake and the $\delta^{18}O_L$ was primarily affected by evaporation.

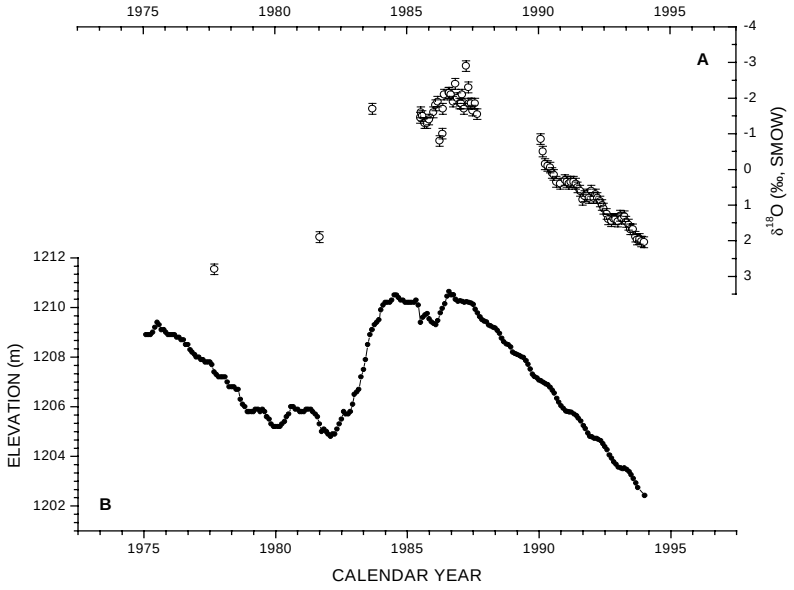

Figure 2-11 Comparison of measured lake level elevation and lake water $\delta^{18}O$ for the period of 1975-1995. The lake level elevation record was observed by USGS and the $\delta^{18}O$ data were taken from (BENSON et al., 1996; NEWTON and GROSSMAN, 1988; PENG and BROECKER, 1980).

However, change in $\delta^{18}O_L$ is not a simple linear function of hydrologic conditions (BENSON and WHITE, 1994). Other factors, such as limnological thermal structural and hypsometric properties of the lake may also play an important role in variations in the $\delta^{18}O_L$ (BENSON et al., 2002; BENSON and

[2] Stream flow is estimated based on long-term annual flow (174 cfs), while rainfall and lake water are estimated based on a lake surface area of 159 km^2.

$\delta^{18}O_L$ record spanning 1985 to 1994 (BENSON et al., 1996) as reference for the HIBAL model and determined the value of f_{ad} by fitting the modeled curve of $\delta^{18}O_L$ changes to that observed.

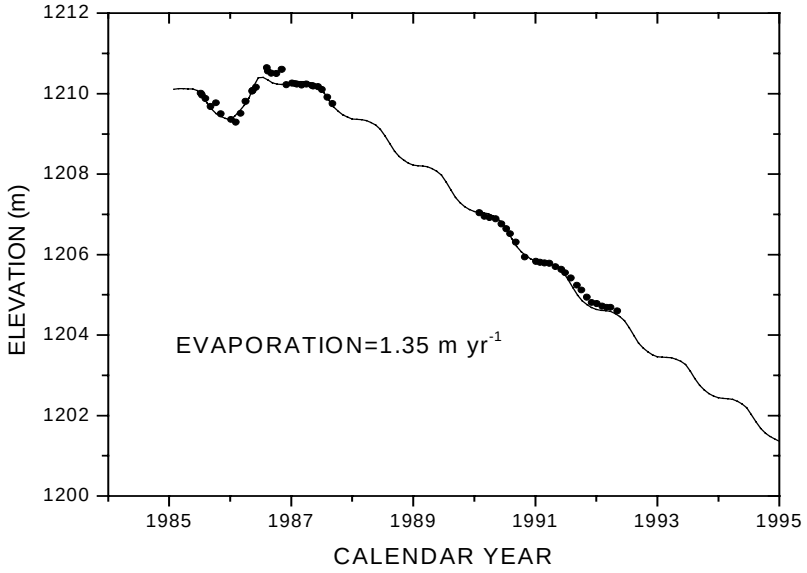

Figure 2-12 Hydrologic balance simulation using fixed rates of on-lake precipitation (0.127 m yr^{-1}) and evaporation (1.35 m yr^{-1}) (original lake elevation data from USGS).

The algorithm for the HIBAL model was kindly provided by Dr. Larry Benson of the U.S. Geological Survey. I modifed the original Fortran source codes of HIBAL and converted them into Visual Basic macros for Microsoft Excel 2000. This Visual Basic program was then simplified and integrated into a comprehensive hydrologic basin model called Paleolake. Paleolake consists of three major components; hydrologic simulation, isotopic simulation, and lake level reconstruction (see Appendix 1 for details). The isotopic simulation component is a simplified version of HIBAL in which relative humidity, on-lake precipitation, and evaporation are treated as constant and the thermal structure of the lake is not taken into account. Paleolake uses corrected daily stream flow readings at the Wabuska gauging station[5] and runs on an arbitrary user-defined time step[6] while HIBAL uses corrected

[5] River flow is corrected by multiplication of 90%.

[6] The model can run hourly time step, but it will not increase the accuracy of model results, as the original data is usually in daily spacing.

an increase in either f_{ad} or *RH*, the model results tend to shift the $\delta^{18}O_L$ curve to lower average values (Figure 2-13B, forward method). An increase in f_{ad} can be offset by a decrease in *RH* during isotopic simulations. In fact, either f_{ad} or *RH* may change year to year. The f_{ad} value of ~33% was estimated according to hydrologic and climatic data in Table 2-2, in which most of the dataset is scaled from those measured in Pyramid Lake.

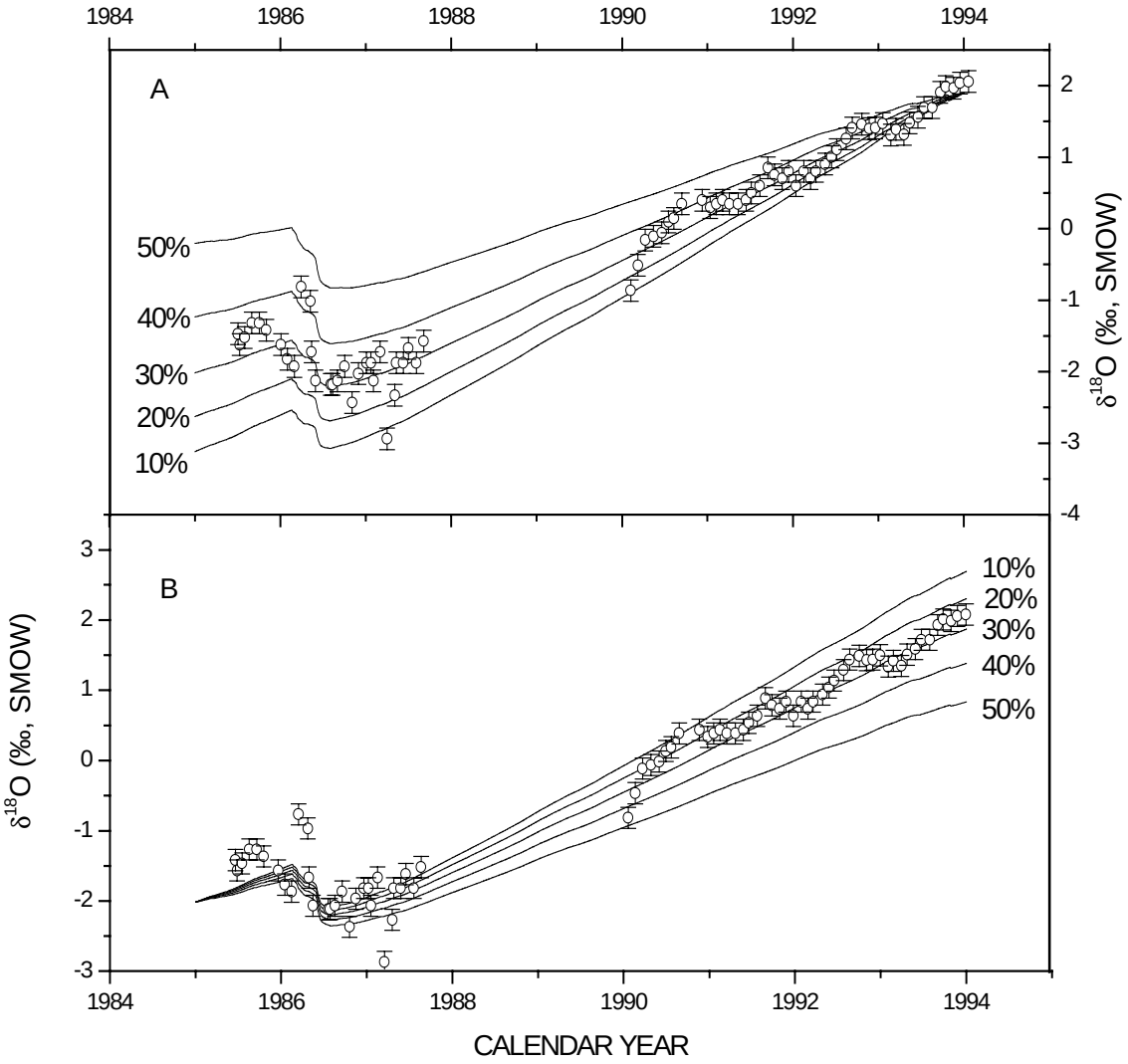

Figure 2-13 Lake water $\delta^{18}O$ simulations through Paleolake using various f_{ad}. A) Backward simulation method. B) Forward simulation method.

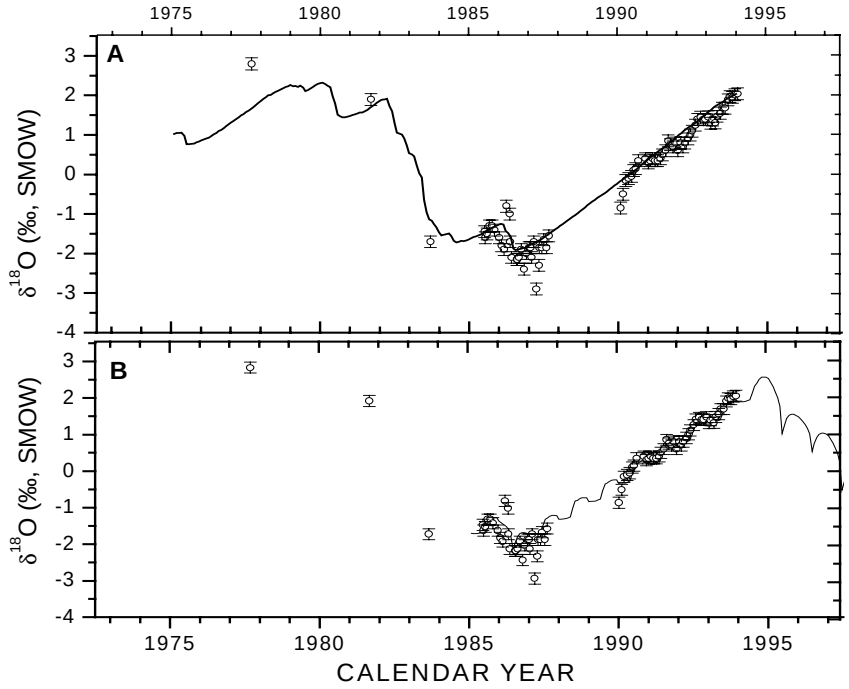

Figure 2-14 Comparison of model simulation results through Paleolake (A) and HIBAL (B). Note that the modeled results from HIBAL captured seasonal variations in lake water $\delta^{18}O$ while Paleolake are capable of reproducing the overall features of variations in lake water $\delta^{18}O$ (assuming RH=60% and f_{ad} =0.3). Open circles with error bar are measured data points (original data extracted from *Benson et al.*, 1996).

In Table 2-2, there are six categories of parameters that may affect the isotopic distribution of the system. These parameters are used to reflect limnological, hydrologic, and the climatic annual cycle of the lake. For example, the mixing depth represents one of the limnological properties. Walker Lake has a thinner mixed layer in summer and early fall and overturns in winter and early spring (COOPER and KOCH, 1984). This limnological cycle is certainly related with hydrologic and climatic conditions of the lake. Hydrological closure, surface water temperature, and relatively high salinity are the primary factors that produce the distinct seasonal limnological pattern. Besides stream flow and on-lake precipitation, evaporation also exhibits a strong seasonal cycle that is higher in summer and early fall seasons and much lower in other seasons (BENSON and WHITE, 1994).

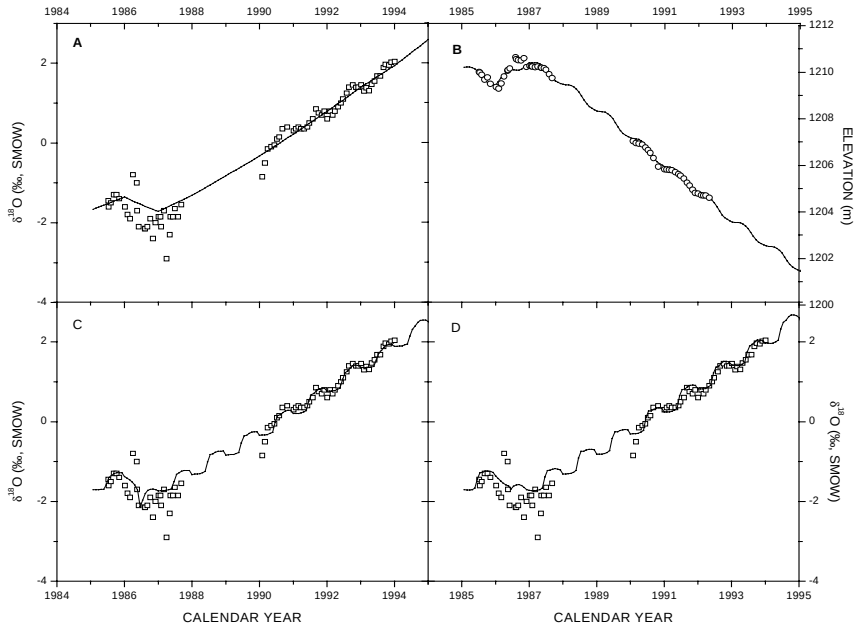

Figure 2-15 Results of HIBAL model experiments (I). Open squires are $\delta^{18}O$ or elevation values observed and solid curves are results of simulations using HIBAL. A) Assuming f_{ad} =0.25, perennial fixed values of precipitation, evaporation, and water temperature, and full mixing conditions. B) Assuming perennial constant inflow. C) Assuming perennial constant rates of precipitation and f_{ad}=0.33. D) Assuming perennial constant inflow and f_{ad} =0.30.

HIBAL-modeled results capture most variations in $\delta^{18}O_L$ using the dataset in Table 2-2. To test the sensitivity of the response of $\delta^{18}O_L$ to these parameters, I removed the seasonal variations of the parameters in Table 2-2 and replaced them with annual averages. For example, the lunar monthly fractions of stream flow, on-lake precipitation, and evaporation are kept constant as 1/13. For water temperature and *RH*, their annual average values are applied, 14ºC and 51%, respectively. The mixing depth is assigned to 1000 m [8], which represents a perennial full mixing condition. Under these circumstances, HIBAL-modeled results are generated and presented in Figure 2-15A. These results are close to the Paleolake-modeled results except for the fact that HIBAL captures the fine or seasonal variations in $\delta^{18}O_L$.

In search for the primary contributors to seasonal variations in $\delta^{18}O_L$, I modified the dataset in Table 2-2 (using annual averages) and re-ran the HIBAL program. From 1985 to 1994, the climate was

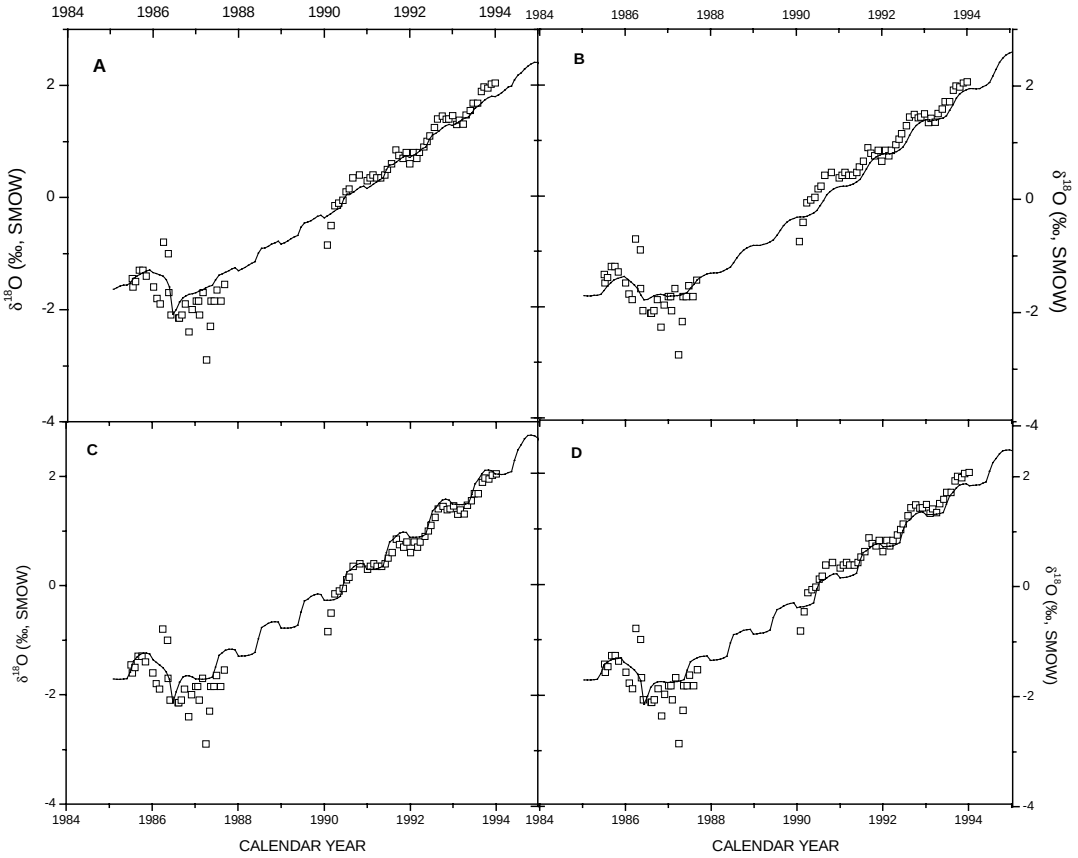

Figure 2-16 Results of HIBAL simulations (II). A) Assuming perennial constant rates of evaporation and f_{ad} =0.30. B) Assuming f_{ad} =0.25 and a perennial full mixing condition. C) Assuming perennial constant water temperature (14ºC) and f_{ad} =0.35. D) Assuming f_{ad} =0.25 and *RH*=51%.

As stated by Benson and Paillet (2002), hydrologic modeling usually has a much higher chance of success when isotopic simulation is confined to "interesting" parts of the record, in which some climatic parameters tend to be relatively well-constrained. This is also true in the Walker Lake isotopic simulations. For example, the HIBAL simulation does a better job for the interval from 1990 to 1995 than from 1985 to 1988. This is because there is little discharge to the lake during the period from 1990 to 1995. Model experiments demonstrate the ability of HIBAL to simulate changes in $\delta^{18}O_L$ of Walker Lake through adapting measured data from Pyramid Lake (except for stream flow and hypsometric data). However, such isotopic simulations are based on a well-defined hydrologic and isotopic system of the lake. The ultimate goal of hydrologic and isotopic model is to extract hydrological and climatic

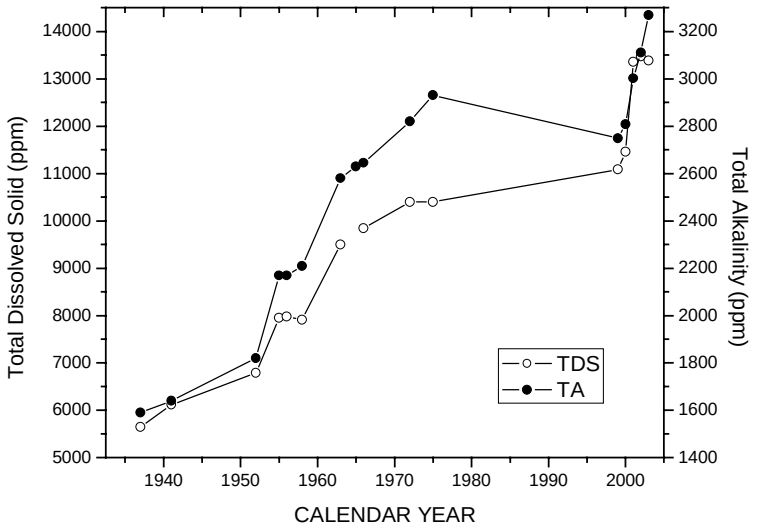

Figure 3-1. Instrumental records of the total dissolved solid (TDS) and total alkalinity (TA) of Walker Lake. Original data were taken from Benson and Spencer (1983) and NDEP (2003).

The purposes of this study are to report carbonate coulometric and isotopic results extracted from a box core collected from Walker Lake in June 2000, compare these results with the historical record of lake level, and examine how the history of variations in hydrological conditions of the lake is transferred to the sedimentary record.

3.3 Method and Materials

A 39.6 cm long boxcore (WLB-003C) was collected from one of the deepest portions of Walker Lake (Figure 3-2) in June 2000. The water depth was approximately 30 m. A distinct water-sediment interface was evident during boxcore recovery. The boxcore was carefully sealed and transferred to the University at Albany. Once it arrived at the University at Albany it was kept refrigerated storage at ~4 ºC. WLB-003C was extruded vertically and sectioned at 0.5-cm intervals. Samples collected were separated into two portions, one was for microfossil analyses and the other was for coulometric analyses. Each sample from the microfossil portion was wet sieved (250 μm) and the coarse fraction transferred into an aluminum weighing dish and oven-dried at 60ºC. The dried ostracode *L. ceriotuberosa* was hand-picked under a microscope with a pen brush, washed with deionized water to remove tiny

particulates stuck on valves, and oven-dried again at 60 ºC. Because at the time when the samples were prepared the University at Albany stable isotope mass spectrometer needed more than 100 µg (ca. 10 to 15 shells) carbonate to get optimal results, every pair of two consecutive samples were merged prior to isotopic analyses. Samples from the other portion were washed several times in deionized water to remove soluble salts until their electrical conductivities were less than 3X those of Albany (New York) tap water. Washed samples were dried, homogenized, and soaked with 2.6% sodium hypochlorite for 6-8 hours to remove organic matter. The soaked sediments were vacuum-filtered with Whatman® glass microfibre filters (1.6 µm), rinsed with deionized water at least five times, and oven-dried at 60 ºC prior to isotopic analysis (BENSON et al., 2002).

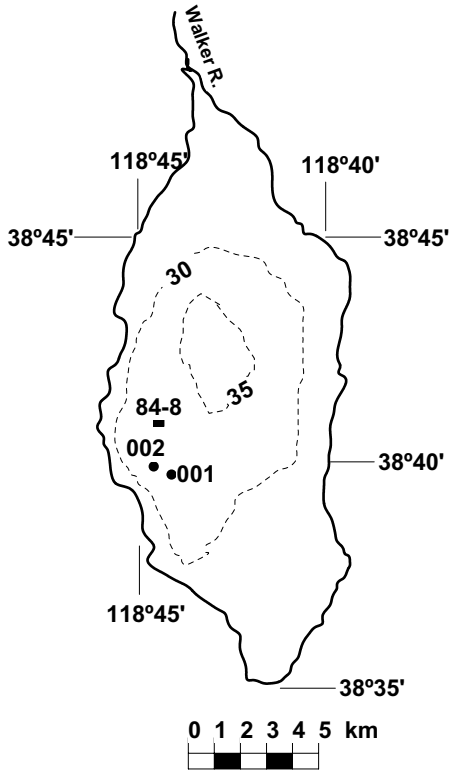

Figure 3-2 Bathymetry and sediment core sites in Walker Lake (After *Benson*, 1988). WLB-003C (not shown here) is very close to WLC002.

will result in the dilution of sedimentary %TIC. It is plausible that the observed decreasing trend in %TIC is caused by increases in primary productivity (BENSON et al., 1991).

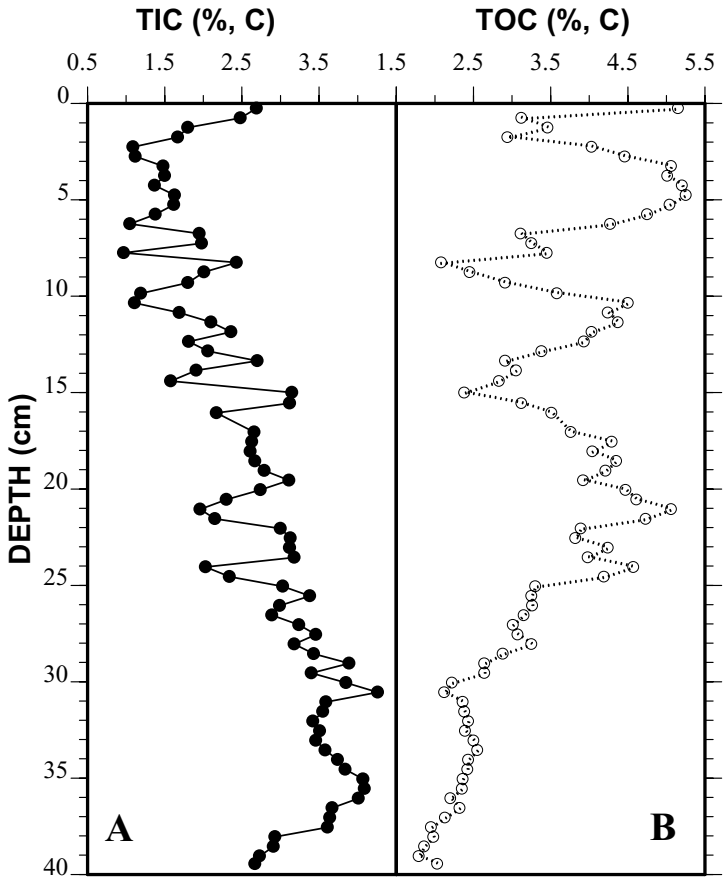

Figure 3-3. Results of measurements of the total inorganic carbon (TIC) and total organic carbon (TOC) of cored sediments from WLB-003C. A) TIC was measured by coulometric analysis. B). TOC was calculated by the difference of total carbon (TC) and TIC.

Carbon and oxygen isotopic analyses were performed on both ostracode shells and the bulk TIC fraction. The results of measurements of the TIC $\delta^{18}O$ and TIC $\delta^{13}C$ are shown in figure 3-4. The TIC $\delta^{18}O$ ranges from –4 to 4 ‰ (PDB) with an average of 0.7 ‰ (PDB) and the TIC $\delta^{13}C$ ranges from 1 to 4 ‰ (PDB) with an average of 3.2‰ (PDB). Both TIC $\delta^{18}O$ and TIC $\delta^{13}C$ progressively increase from a depth of 39.6 cm to 15 cm. TIC $\delta^{18}O$ and $\delta^{13}C$ variability becomes larger from a depth of 15 cm to the water-sediment interface. This is probably related to increases in isotopic sensitivity due to a

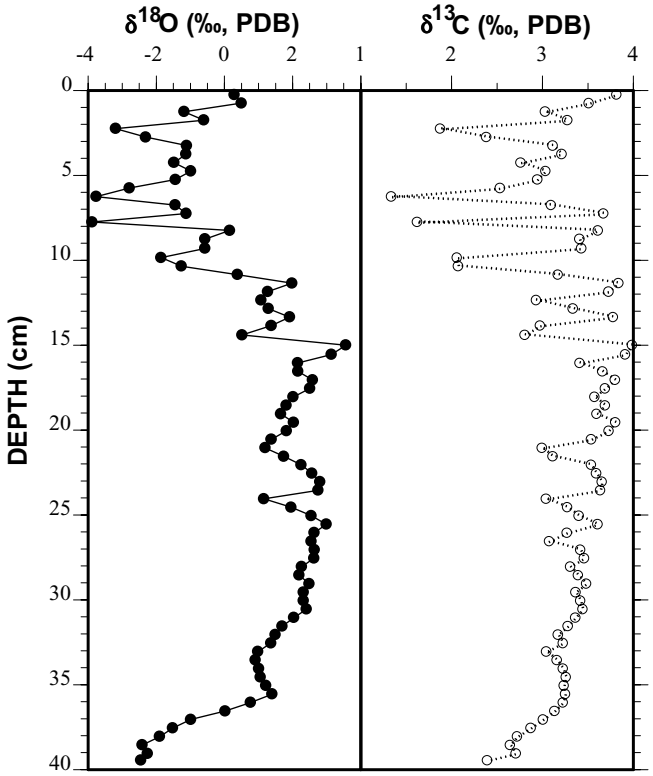

Figure 3-4. Results of measurements of TIC $\delta^{13}C$ and TIC $\delta^{18}O$ of cored sediments from WLB-003C.

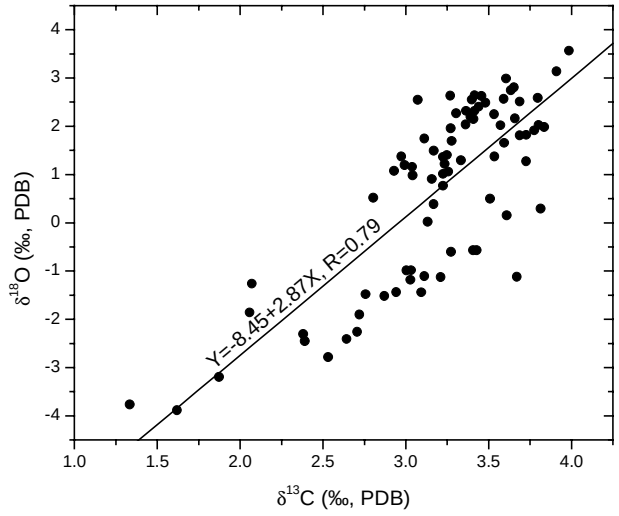

Figure 3-5. Positive correlation between TIC $\delta^{13}C$ and TIC $\delta^{18}O$ of cored sediments (WLB-003C)

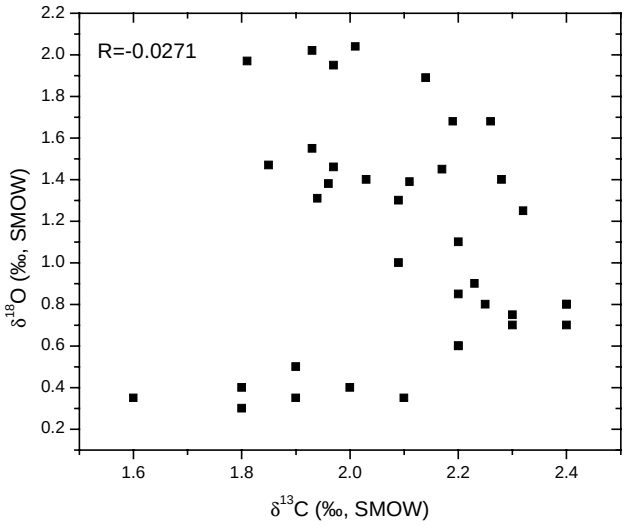

Figure 3-6. Plot of Walker Lake isotopic data: $\delta^{13}C$ vs. $\delta^{18}O$, based on the results of 37 measurements of lake water samples for the period of 1991-1994 (original data from *Benson et al*., 1996).

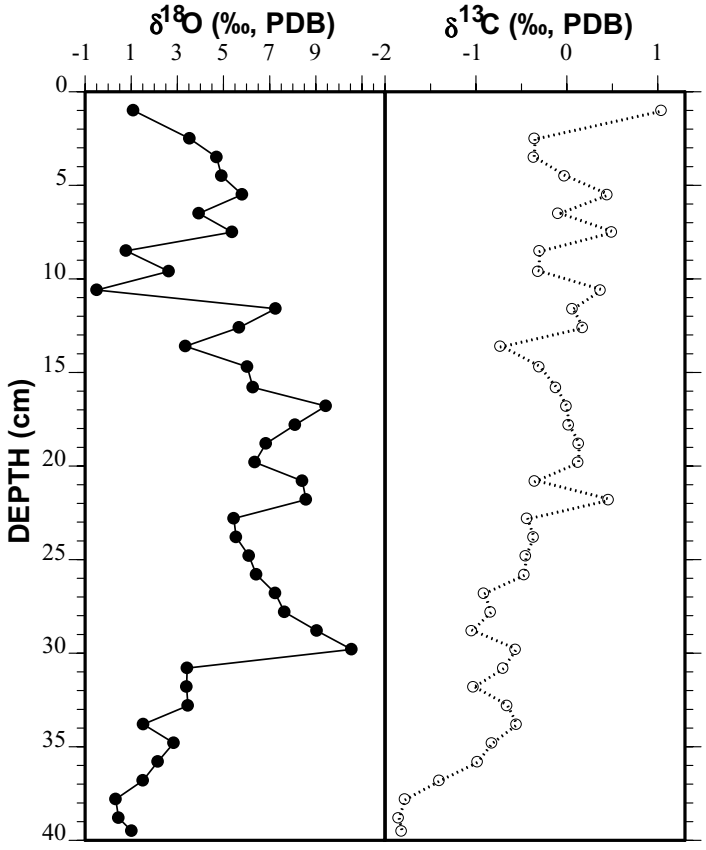

Figure 3-7. Results of measurements of $\delta^{13}C$ and $\delta^{18}O$ preserved in down-core ostracode shells (*L. ceriotuberosa*) of cored sediments from WLB-003C.

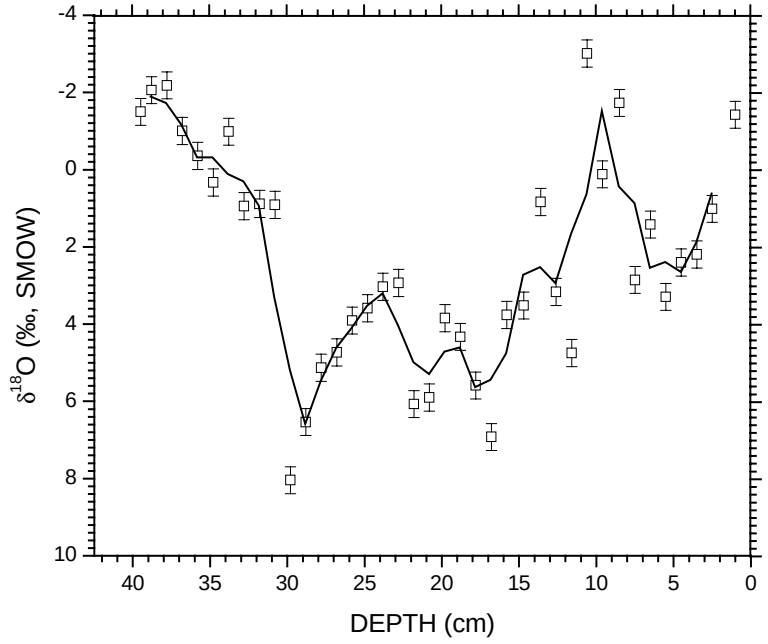

Figure 3-8. Computed $\delta^{18}O_L$ record from down-core ostracode $\delta^{18}O$ (see text for details). Errors of the computed $\delta^{18}O_L$ record (open squares with error bar) are induced by the uncertainty of water temperature (6 ± 2ºC). The solid line represents 3-point running average of the computed $\delta^{18}O_L$ record.

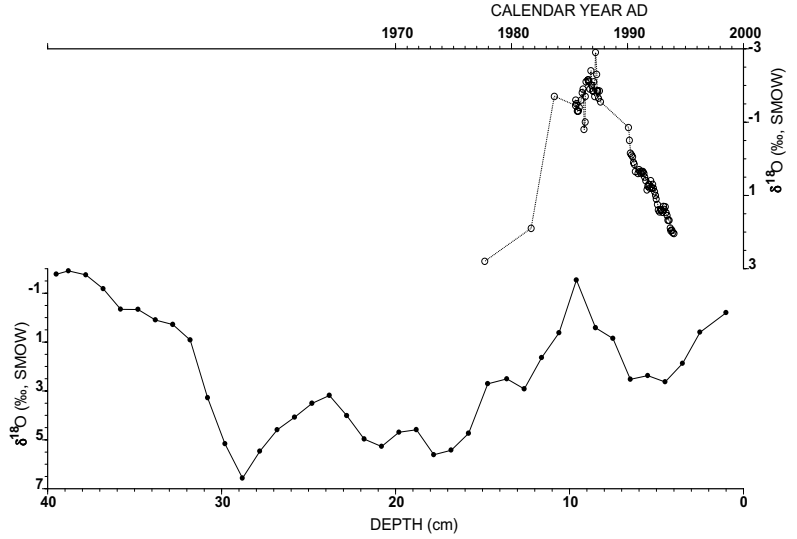

Figure 3-9. Comparison between the 3-point running average computed $\delta^{18}O_L$ and instrumental $\delta^{18}O_L$ records spanning 1985 to 1994. Original instrumental data were taken from Benson et al. (1996).

The bottom-most sediments in box core WLC-003C are equivalent to a depth of 29 cm in piston core WLC002 with a calendar age of ~1928 AD (refer to Chapter 4 in this dissertation). As the water-sediment interface was evident during box core recovery, the calendar age of the topmost sediments is assumed to be AD 2000. The comparison of proxy and instrumental $\delta^{18}O$ records supplies extra age constraints for WLC-003C. A second-order polynomial fit is made to establish an age model for box core WLC-003C (Figure 3-10). The sediment accumulation rate was apparently higher in uppermost sections than in the lower part of the core.

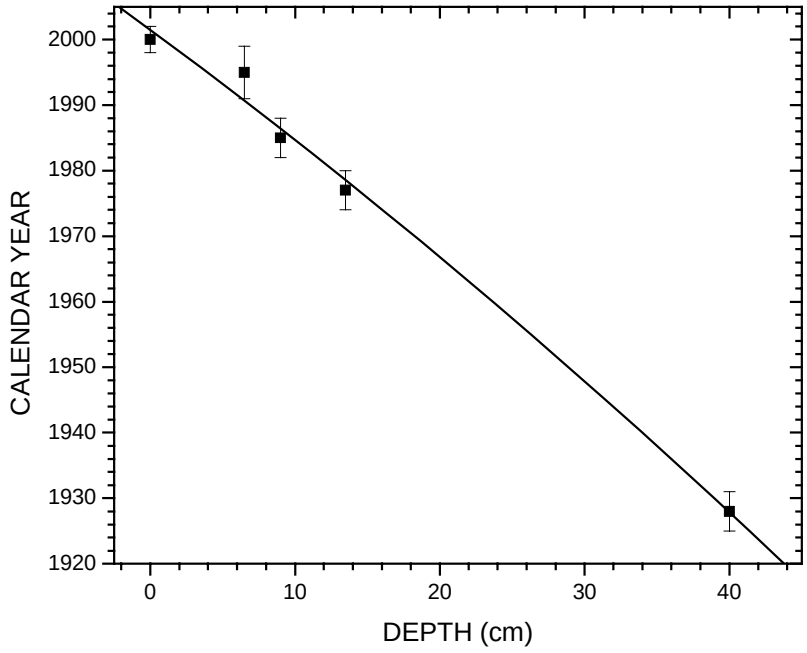

Figure 3-10. Plot of age model for WLB-003C: age vs. depth. The age of topmost sediments was assumed to be 2000AD as a sediment-water interface was preserved during core recovery. The age of bottommost sediments was assumed to be 1928AD (see Chapter 4 for details). Other age constraints were picked from figure 3-9 according to curve match. A 2nd order polynomial fit was performed to calculate the ages at various depths in the core.

The calendar age of sediments at various depths is calculated, through the second-order polynomial equation indicated in figure 3-10, to produce a 72-year proxy record of WLC-003C. This

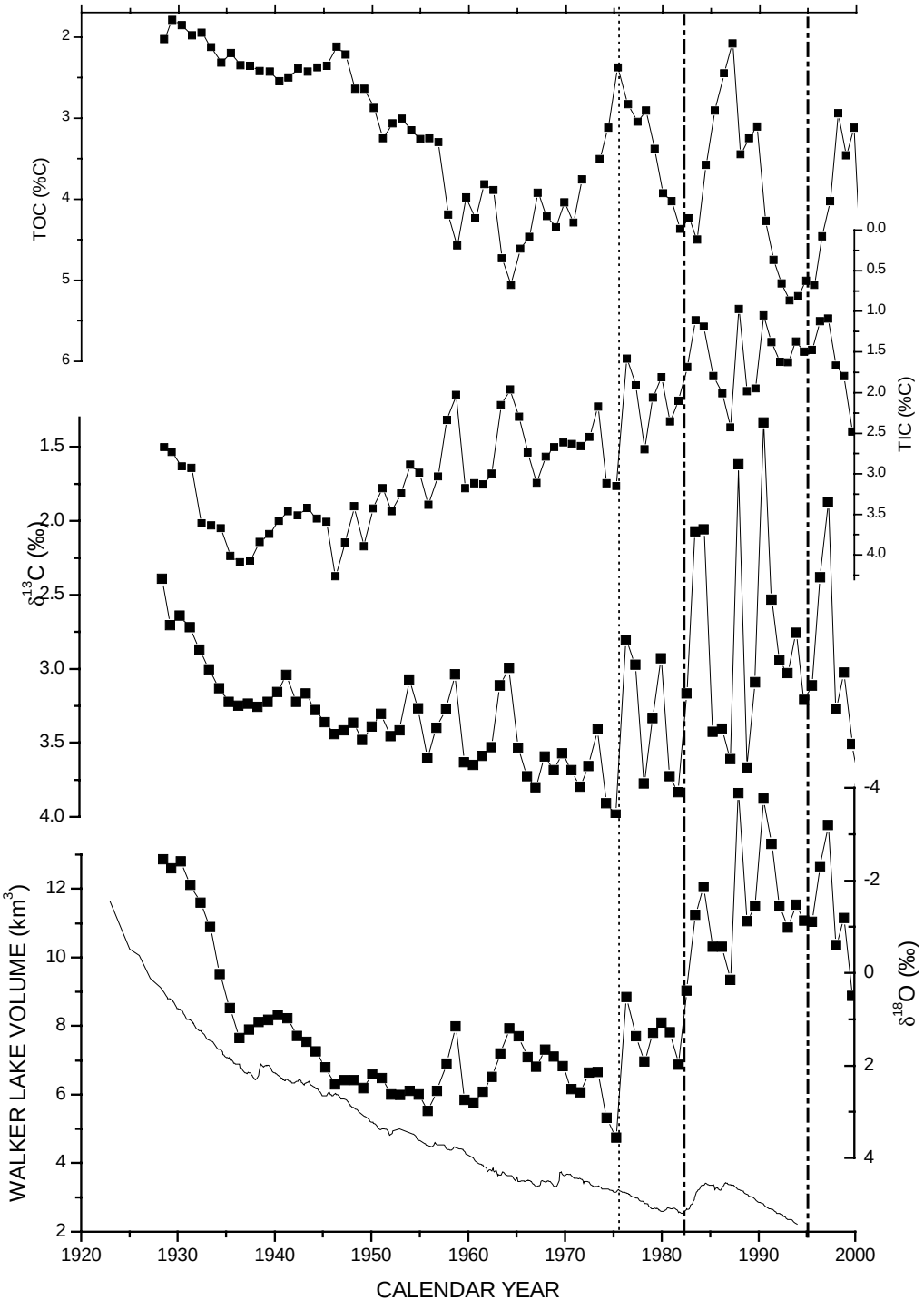

Figure 3-11. 72-year records of TIC, TOC, TIC $\delta^{13}C$, TIC $\delta^{18}O$ from WLB-003C and their comparison with historical lake level record (USGS). Vertical dotted line indicates a regime shift in 1976AD and two vertical dashed lines refer to the El Niño events of 1982/83 and 1997/98.

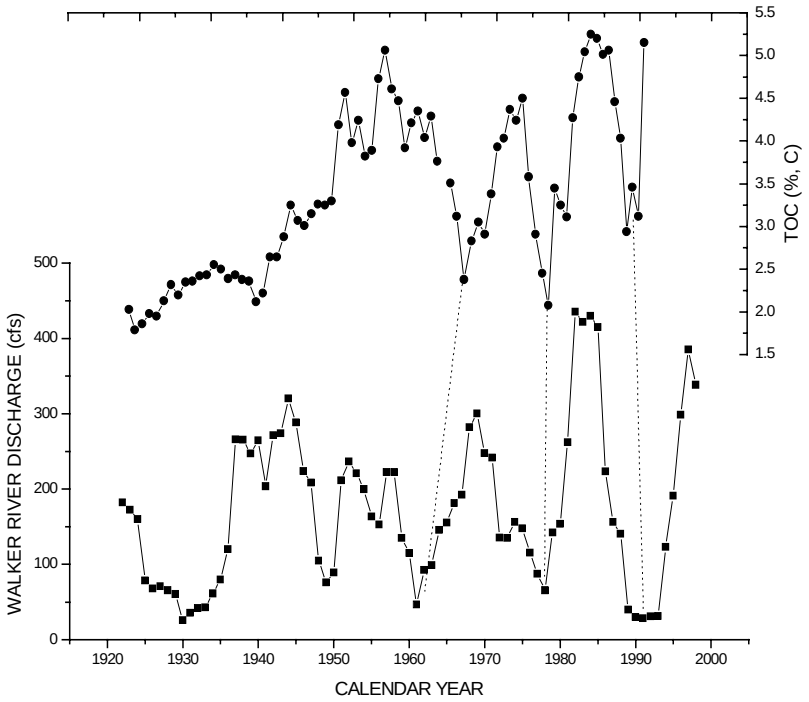

Figure 3-12. Comparison of down-core % TOC and the Walker River discharge. Dotted lines denote possible correlation between these two records. Note that the Walker River discharge data were taken from USGS and a five-point moving average was employed.

Changes in lake level or hydrological conditions usually lead to variations in TIC, TOC, $\delta^{13}C$ and $\delta^{18}O$ of the lake. TIC, TOC, and $\delta^{13}C$ are also associated with biological primary productivity and post-depositional diagenesis, which are indirectly linked with hydrological conditions, i.e., changes in hydrological conditions in general have indirect influence on these proxy indicators. In contrast, biological activities may have little effect on the $\delta^{18}O$ signal of the lake. Most variations in down-core $\delta^{18}O$ from a closed-basin lake are induced by changes in hydrologic and /or climatic conditions, such as river flow, evaporation, surface temperature, relative humidity, and wind speed etc. Although change in the $\delta^{18}O$ value of a closed-basin lake is not a simple function of the amount of change in lake volume (BENSON et al., 1991), model experiments indicate that the oxygen isotopic system is relatively simple because hydrologic models like Paleolake and HIBAL (BENSON and PAILLET, 2002) are capable of

simulating variations in $\delta^{18}O_L$ of Walker Lake over the last several decades, using just the historical stream flow record (refer to Chapter 2 and 5 in this dissertation).

Because Walker Lake is today an alkaline lake, 90% of the dissolved inorganic carbon (DIC) in the lake is in the form of HCO_3^- (BENSON et al., 1996). Results of measurements of the DIC $\delta^{13}C$ in Walker Lake back to 1966 have also been previously published. Peng and Broecker (1980) reported that the DIC $\delta^{13}C$ values of Walker Lake were 4.0‰, 3.0‰, and 3.0‰ in July 1966, September 1976, and May 1978, respectively. Based on measurements of 13 water samples collected from the lake in September 1977, Newton and Grossman (1988) reported an average $\delta^{13}C$ value of 2.8‰. In addition, Benson et al. (1996) presented 37 measurements for the $\delta^{13}C$ in Walker Lake during the interval from January 1991 to January 1995. These results are collected and shown in figure 3-13. In comparison with variations in the $\delta^{18}O_L$ observed (Figure 2-11), variations in the DIC $\delta^{13}C$ of Walker Lake are relatively small. As stated above, instrumental records in figure 3-13 show that lake DIC $\delta^{13}C$ appears to be associated with lake level change. For example, the DIC $\delta^{13}C$ was higher during relatively high stands in 1966 than during relatively low stands in 1990s.

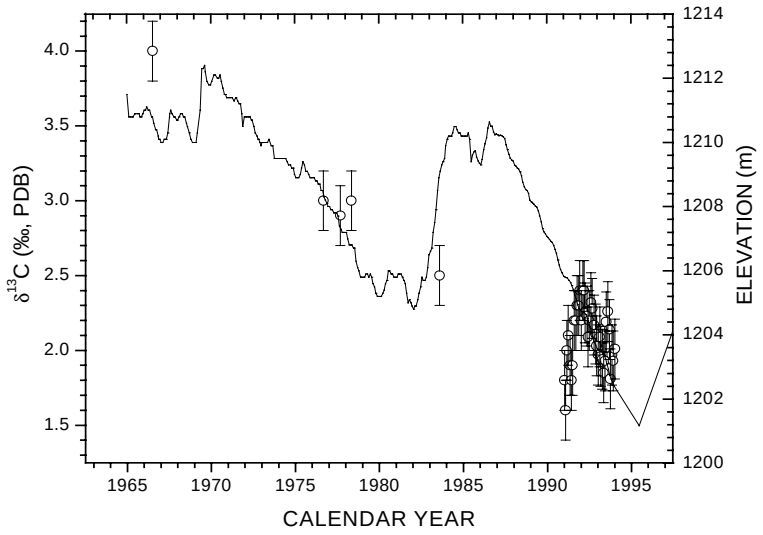

Figure 3-13. Comparison of lake water $\delta^{13}C$ and lake level elevation (carbon isotopic data originally from *Benson et al., 1996* and lake elevation data taken from USGS).

1975 to 1985. In addition, variability in the ostracode $\delta^{18}O$ is apparently larger than that in TIC $\delta^{18}O$. This apparently contradicts the stable environments near water-sediment interface where *L. ceriotuberosa* inhabits. This probably relates with the mobility and immaturity of *L. ceriotuberosa*, which have the potential to lead relatively large fluctuations in the $\delta^{18}O$ of ostracode shells.

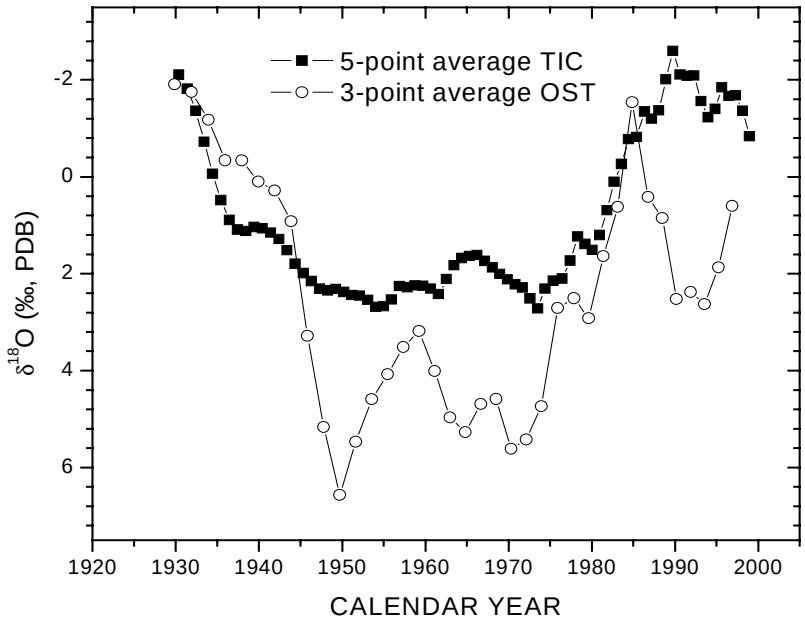

Figure 3-14. Comparison of TIC $\delta^{18}O$ (TIC) and ostracode $\delta^{18}O$ (OST) from cored sediments (WLB-003C).

Today, monohydrocalcite is the dominant carbonate precipitate in Walker Lake (SPENCER, 1977). Although the oxygen isotope fractionation factor for monohydrocalcite-H_2O is very close to that for calcite-H_2O[9] (JIMENEZ-LOPEZ et al., 2001), monohydrocalcite is metastable and subject to recrystallization. Isotopic fractionation between monohydrocalcite and calcite remains unknown, but systematic calculations for isotopic fractionation between calcite and aragonite (ZHENG, 1999; ZHOU

[9] The oxygen isotope fractionation factors for monohydrocalcite-H_2O and calcite-H_2O (25ºC, 1atm) are 27.8±0.1‰ and 28.0±0.2‰, respectively. Jimenez-Lopez C., Caballero E., Huertas F. J., and Romanek C. S. (2001) Chemical, mineralogical and isotope behavior, and phase transformation during the precipitation of calcium carbonate minerals from intermediate ionic solution at 25ºC. *Geochimica et Cosmochimica Acta* **65**(19), 3219-3231.

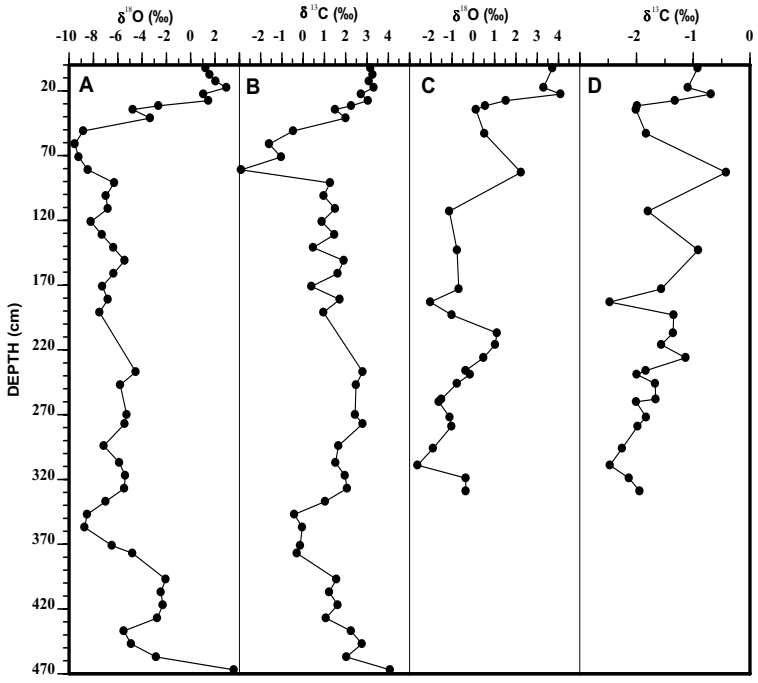

Figure 4-1. Results of measurements of oxygen and carbon isotopes from WLC84-8. A) TIC $\delta^{18}O$ record, B) TIC $\delta^{13}C$ record, C) $\delta^{18}O$ record of ostracod *L. ceriotuberosa* shells, D) $\delta^{13}C$ record of ostracod (*L. ceriotuberosa*) shells.

These isotopic results from bulk carbonate sediments and ostracode shells show maximum $\delta^{13}C$ and $\delta^{18}O$ values at a depth of ~20 cm. The transition in this interval is associated with the anthropogenically-induced lake level lowering that occurred starting in 1922/23. The ostracode $\delta^{13}C$ value is on average 3 ‰ lower than that of bulk carbonate sediments while the ostracode $\delta^{18}O$ values is on average 4 ‰ higher than that of bulk carbonate sediments. This is consistent with previous results from piston core WLC84-8 (BENSON et al., 1991) and box core WLC-003C (Chapter 3 in this dissertation). The difference of $\delta^{18}O$ values between ostracode and bulk carbonate sediments can be ascribed to vital effect (i.e., different organisms fractionate to varying degrees) (XIA et al., 1997a; XIA et al., 1997b) and the temperature difference between surface and bottom water (BENSON et al., 1991) since this ostracod (*L. ceriotuberosa*) tends to inhabit the water-sediment interface (BRADBURY et al., 1989; CHIVAS et al., 1985; HOLMES, 1996). The relatively ^{13}C-depleted ostracode shells may be in part related to the presence of organic material inside and /or outside of their valves since no sample

pre-treatment to remove organic matter was taken prior to isotopic analysis. $\delta^{18}O$ and $\delta^{13}C$ are positively correlated (for bulk carbonate, r^2=0.55, n=45; for ostracod shells, r^2=0.57, n=27). However, no correlation between ostracode $\delta^{18}O$ and ostracode $\delta^{13}C$ was found for the core WLC84-8 samples.

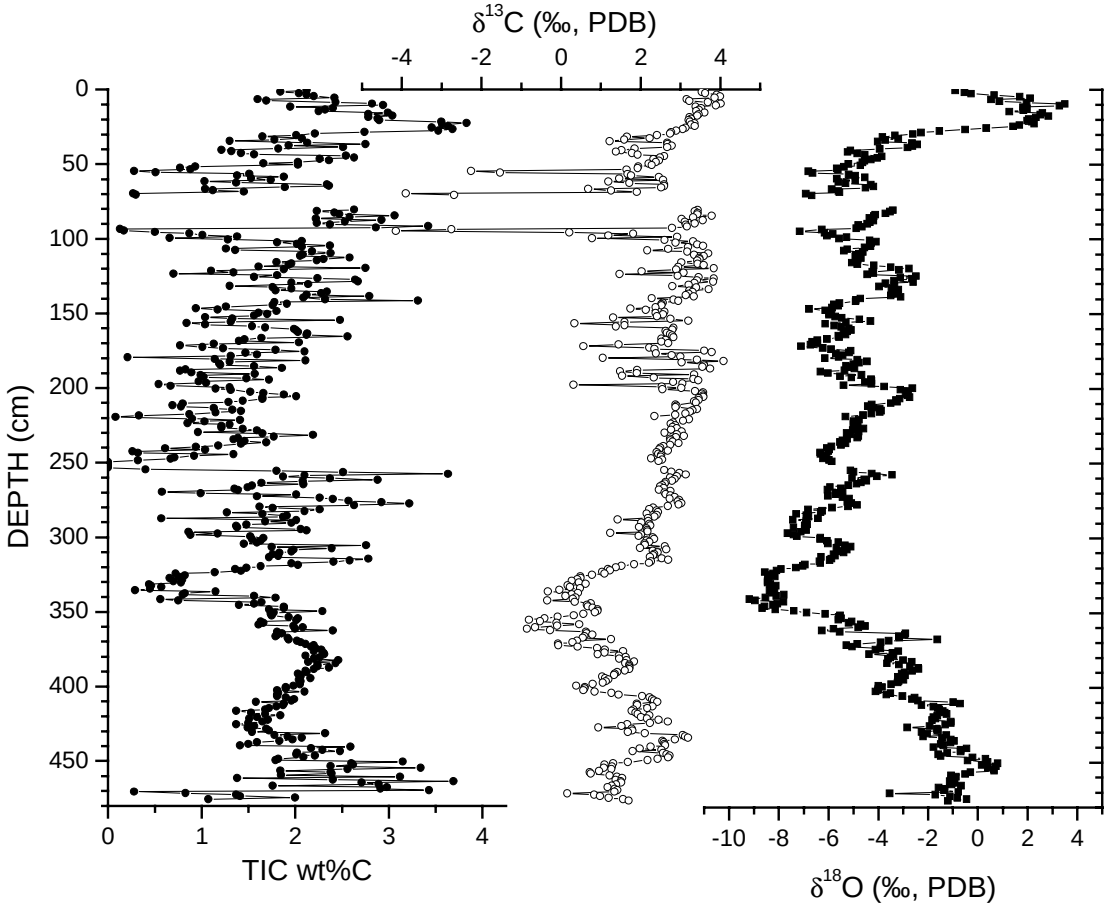

Figure 4-2. TIC, $\delta^{13}C$, and $\delta^{18}O$ results were performed on the total inorganic carbon fraction of sediments from core WLC002. Carbon and oxygen isotopic analyses were conducted after organic carbonate matter was removed by 2.6% NaClO solution.

4.3.2 Core WLC002

The TIC and isotopic results from the bulk carbonate content of WLC002 are plotted vs. depth cm in Figure 4-2. The gap indicated in the dataset is due to a loss of ~10-15 cm of core (previously estimated by Dr. S. Lund and Dr. J. Smoot) at the bottom of the uppermost core section during core recovery. Although $\delta^{18}O$ and $\delta^{13}C$ are not significantly correlated (r^2 = 0.11,

n = 461), the $\delta^{13}C$ minima are usually concurrent with the $\delta^{18}O$ minima as well as the TIC minima. In general, weight % TIC (Figure 4-2) shows larger variability than $\delta^{18}O$ and $\delta^{13}C$.

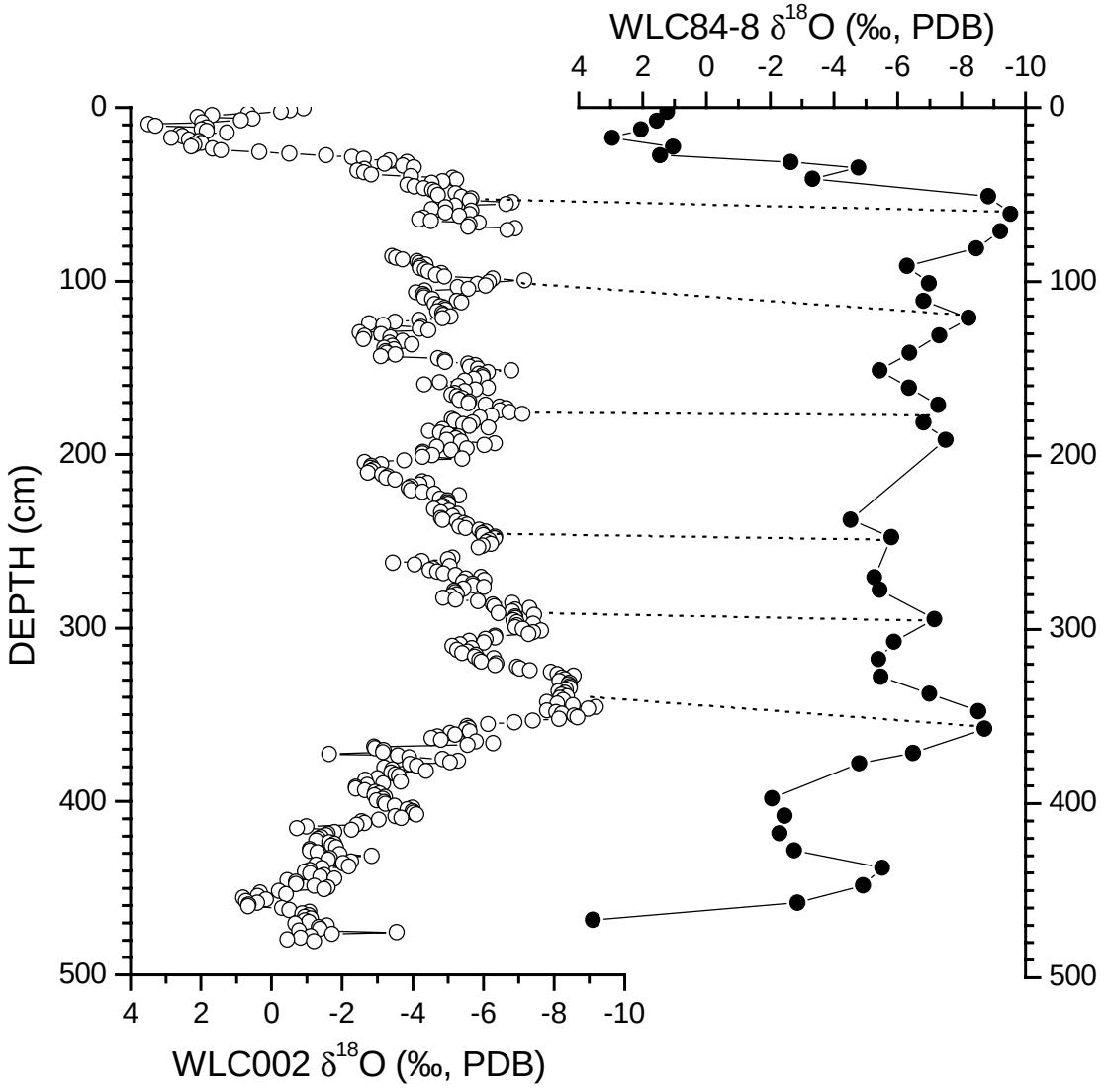

Figure 4-3. Comparison of TIC $\delta^{18}O$ records derived from WLC84-8 and WLC002. Note that the two records are generally consistent.

In the oldest part of the record $\delta^{18}O$ is higher except for the historical interval (0-45 cm) and then becomes progressively lower until it reaches a minimum of < -8 ‰ at depths of 330

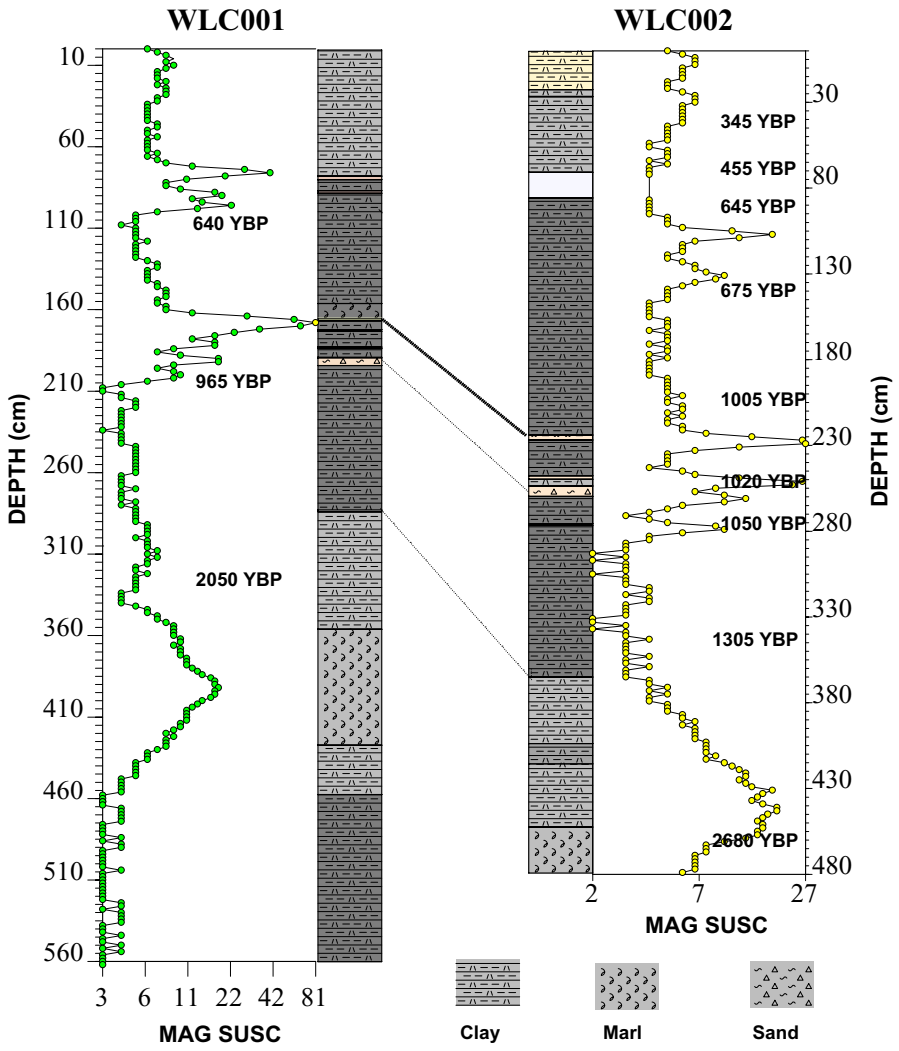

Figure 4-4. Stratigraphic correlations between WLC001 and WLC002. Magnetic susceptibility data were obtained by Dr. Steve Lund of the University of Southern California. Dates are uncorrected radiocarbon ages measured on the TOC fraction of carbonate materials of WLC001 and WLC002 by USGS.

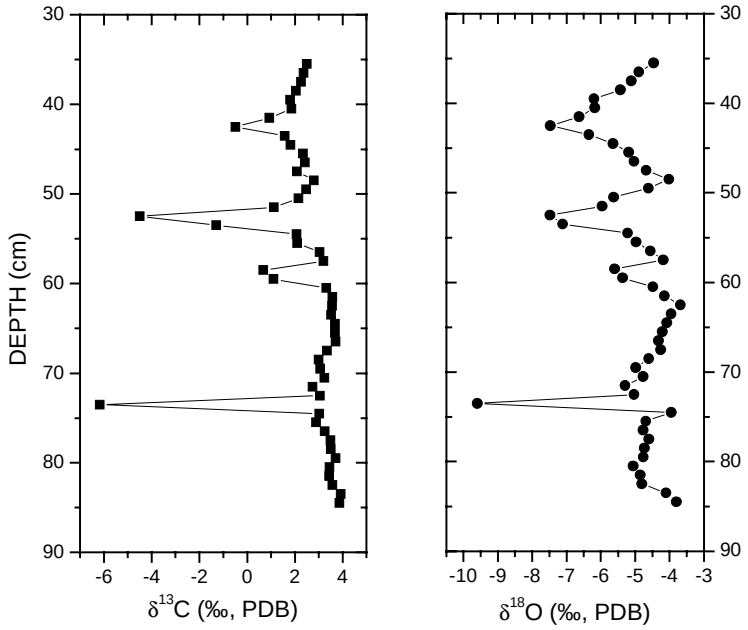

Figure 4-5. TIC $\delta^{13}C$ and TIC $\delta^{18}O$ records derived from piston core WLC001 to in the interval that spans the gap in WLC002.

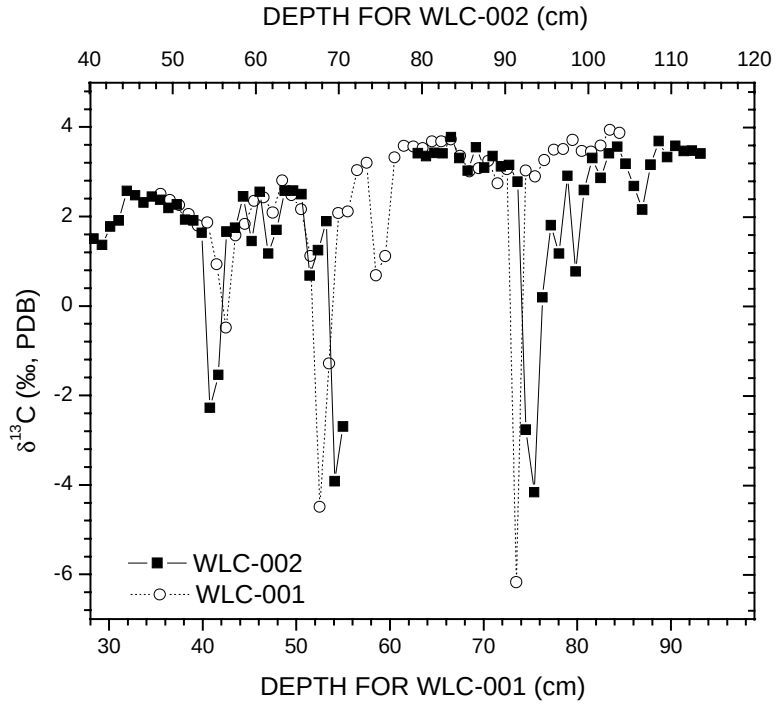

Figure 4-6. $\delta^{13}C$ records from WLC001 (open circles) and WLC002 (solid squares).

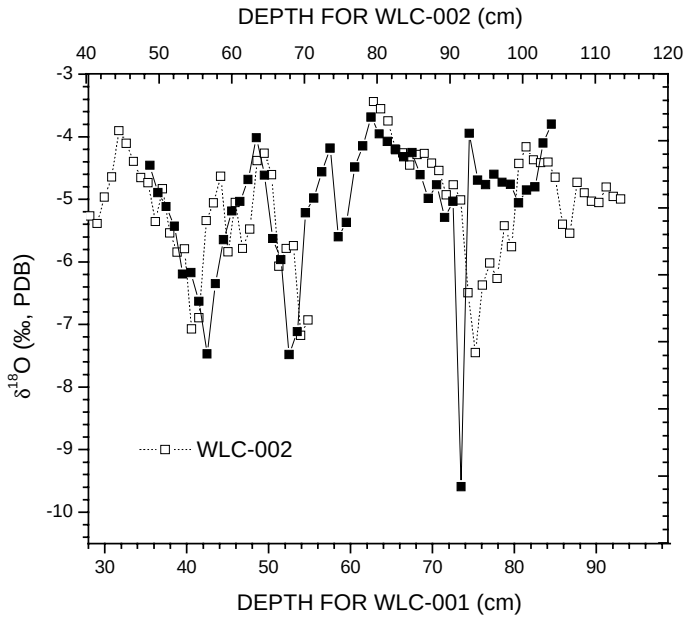

Figure 4-7. $\delta^{18}O$ records from WLC001 (solid square) and WLC002 (open square). In conjunction the $\delta^{13}C$ record presented in Figure 4-6, there is 8 cm loss at the bottom of the top segment of WLC002.

4.4 Core Chronology

4.4.1 Reservoir Effect

Because the radiocarbon-dated material is from the TOC fraction, that is mostly lake-derived organic matter (MEYERS, 1990), the reservoir effect of Walker Lake needs to be taken into account prior to ^{14}C date calibration. The reservoir effect on radiocarbon in Great Basin lakes is somewhat basin-specific. For example, Pyramid Lake has a 600-year reservoir effect (BENSON et al., 2003a; BENSON et al., 2002) while Mono Lake has a reservoir effect ranging from 1100 to 5300 years (BENSON et al., 2003a; BENSON et al., 1990). The reservoir effect is related with the residence time of the dissolved inorganic carbon (DIC) in the lake. Also, non-atmosphere borne carbon inputs, such as dissolution (weathering or reworking) of old carbonate sediments and DIC-bearing groundwater baseflow, will lead to lower $^{14}C/^{12}C$ ratio and apparently older ^{14}C dates.

One way to determine the reservoir effect of a lake is to compare radiocarbon dates and calendar ages of topmost sediments. If the calendar ages of topmost sediments can be determined through identification of regional and /or global historical events such as mining activities, river

diversions, and nuclear bomb tests, then these ages can be compared to radiocarbon ages of TOC in the same sediment horizons. In Walker Lake, two historical events are documented in down-core sediments; mining activities in 1860 (SMITH, 1998) and construction of Lake Topaz and Bridgeport reservoir completed in 1922/23.

A hydrological and isotopic balance modeling study on Pyramid Lake and Walker Lake (BENSON and PAILLET, 2002) suggested that the overall shapes of the lake volume and $\delta^{18}O$ records are similar and that minima and maxima in simulated TIC $\delta^{18}O$ records correspond to minima and maxima in the reconstructed lake volume records. The $\delta^{18}O$ signals preserved in carbonate sediments from the uppermost section of piston core WLC002 agree with this conclusion and have recorded the abrupt lake level lowering that began in 1922/23 due to an anthropogenically induced reduction of stream flow (Figure 4-8).

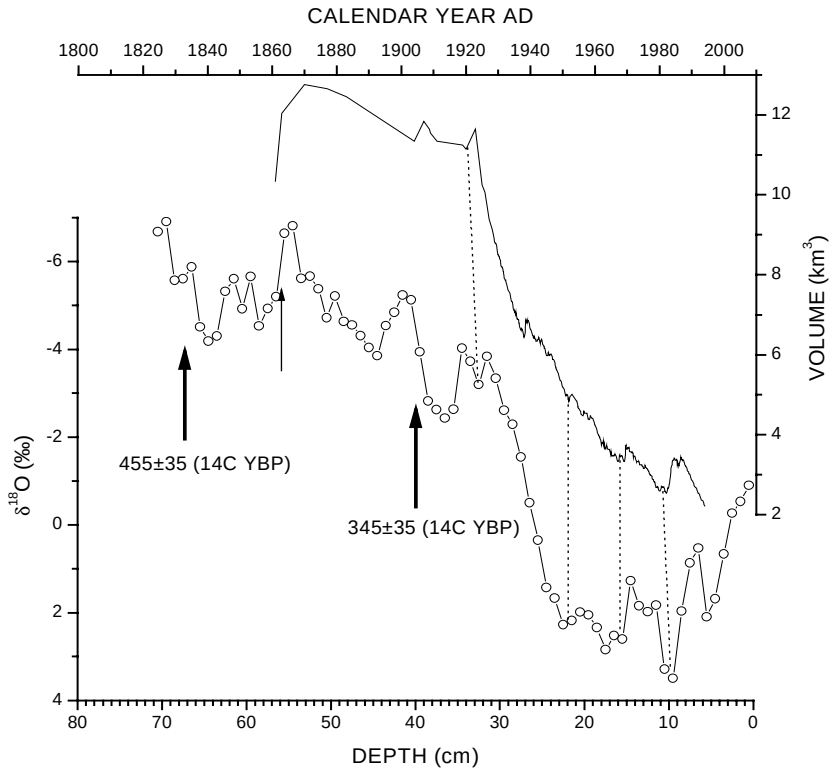

Figure 4-8. Direct comparison of historic lake level record (USGS) and the raw $\delta^{18}O$ record from the uppermost section of WLC002. Solid arrows refer to uncorrected radiocarbon dates and the thin arrow stands indicates a rise in Hg concentration due to Hg amalgamation processes around 1860 AD (*Michael Lico, personal communication*, 2002). Dotted lines denote possible correlation of these two records.

Table 4-2 Estimates of the reservoir effect of Walker Lake. Calendar year dates were calculated through applying the computer program Calib 4.3 (STUIVER and REIMER, 1993; STUIVER et al., 1998). Calibrated age is the 50% median probability (SMITH et al., 2002).

τ_r (years)	CAMS87139		CAMS87140	
	Calibrated Year (AD)	2-σ range Year (AD)	Calibrated Year (AD)	2-σ range Year (AD)
290	1865	1692-1955	1775	1660-1950
300	1875	1693-1955	1780	1665-1950
310	1895	1813-1955	1805	1668-1950
320	1895	1813-1955	1815	1671-1951

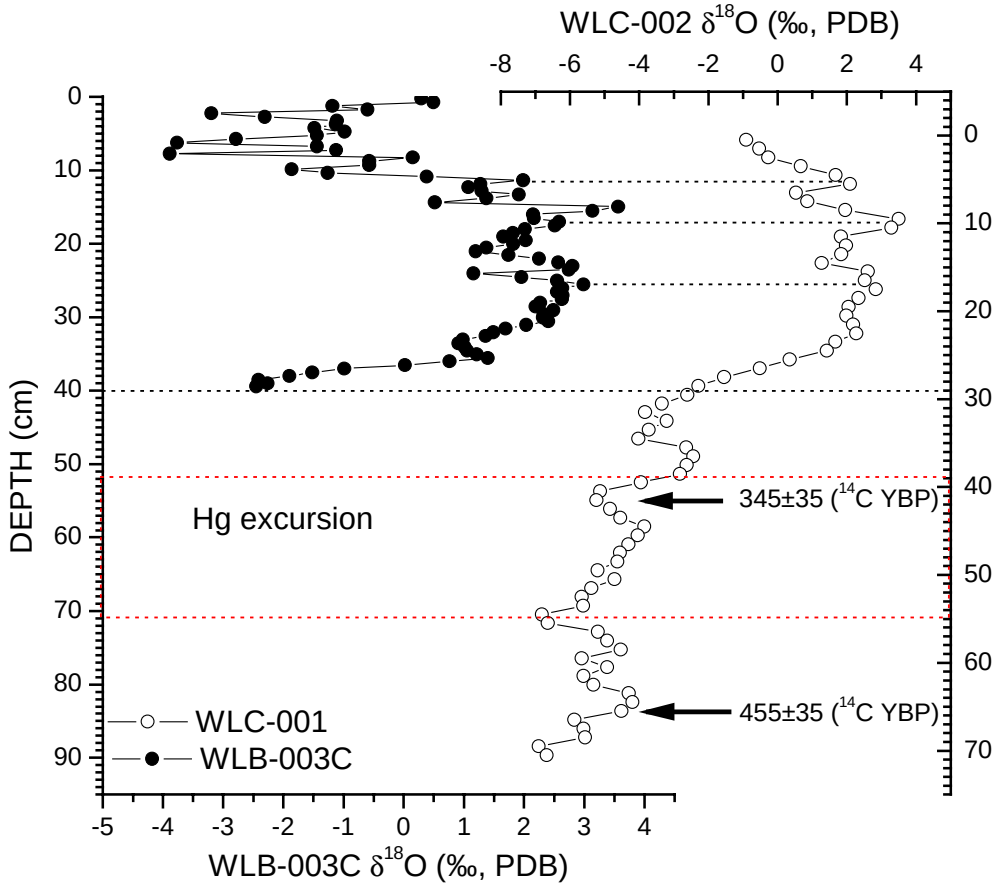

Figure 4-9. $\delta^{18}O$ records of WLB-003C (solid dots) and the uppermost section of WLC002 (open circles). Compared results indicate that topmost loss of WLC-002 is minor. Solid arrows refer to uncorrected radiocarbon dates.

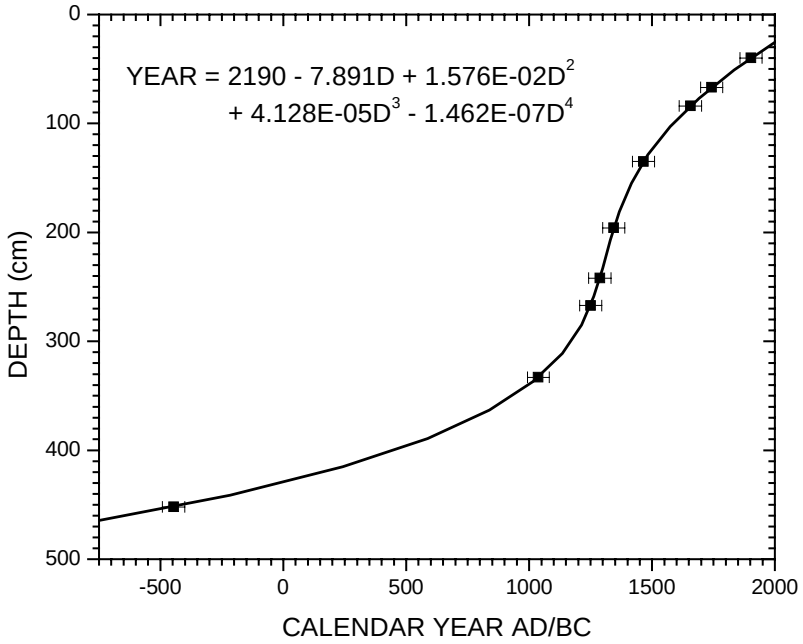

Figure 4-10. Plot of calibrated ^{14}C ages vs. depth for WLC002. Individual error bar is marked according to 2-σ range in Table 4-3. Solid line is a fourth-order polynomial fit of nine calibrated dates. Depth means the distance between the dated sample position and the water-sediment interface.

4.5 Discussion

The $\delta^{18}O$ results from WLC001 and WLC002 were merged to produce a high-resolution multi-proxy record spanning the last 3000 years (see Figure 4-11). The proxy record is characterized by lower accumulation rates and lower variability in % TIC, $\delta^{13}C$, and $\delta^{18}O$ prior to 800 AD. The values of magnetic susceptibility after 800 AD are relatively lower except for two pronounced excursions centered on ~1250 and ~1550 AD. On the basis of variations in magnetic susceptibility, TIC, $\delta^{13}C$, and $\delta^{18}O$, this late Holocene proxy record are divided into three periods; Period LH-1 (from 1000 BC to 800 AD), Period LH-2 (from 800 AD to 1900AD), Period LH-h (from 1900 AD to 2000AD). These intervals are discussed in more detail below.

4.5.1 Period LH-1, 1000BC to 800AD

The $\delta^{18}O$ values of down-core bulk carbonate sediments in Walker Lake are relatively high during Period LH-1 (Figure 4-11). The interval with highest $\delta^{18}O$ values (~0.8 ‰, PDB) is centered on

~400BC. This interval has the highest $\delta^{18}O$ of the entire late Holecene section from Walker Lake. In addition, the values of magnetic susceptibility are generally high during this period. This is interpreted to indicate that Walker Lake had a low stand at this time allowing terrestrial magnetic-bearing materials to reach in core sites. The average values of $\delta^{13}C$ are relatively low in this period, which probably indicates low primary productivity. This is consistent with low accumulation rates during Period LH-1.

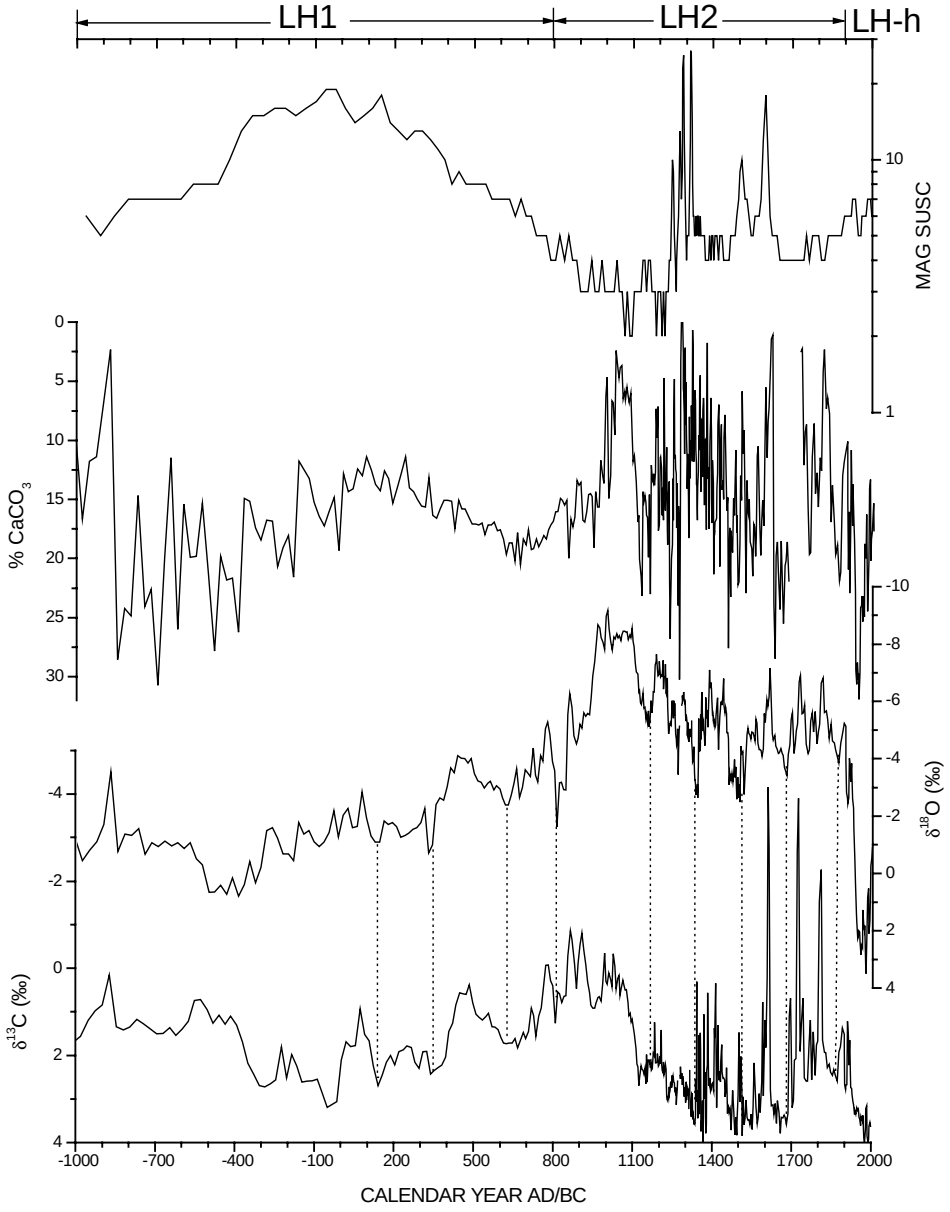

Figure 4-11. 3000-year records of TIC, magnetic susceptibility (Steve Lund), TIC $\delta^{13}C$, and TIC $\delta^{18}O$ of Walker Lake. Eight points were taken from WLC001 to fill the gap of WLC002. Vertical dotted lines denote correlation between $\delta^{13}C$ and $\delta^{18}O$.

On the basis of the core chronology (Figure 4-11), Walker Lake level elevation is interpreted to have been relatively low during Period LH-1. This result is comparable with previous findings except for the beginning of the period, in which previously results (BENSON and THOMPSON, 1987; BRADBURY, 1987; DAVIS, 1982) suggest that Walker Lake elevation was high (see Figure 4-12). A shallow brine Walker Lake (2400 to 2000 years BP) was documented in down-core limnological records of diatoms, ostracodes, and pollen (BRADBURY, 1987; BRADBURY et al., 1989). Benson et al. (1991) previously suggested relatively low lake levels during 2700-1250 years BP. However, whether the low lake stands during Period LH-1 were induced by climate changes or river diversions still remains uncertain. The fact that Mono Lake was also low during 1800-1000 years BP (STINE, 1990) favors climate-driving fluctuations in hydrologic conditions instead of river diversions.

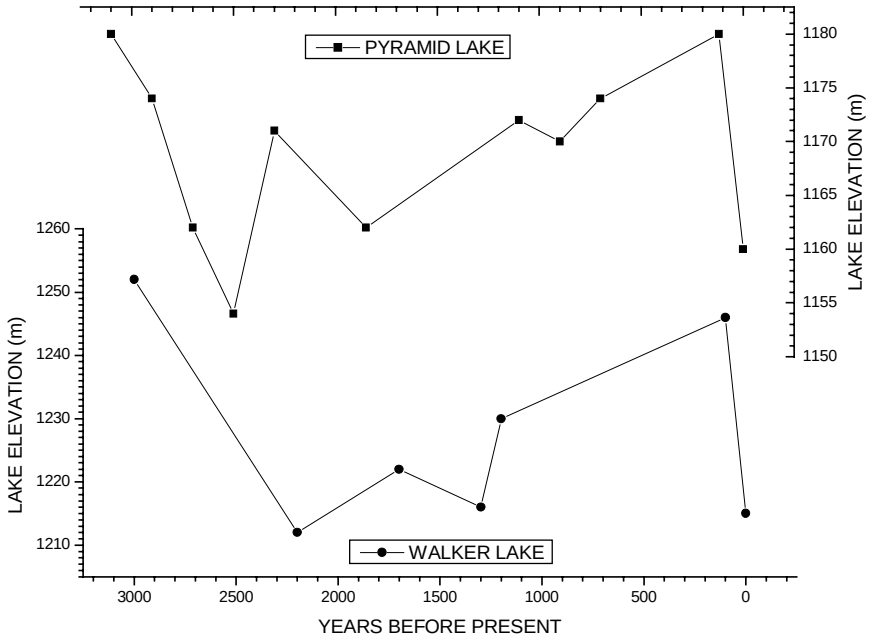

Figure 4-12 Late Holocene variations in lake level of Pyramid and Walker Lakes according to radiocarbon dated tufas and archaeological materials (after BRADBURY, 1987). Original data from Benson (1978) and Davis (1982)

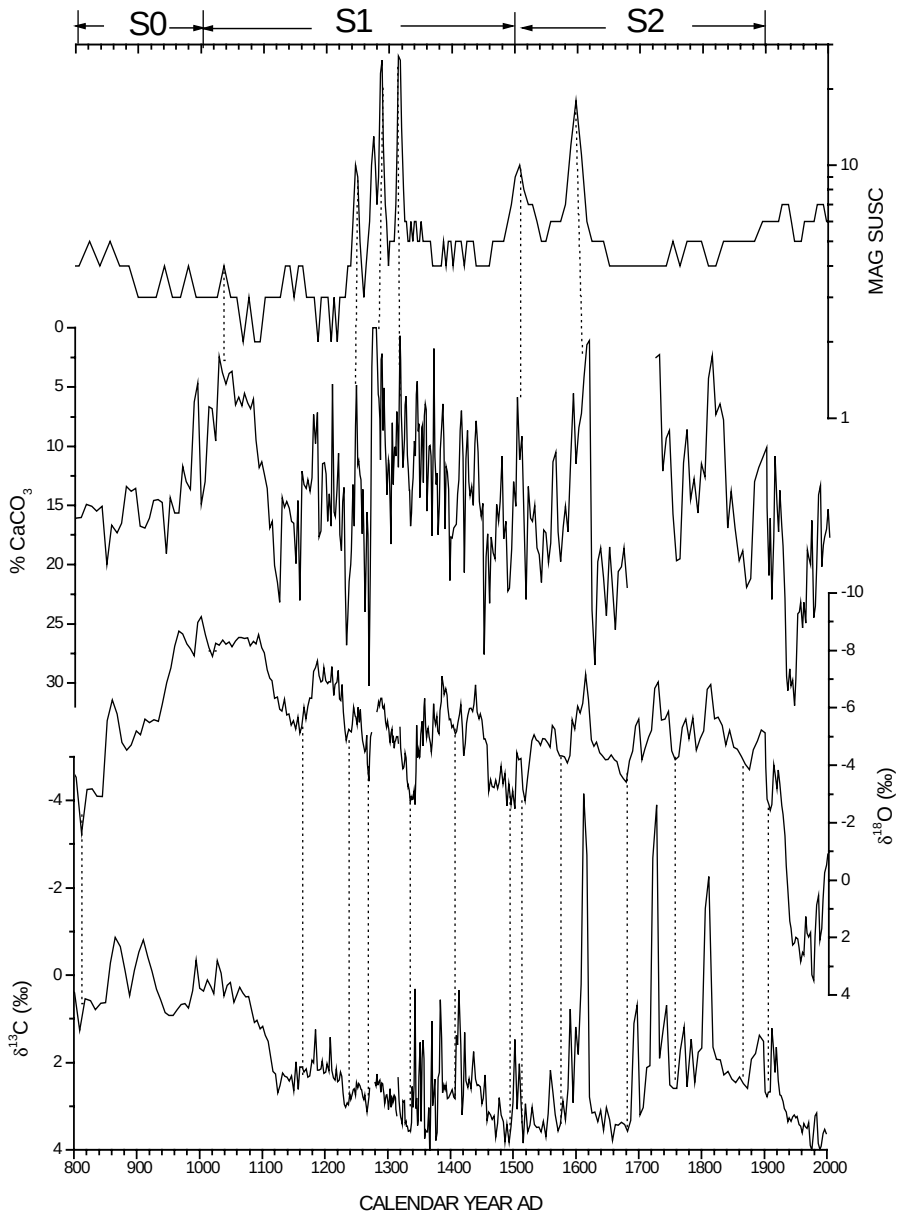

Figure 4-13. High-resolution (3.3 years per sample on average) 1200- year records of TIC, magnetic susceptibility (Steve Lund), $\delta^{13}C$, and $\delta^{18}O$ of Walker Lake. Dotted lines denote correlation between these records.

4.5.2 Period LH-2, 800AD to 1900AD

Down-core sediments in Period LH-2 are characterized by high accumulation rates with an average of ~0.3 cm yr^{-1}. High-resolution records of magnetic susceptibility, TIC, $\delta^{13}C$, and $\delta^{18}O$ are shown in Figure 4-13. The TIC, $\delta^{13}C$, and $\delta^{18}O$ records exhibit several multi-decadal to centennial time

950 to 1100 AD. If this interpretation is correct it contradicts Stine's (1994) tree-stump results that show drier conditions and lower lake levels during this time of the MWE, but agrees with the tree-ring-based streamflow record of the Sacramento River (see figure 4-15). In addition, both TIC $\delta^{18}O$ records of Pyramid Lake and Walker Lake show low lake stands in ~1265, ~1335, and ~1470 AD. Except for the proposed low stand of Walker Lake in 1265AD, the other two are also evident in tree-ring based river flow record (40-yr moving average) of the Sacramento River (MEKO et al., 2001).

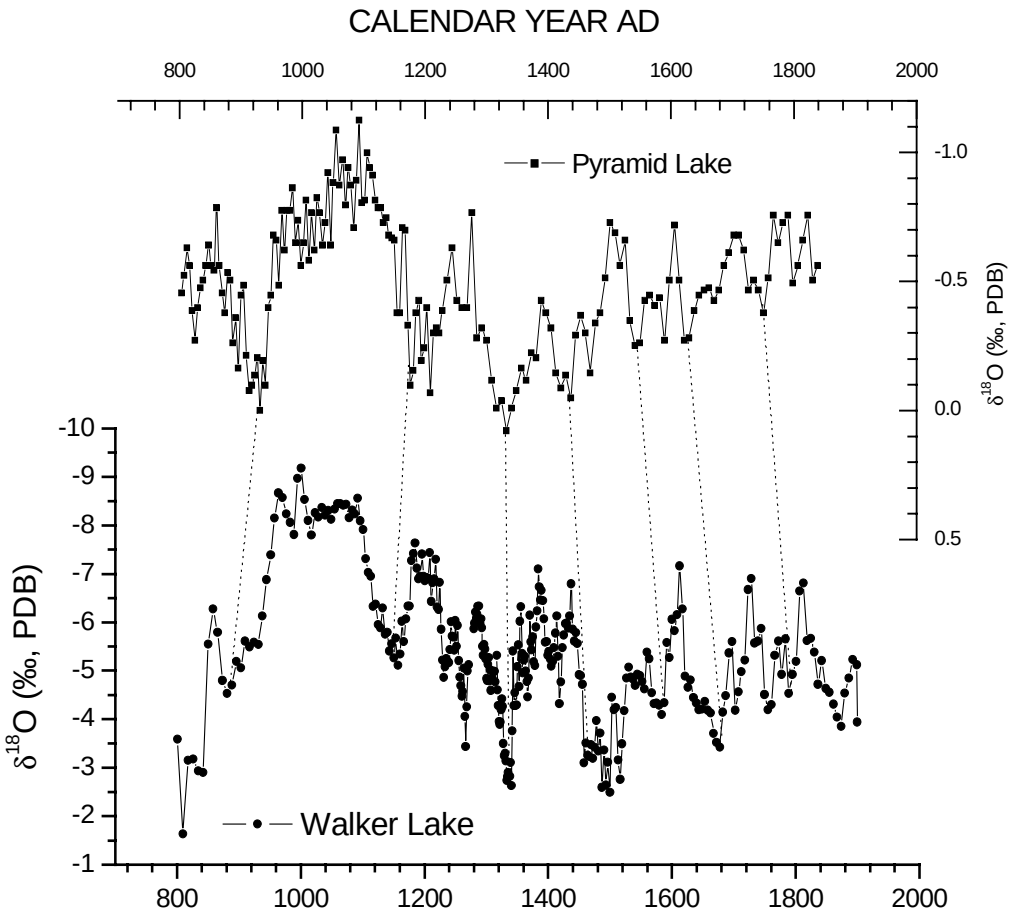

Figure 4-14. Comparison of $\delta^{18}O$ records from Walker Lake and Pyramid Lake (PLC97-1) (BENSON et al., 2002). Dashed lines denote possible correlation between these two $\delta^{18}O$ records.

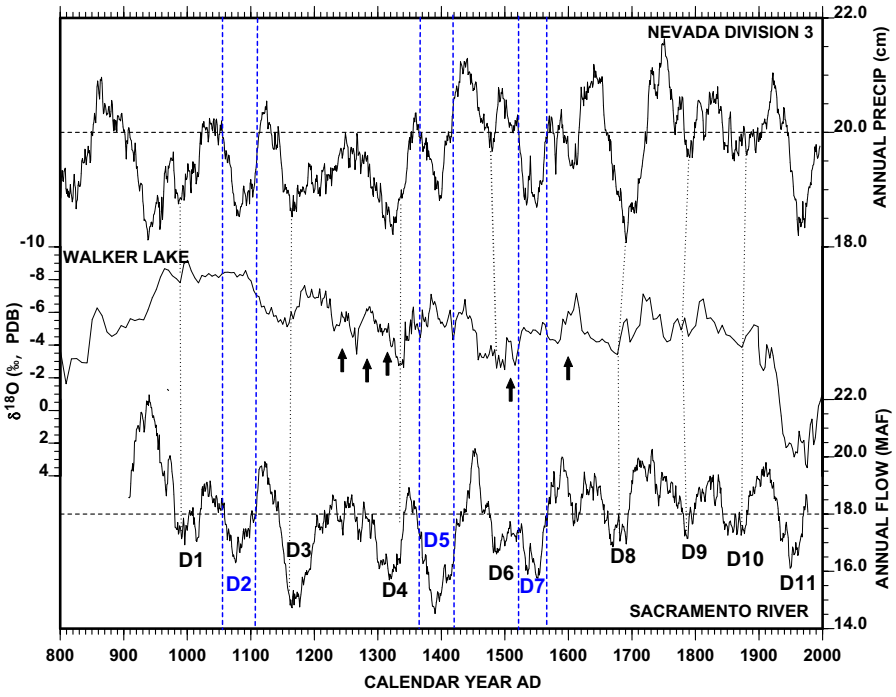

Figure 4-15. Comparison of sediment-based record of Walker Lake and tree-ring based records in adjacent areas. Proxy precipitation record of Nevada Division 3 and river flow record of the Sacramento River are 40-year moving averages of the data obtained by Hughes and Graumlich (1996) and Meko et al. (2001), respectively. D1 to D11 are 11 dry intervals evident in the Sacramento River flow record. The coarser solid line is also a 40-year moving average of $\delta^{18}O$ record from Walker Lake. Solid arrows represent the peaks of magnetic susceptibility.

The Walker Lake TIC $\delta^{13}C$ record is not as easily interpreted. The $\delta^{13}C$ record of Walker Lake and the streamflow record of the Sacramento River are only weakly correlatable (Figure 4-16). Wet intervals (high discharge) of the Sacramento River tend to correlate with minima of $\delta^{13}C$ and TIC values after 1550 AD, while the dry intervals are correlated with minima of $\delta^{13}C$ and TIC values before 1550 AD. The fact that the minima of $\delta^{13}C$ are concurrent with the minima of TIC values suggests the $\delta^{13}C$ is affected by biological productivity and /or TOC. In Chapter 3, I illustrated that downcore TOC content is associated with the stream discharge. When the stream discharge is larger, the Walker River tends to carry more nutrients to the lake and results in higher productivity or % TOC, which has the potential to produce a more negative signal of $\delta^{13}C$.

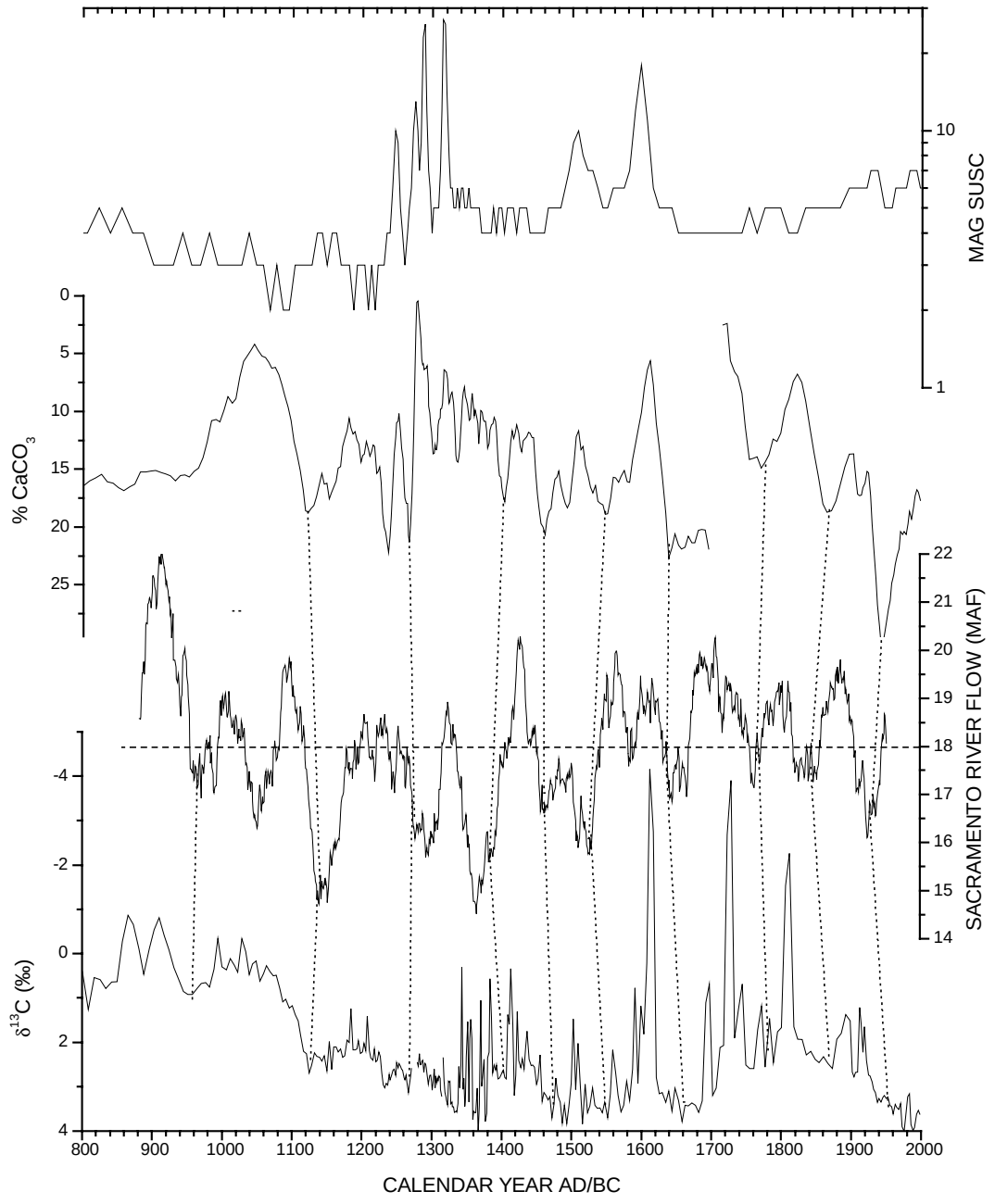

Figure 4-16. Comparison of magnetic susceptibility (Steve Lund), TIC, and $\delta^{13}C$ records from Walker Lake with the tree-ring based river flow record of the Sacramento River (MEKO et al., 2001). Vertical dashed lines are possible connections between these proxy records and horizontal dotted line denotes the average river discharge of the Sacramento River over the last 1130 years.

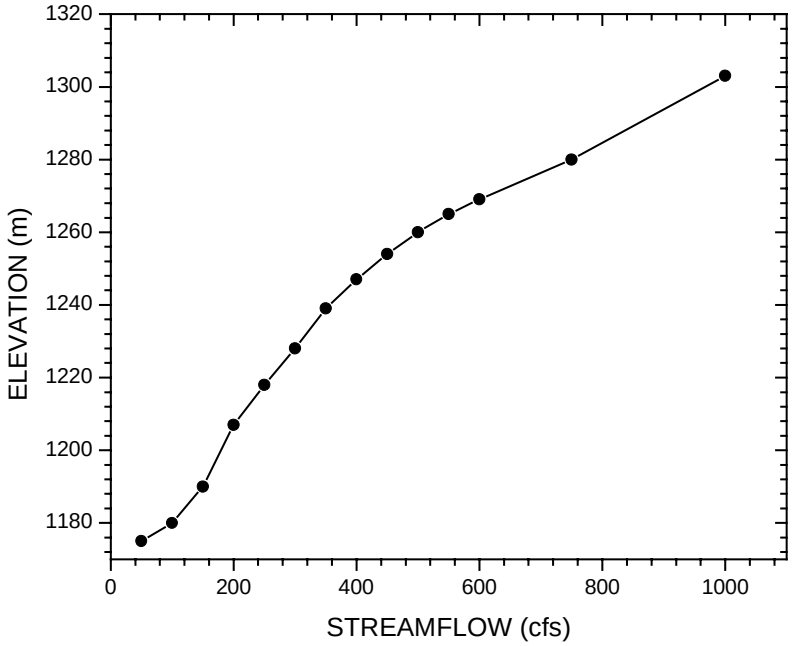

Figure 5-1. Steady-state lake elevation of Walker Lake corresponding to long-term average value of the Walker River discharge. The elevation of spilling sill is 1308.0 m and the lake bottom elevation is 1171.5 m (MILNE, 1987).

Walker Lake presently has not reached a hydrologic steady-state following the lowering that began in the early 1920s, as the actual lake elevation is slightly above to the steady-state level of 1198 m for the average river flow of 174 cfs. The average values of the reconstructed river flow of the Walker River are 330 cfs in the late Holocene, 550 cfs in the last millennium, and 640 cfs in MWE (1000 to 1430 AD) (see Chapter 5). The 20-year running average values of the reconstructed river flow of the late Holocene Walker River also varies within 1000 cfs, indicating that Walker Lake remained in hydrologic closure in the late Holocene.

Variations in the $\delta^{18}O_L$ have been successfully simulated using HIBAL (see chapter 2 in this dissertation). The natural river flow (Q) of the Walker River, as well as other climatic signals tends to fluctuate periodically, $Q = \sum_{i=1}^{n} A_i \sin(\frac{2\pi t}{\lambda_i}) + M$, where A is the amplitude of river discharge in cfs, λ the wavelength in year, t the time in year, M the mean value of river flow in cfs, i=1, 2, … , n denoting n

discharge (Figure 5-2A and 5-2B). Under approximate steady-state conditions, the $\delta^{18}O_L$ values of epilimnion and hypolimnion vary in phase with changes in river discharge (Figure 5-2C and 5-2D). For interdecadal variations in river discharge (e.g., λ=25 yr), both the initial and steady-state responses of epilimnion and hypolimnion $\delta^{18}O_L$ tend to be synchronous with change in river discharge (Figure 5-3A, B, C, and D). However, for century-timescale like λ=100 yr, both the initial and steady-state responses of the epilimnion and hypolimnion $\delta^{18}O_L$ appear to lead by ~10 years changes in river discharge (Figure 5-4A, B, C, and D). If this result can be confirmed, the low-frequency $\delta^{18}O_L$ signal stored in down-core sediments can be used to predict the long-term future climate (discharge) changes. As this result is opposite to previous studies (BENSON and PAILLET, 2002), more modeling work is needed.

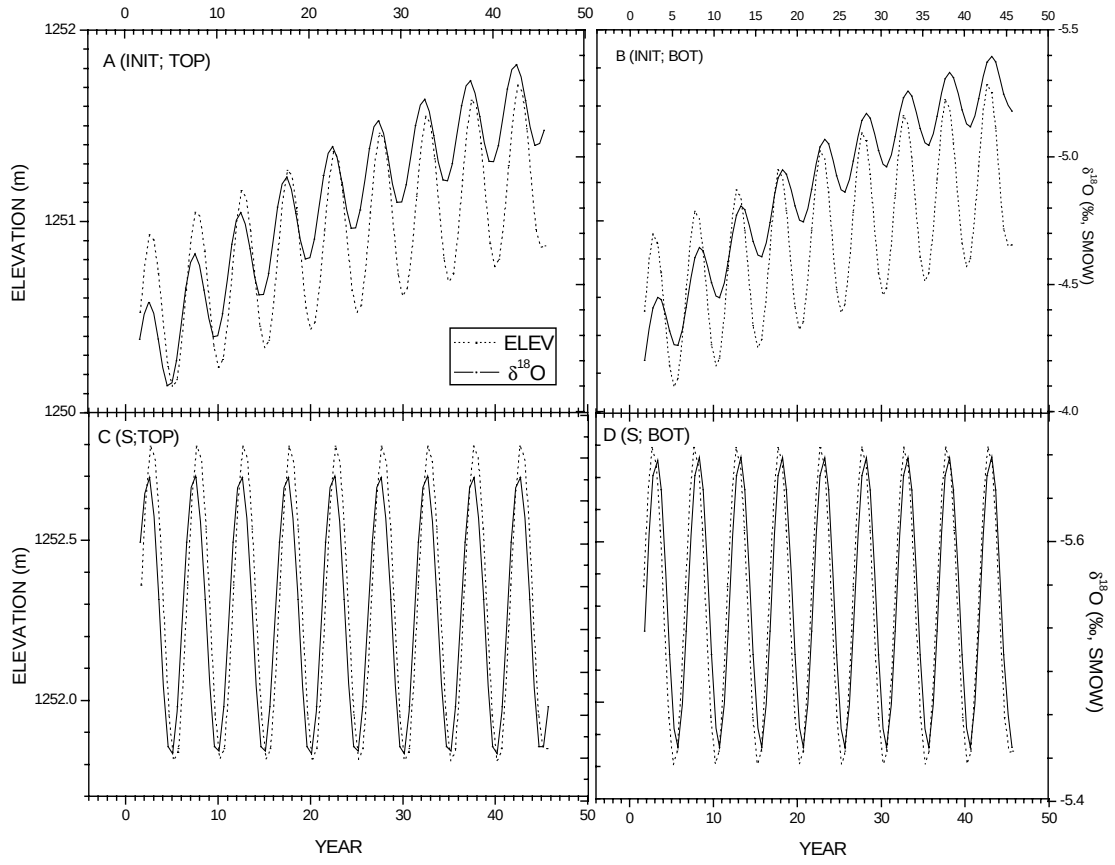

Figure 5-2. Oxygen isotopic responses to oscillatory changes in the Walker River discharge with a wavelength of 5-yr. A) Initial response of the top water. B) Initial response of the bottom water. C) Steady-state response of the top water. B) Steady-state response of the bottom water.

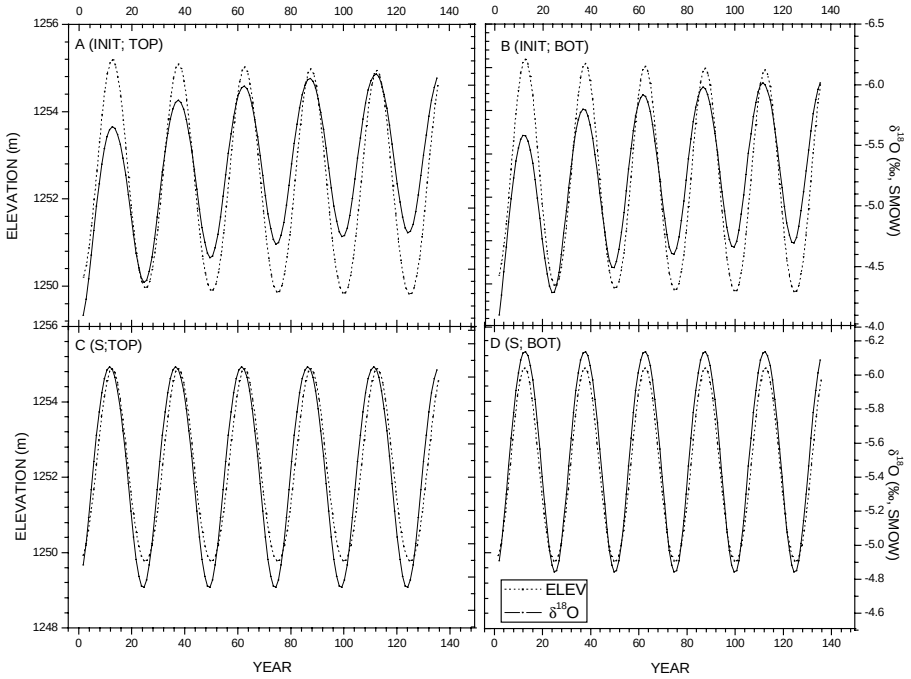

Figure 5-3. Oxygen isotopic responses to oscillatory changes in the Walker River discharge with a wavelength of 25-yr. A) Initial response of the top water. B) Initial response of the bottom water. C) Steady-state response of the top water. D) Steady-state response of the bottom water.

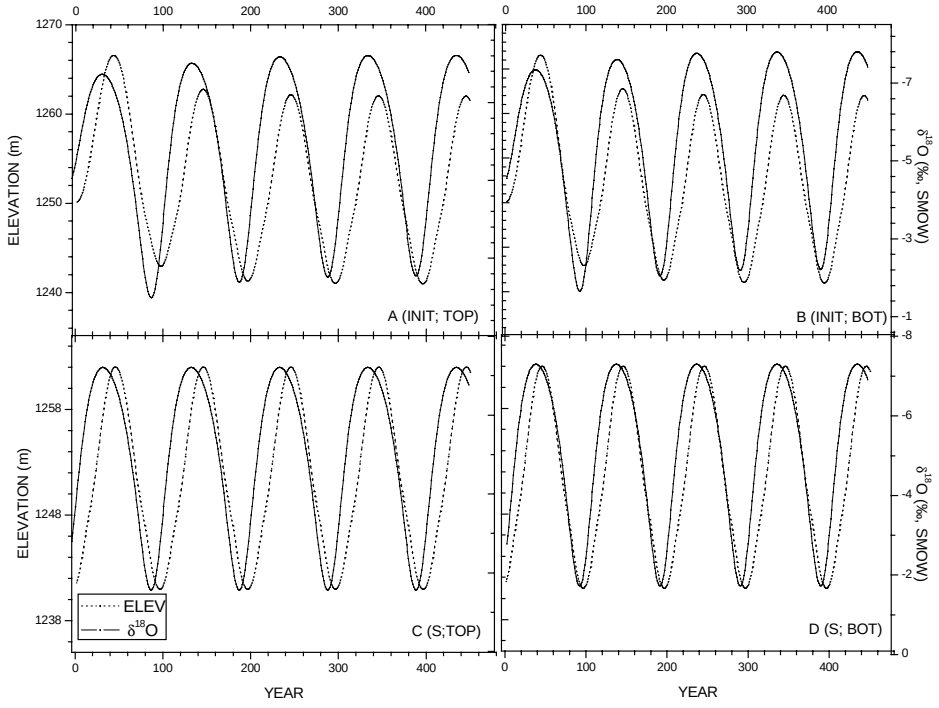

Figure 5-4. Oxygen isotopic responses to oscillatory changes in the Walker River discharge with a wavelength of 100-yr. A) Initial response of the top water. B) Initial response of the bottom water. C) Steady-state response of the top water. D) Steady-state response of the bottom water.

In Appendix 2 of this dissertation, I will discuss the isotopic relationship between lake water and river water, and suggested that the long-term average $\delta^{18}O_R$ can be inferred from the steady-state $\delta^{18}O_L$. In this section, the amplitude of variations in $\delta^{18}O_L$ that are induced by change in river discharge is addressed.

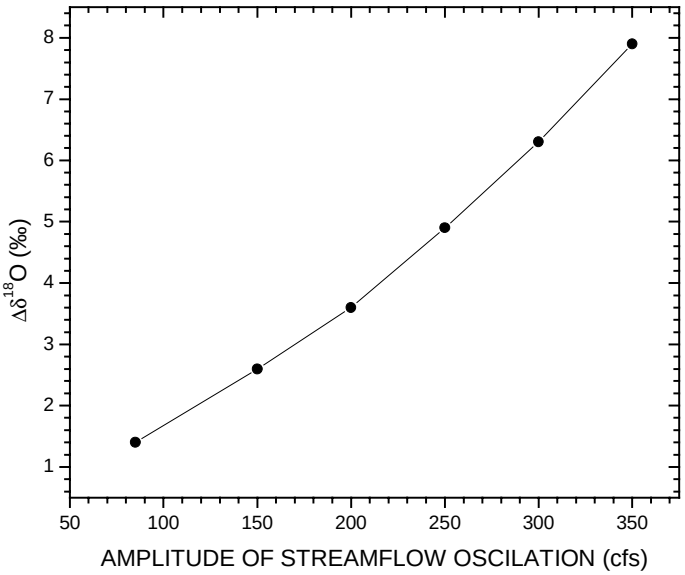

Figure 5-5. Relationship between the amplitude of oscillations in the $\delta^{18}O_w$ and the amplitude of fluctuations in the Walker River discharge.

The river discharge signal (function) can be decomposed into three components, the amplitude (A), the wavelength (λ) or frequency ($1/\lambda$), and the mean discharge value (M). The amplitude ($\Delta\delta^{18}O = \delta^{18}O_{max} - \delta^{18}O_{min}$) of variations in $\delta^{18}O_L$ increases in proportion to the amplitude of river discharge (Figure 5-5). However, it increases with the decrease in the mean value of river discharge (Figure 5-6), indicating that $\delta^{18}O_L$ is more sensitive when the lake is volumetrically smaller. The amplitude of variations in $\delta^{18}O_L$ is also in inverse proportion to the frequency of river flow signal (Figure 5-7). This means that the lower frequency component has larger spectral power. In addition, the amplitude of changes in river flow is positively correlated with the $\delta^{18}O_R$ (Figure 5-8).

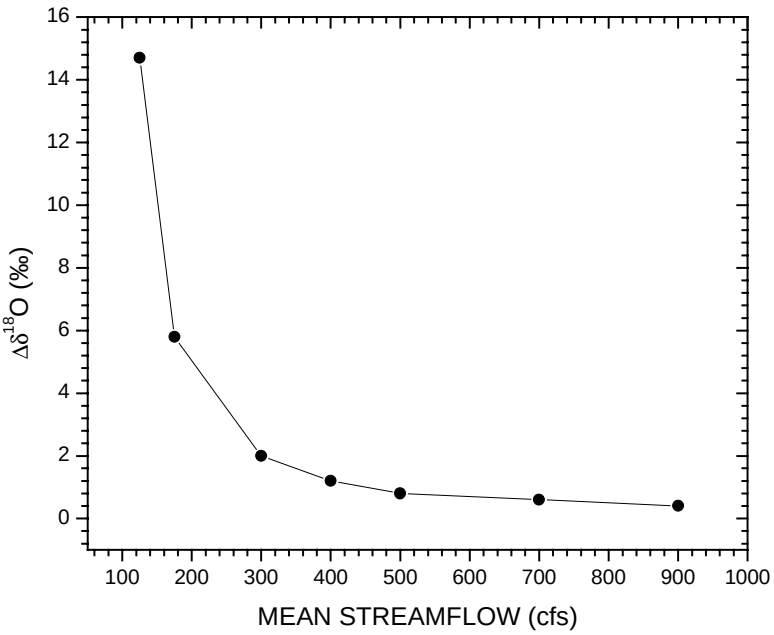

Figure 5-6. Relationship between the amplitude of oscillations in the $\delta^{18}O_L$ and the mean value of the Walker River discharge showing that the sensitivity of the $\delta^{18}O_L$ is exponentially proportional to the amount of stream flow when a lake becomes volumetrically small.

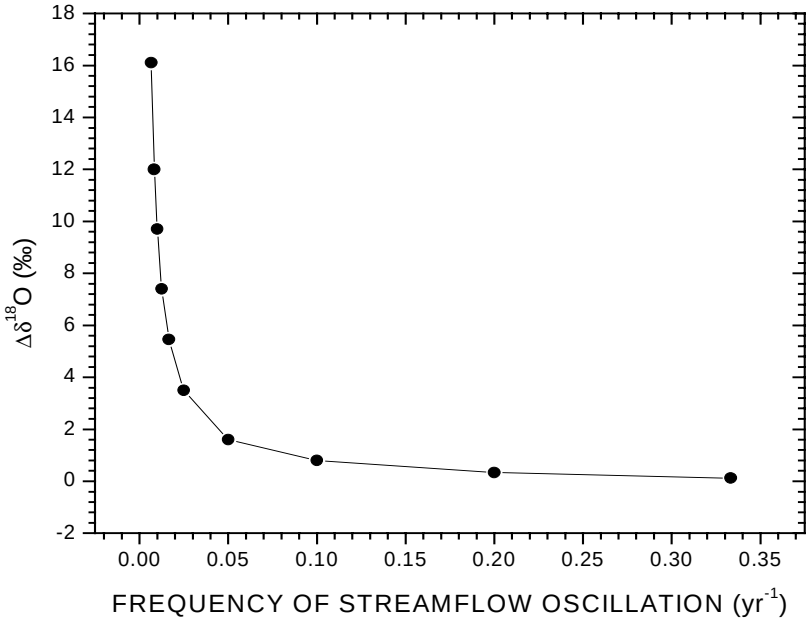

Figure 5-7. Relationship between the amplitude of oscillations in the $\delta^{18}O_L$and the frequency component of oscillations in the Walker River discharge showing that the sensitivity of the $\delta^{18}O_L$ becomes exponentially large for lower frequency climatic forcing.

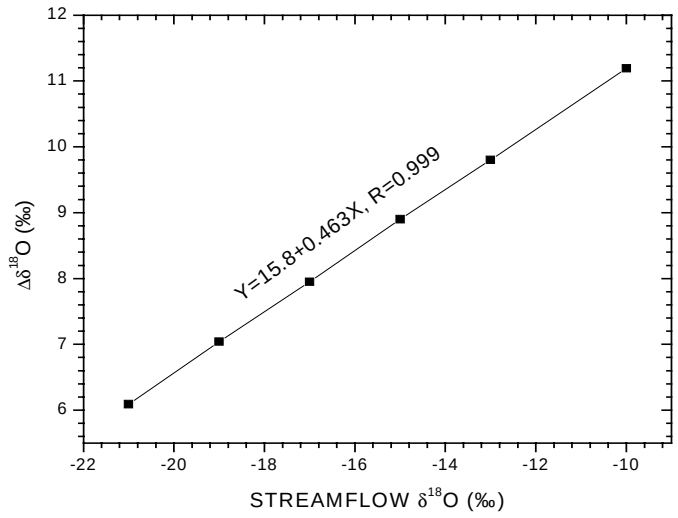

Figure 5-8. Relationship between the amplitude of oscillations in the $\delta^{18}O_L$ and the $\delta^{18}O_R$ value of the Walker River discharge showing that the sensitivity of the $\delta^{18}O_L$ is positively correlated with the value of $\delta^{18}O_R$.

In summary, changes in river discharge will lead to fluctuations in the $\delta^{18}O_L$ at different timescales, such as interannual, interdecadal, and centennial timescales. Most frequencies of variations in river discharge are reflected in the $\delta^{18}O_L$ and thereby $\delta^{18}O_C$ record and only slight changes are noticeable. The lower frequency component of the river flow signal tends to have higher spectral power in affecting the $\delta^{18}O_L$. This is consistent with observation from spectral analysis that lower frequency geophysical signal usually has larger spectral power.

5.4 Age model revision

The chronology of core WLC002 derived and presented in Chapter 4 is mainly based on nine AMS radiocarbon dates. Because of large uncertainty in conversion from radiocarbon dates to calendar ages (especially for those relatively young dates), here I use Table 1 and 2 in Stuiver et al. (1998) to reinterpret the radiocarbon dates and try to get their best probable calendar ages (Table 5-1). LH-2 in Figure 5-9 denotes the interval of interest from AD 800 to 1900, based on the age model presented in this figure. In chapter 4, it has been noted that the $\delta^{18}O$ record of Walker Lake has a great deal of similarity with the tree-ring-based Sacrament flow data over the last 1200 years. This similarity is not unexpected because both the Walker River and the Sacramento River receive water originating from the

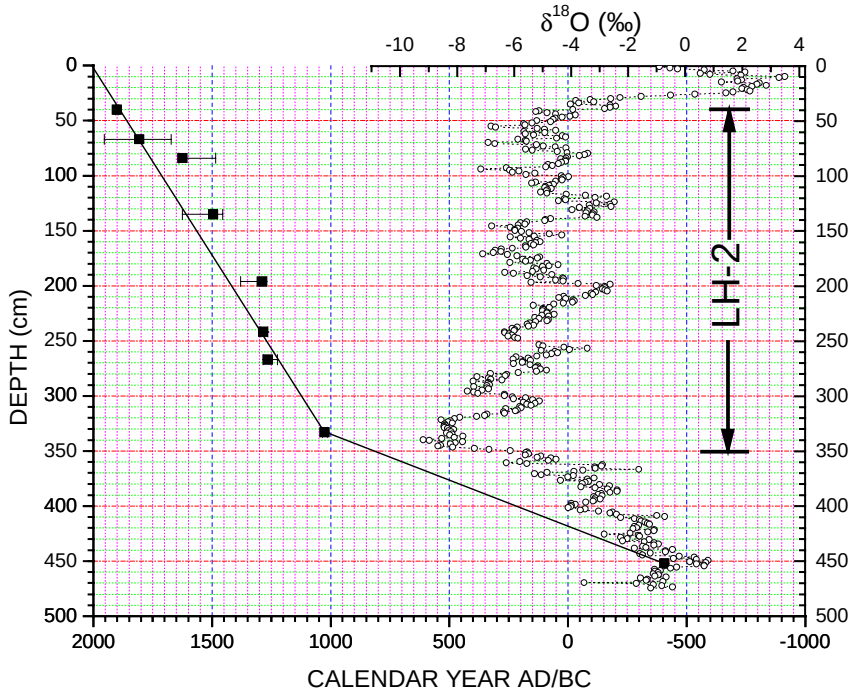

Figure 5-9 Plots of revised age model and original $\delta^{18}O$ results from Walker Lake. LH-2 denotes the interval of interest (AD 800 to 1900) according to this new age model.

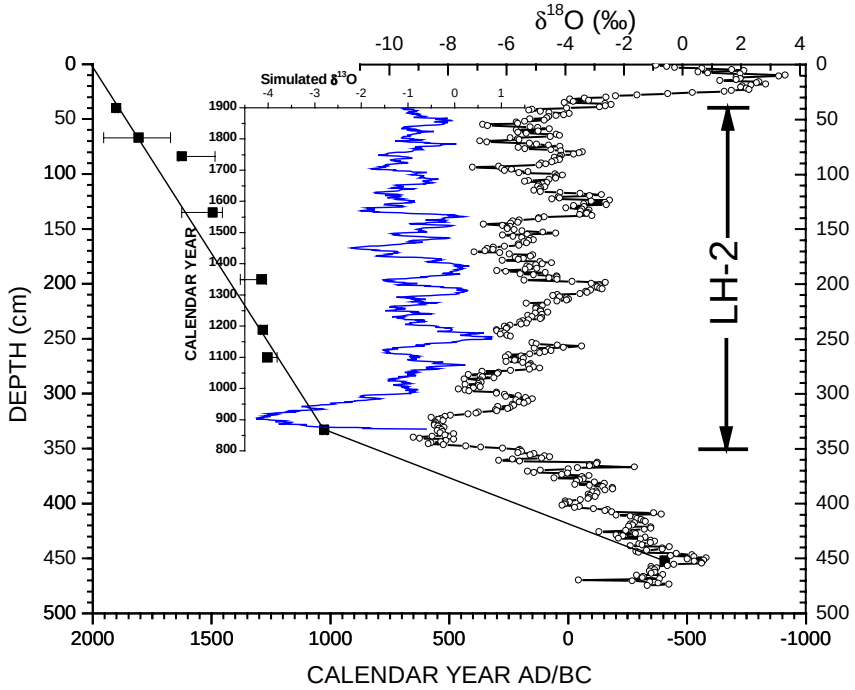

Figure 5-10 Plots of revised age model, original and simulated $\delta^{18}O$ results from Walker Lake. Embedded graph is a chronology of simulated $\delta^{18}O_L$ results of Walker Lake using the scaled Walker River flow data according to the tree-ring-based Sacramento River flow record (MEKO et al., 2001) and a hydrologic-isotopic model-HIBAL (BENSON and PAILLET, 2002).

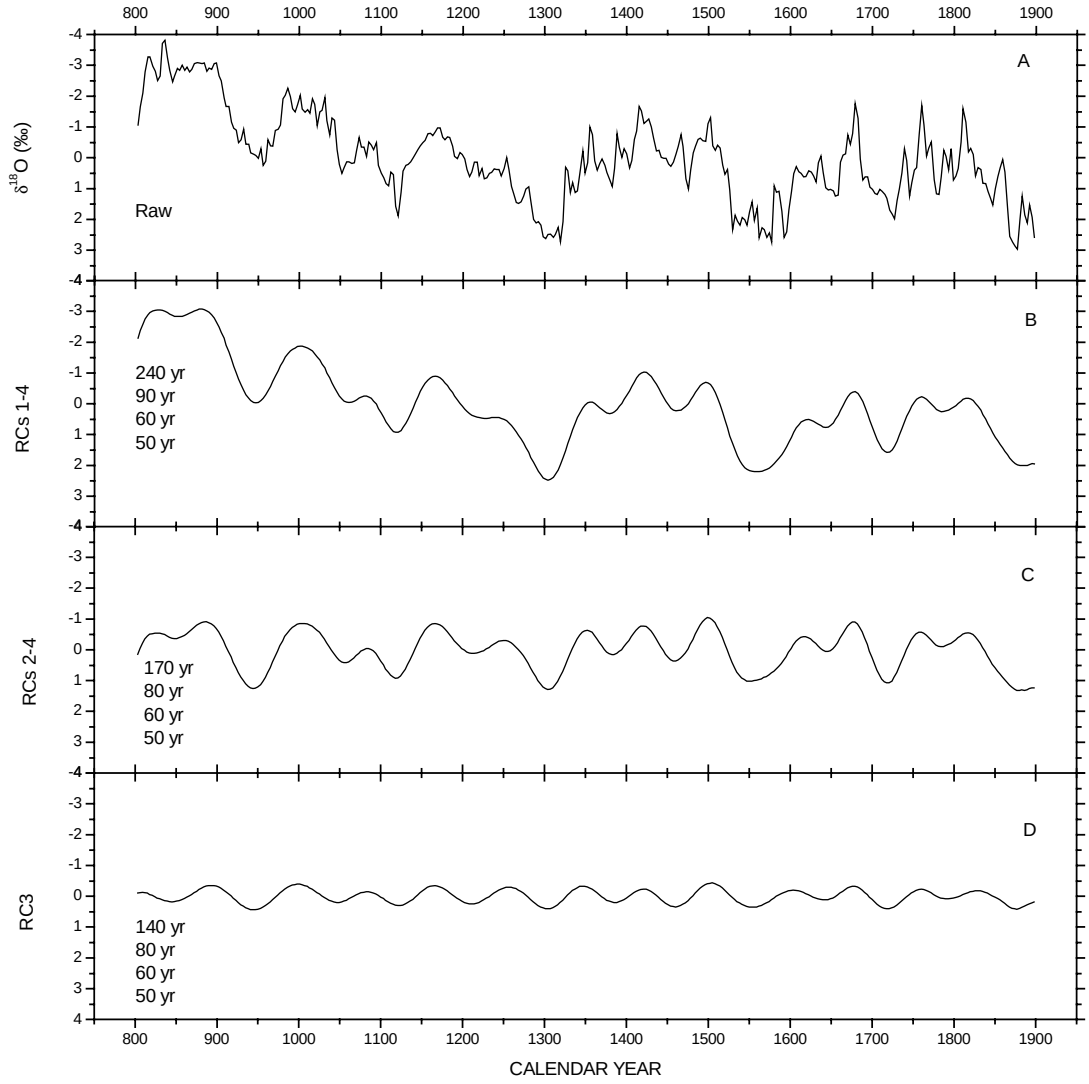

Figure 5-11. Singular spectrum analysis (SSA) (DETTINGER et al., 1995; VAUTARD and GHIL, 1989) on time series from Walker Lake for the intervals from 800 to 1900AD. A: Raw centered $\delta^{18}O_C$ record of bulk inorganic carbonate sediments. B: First four reconstructed components (RCs 1-4) derived from SSA. A cubic spline is used to extract the $\delta^{18}O_C$ data every 3-yr prior to SSA and SSA is implemented using the SSA-MTM Toolkit 4.1 (DETTINGER et al., 1995; GHIL et al., 2002). Window length N is 36. The first four RCs together account for 89% of total variance and have significant frequency lines of 240, 90, 60, and 50 yr. These frequency lines are detected using MultiTaper method (MTM) (PARK et al., 1987; PERCIVAL and WALDEN, 1993; THOMSON, 1982). C: The second to fourth reconstructed components (RCs 2-4) of SSA representing 27% of total variance and having dominant periodicities of 170, 80, 60, and 50 yr. D. The third reconstructed component (RC 3) accounting for 6.8 % of total variance and having dominant cyclicities of 140, 80, 60, and 50 yr.

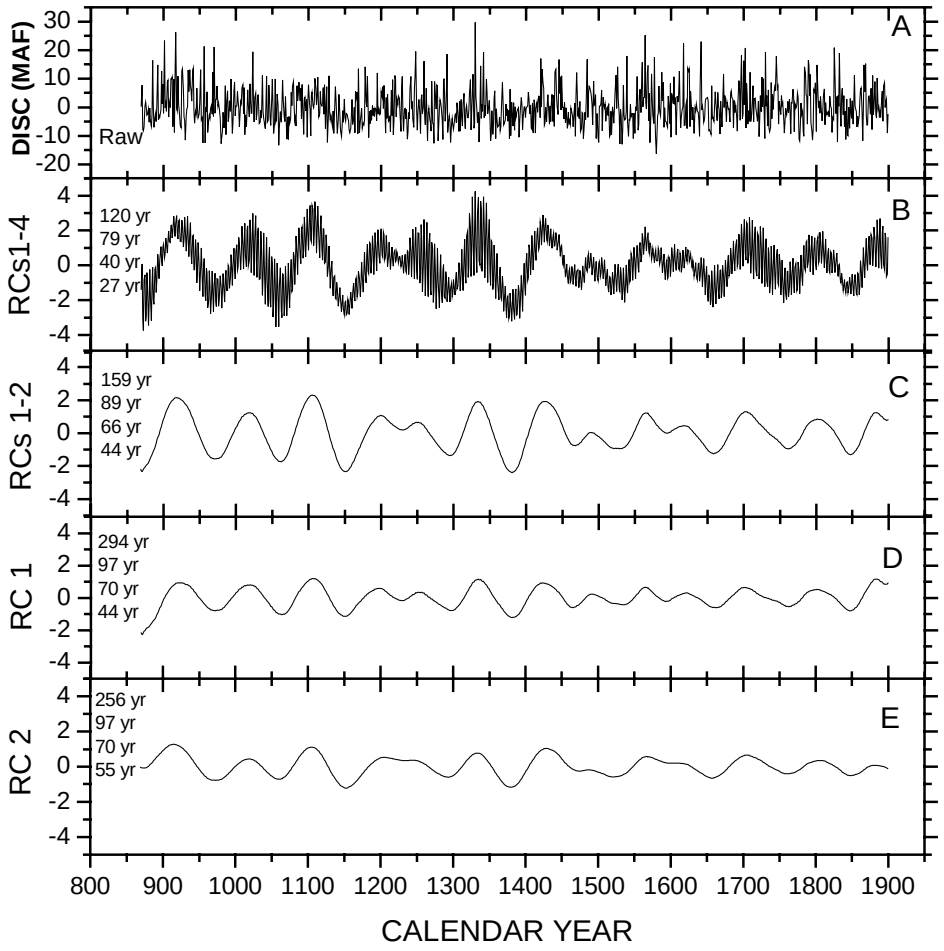

Figure 5-12. Singular spectrum analysis (SSA) (DETTINGER et al., 1995; VAUTARD and GHIL, 1989) on time series of the tree-ring based Sacramento River for the intervals from AD 869 to 1900. A: Centered river flow record (MEKO et al., 2001). MAF denotes million acre feet. B: First four reconstructed components (RCs 1-4) derived from SSA. SSA is implemented using the SSA-MTM Toolkit 4.1 (DETTINGER et al., 1995; GHIL et al., 2002). Window length N is 103. The first four RCs together account for 7.0 % of total variance and have significant frequency lines of 120, 79, 40, and 27 yr. These frequency lines are detected using MultiTaper method (MTM) (PARK et al., 1987; PERCIVAL and WALDEN, 1993; THOMSON, 1982). C: The first two reconstructed components (RCs 1-2) of SSA representing 3.6% of total variance and having dominant periodicities of 159, 89, 66, and 44 yr. D. The first reconstructed component (RC 1) accounting for 1.85 % of total variance and having dominant cyclicities of 294, 97, 70, and 44 yr. E. The second reconstructed component (RC 2) accounting for 1.77% of total variance and having dominant periodicities of 256, 97, 70, and 50 yr.

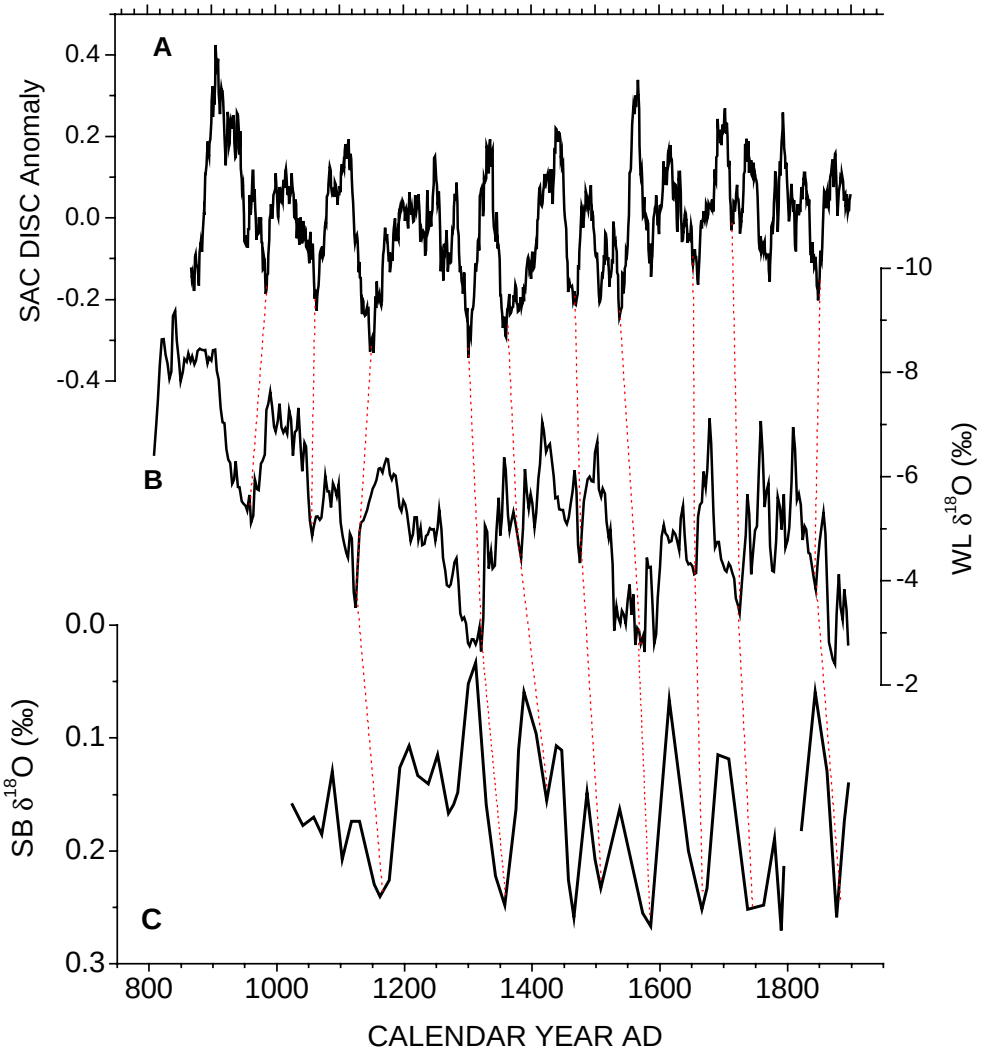

Figure 5-13 Comparison of the tree-ring reconstructed Sacramento River flow (MEKO et al., 2001), Walker Lake $\delta^{18}O$, and Santa Barbara $\delta^{18}O$ records (FIELD and BAUMGARTNER, 2000). The Sacramento discharge anomaly (upper panel: A) is calculated using the reconstructed river flow data and the Santa Barbara $\delta^{18}O$ record (lower panel C) is Lowess smoothing (f=0.04) of average *N. dutertrei* $\delta^{18}O$ values (see Figure 7b in Field and Baumgartner, 2000).

Although the variance concentrations detected from the Walker Lake $\delta^{18}O$, the Sacramento River discharge, and the Santa Barbara $\delta^{18}O$ records are not exactly the same, most of them are within 50-70 yr, the most energetic periodicities of PDO-related climate variability (MINOBE, 1997). The fact that these two proxy records in the Sierra regions are almost in phase with fluctuations in the California Current suggests that the climate of the Sierra is linked the dynamics of the Pacific Ocean. During the

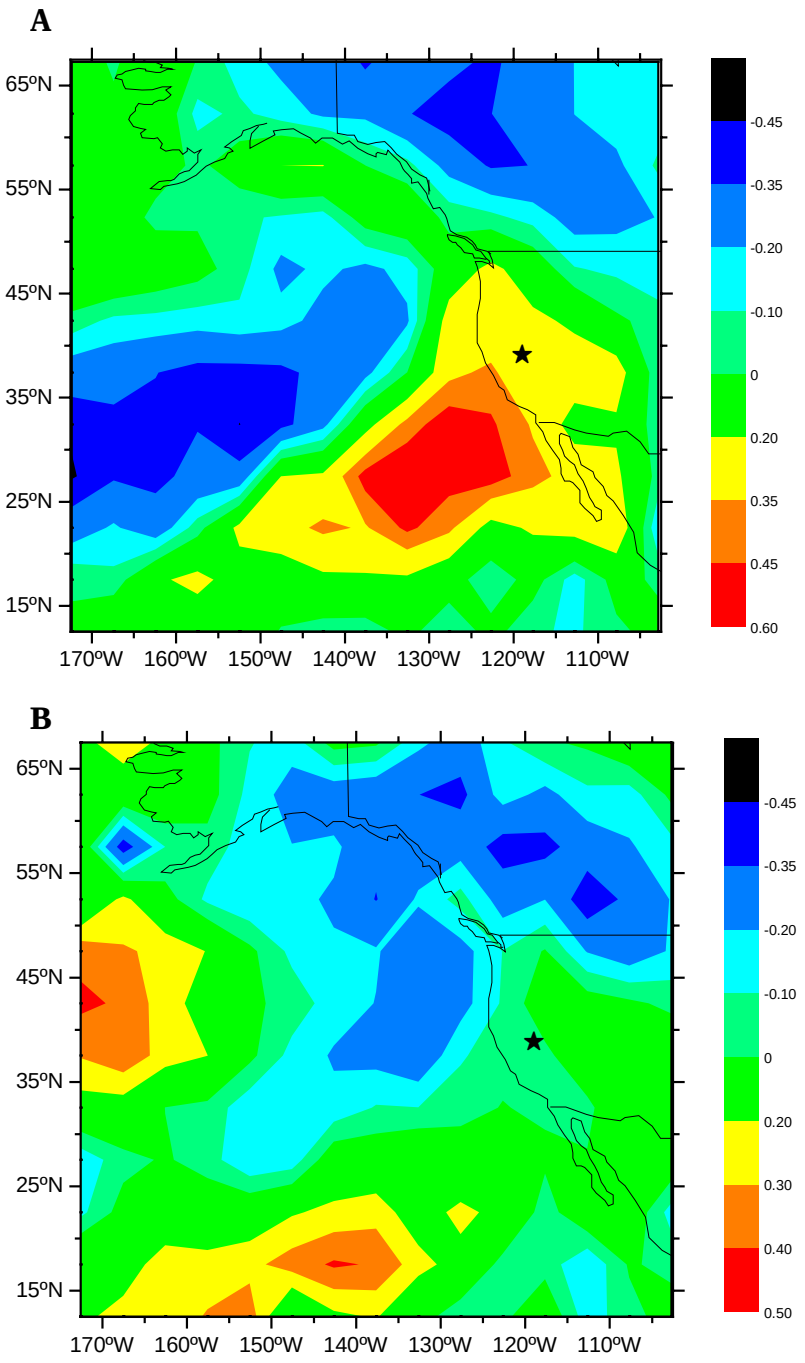

Figure 5-14 Regression analysis of the winter mean (January, February, and March) 5°x5°surface temperature (HadCRUTv dataset) against the West Walker River discharge during the positive PDO phase of 1978 to 2000 (A) and the negative PDO phase of 1948-1977 (B). Stars denote the geographical location of the Walker Lake Basin.

cores, marine and lacustrine sediments. For examples, the ^{14}C record from tree rings shows a pronounced 126-yr peak in the past 4000 years (STUIVER and BRAZIUNAS, 1993). A 2100-yr lake sediment-based salinity record from Rice Lake, a closed-basin lake in the northern Great Plains exhibits significant periodicities of 400, 200, 130 and 100 yr (YU and ITO, 1999).

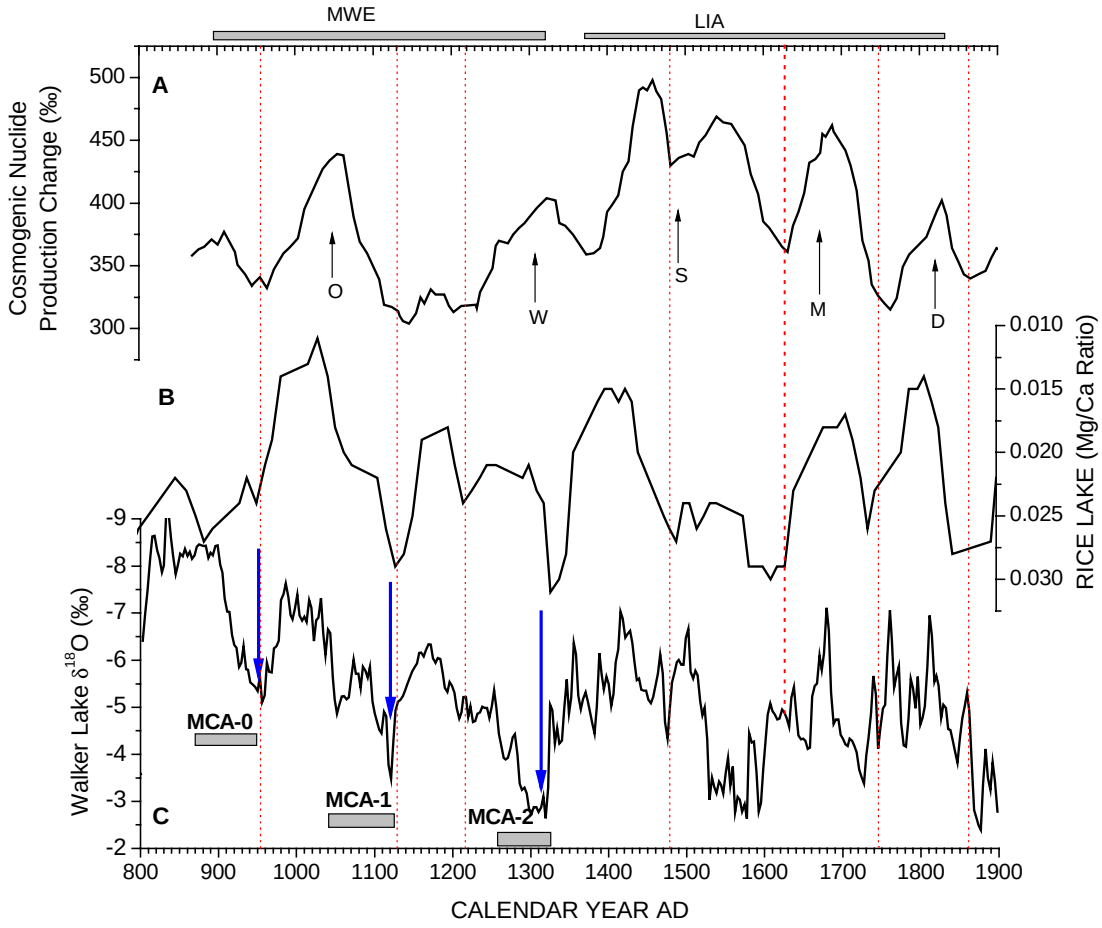

Figure 5-15. Correlation of paleoclimate and paleo-solar proxies. A) The record of the cosmogenic nuclide production changes (BARD et al., 2000; BARD et al., 2003). B) Mg/Ca molar ratio record from Rice Lake (YU and ITO, 1999). C) The $\delta^{18}O_C$ record of Walker Lake. Minima of solar activity: D-Dalton (1810 AD), M-Maunder (1645-1715), S-Spörer (1420-1530), W-Wolf (1280-1340), and O-Oort (1010-1050) (BARD et al., 2000; EDDY, 1976). MWE-Medieval Warm Epoch, LIA-Little Ice Age. Vertical dotted lines denote probable correlations among these records and three major arrows symbolize terminations of three major droughts that occurred during the MWE. MCA-Medieval Climate Anomaly. Note that MCA-1 (AD910-1110) and MCA-2 (AD 1210-1350) were previously proposed by Stine (1994).

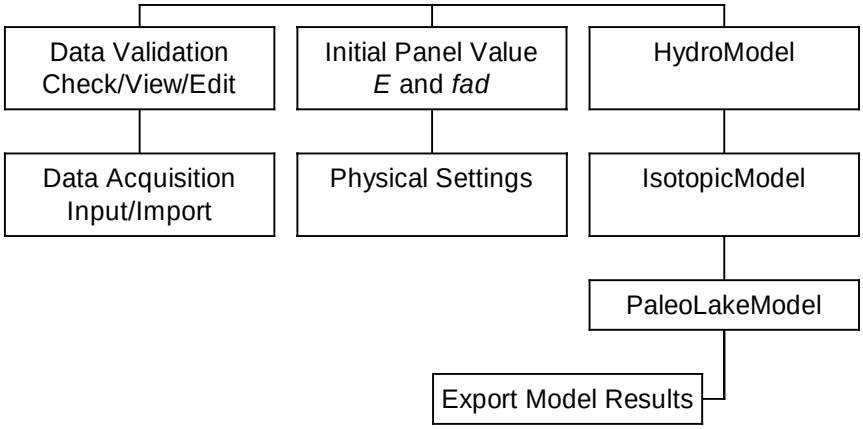

Fig. A1-1. A block diagram lists the major modules or components of the program. The left column functions as data acquisitions and validations. The middle column consists of two components; the physical settings (such as lake geometry) and tuning parameters (such as model parameters and model interval of interest). The right column includes three key modules plus a data export module.

A1.3.1 Data acquisition and validation

The model assumes that the following aspects of information are available; the lake geometry, the historic lake surface levels, daily stream gauge readings, the $\delta^{18}O$ of stream and lake water, the $\delta^{18}O$ record of lake carbonate sediments, and its corresponding age control. Usually, hydrologic models use polynomial equations to define the relationships between surface area, volume and lake water depth (BENSON and PAILLET, 2002). Instead, this program applies the spline interpolation technique to get the corresponding value. In the Data submenu, the program gives a graphic interface to compare the spline curve with that measured.

The record of historic stream gauge readings is the primary input variable for the hydrologic and isotopic mass balance modeling modules. This program uses the daily stream flow readings. The unit is in cubic feet per second (cfs). In the case of multiple stream inputs into the same lake, the sum of these stream gauge readings is applied.

The historic lake surface level (elevation) record is used as key references for hydrologic mass balance and paleolake level recovery modeling modules. In the hydrologic mass balance module the model uses this record as a baseline to determine the mean annual evaporation rate, while in the

(*f*) stands for the fraction of water that actually flows into the lake of interest since there maybe some water loss between the gauge station and the lake inlet. The isotopic and dynamic parameter settings are designed for the isotopic mass balance and paleolake level recovery models, which are not visible at the first stage of modeling, i.e. the HydroModel. The $\delta^{18}O$ of free air vapor, on-lake precipitation, and stream water need to be clear. For those lakes with multiple stream inlets, the stream $\delta^{18}O$ value should be the weighted average. α_{kin} is the kinetic fractionation factor, and the mean annual surface temperature, precipitation and relative humidity (*RH*) can be obtained from the local weather station. These values are stored in the same database file of the input dataset.

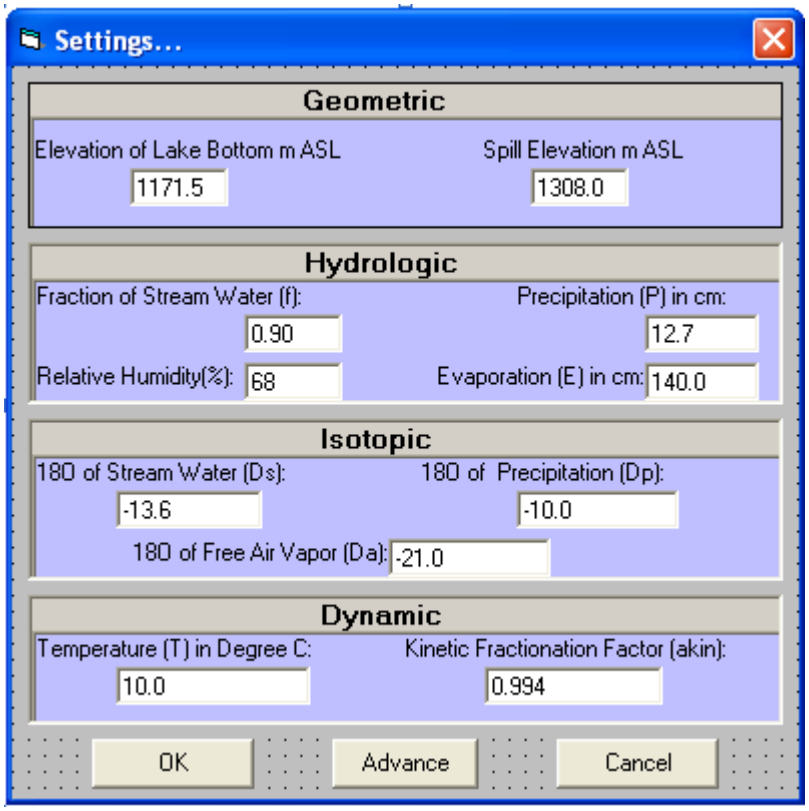

Figure A1-2. A model parameter settings panel consists of four categories: geometric, hydrologic, isotopic, and dynamic settings.

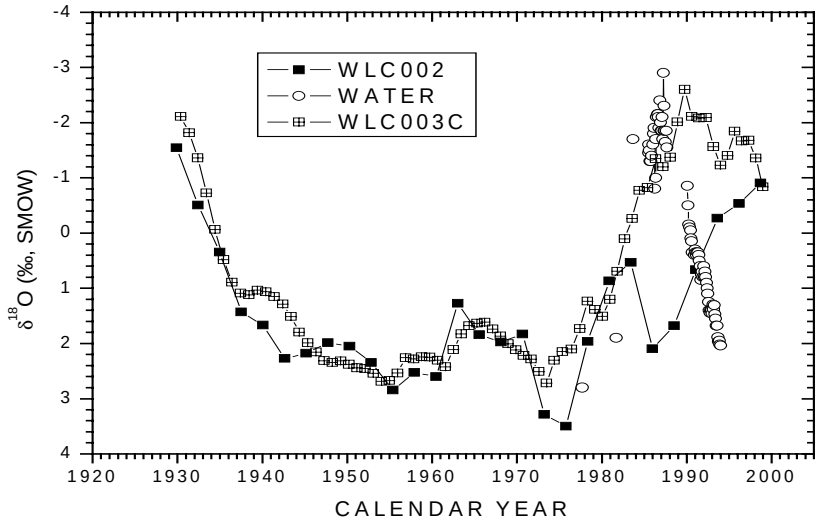

Figure A2-1. Comparison of measured and computed $\delta^{18}O_L$ records for Walker Lake. The measured $\delta^{18}O_L$ data were taken from Benson et al. (2002). Grossman and Ku's (1986) equation was used to compute corresponding $\delta^{18}O_L$ value for WLC002 and WLB-003C, assuming T= 22 ºC. The computed $\delta^{18}O_L$ values were smoothed by the 6-point running average. Discrepancies among these records appear to be induced by the uncertainties of ages and possible minor loss at the top of WLC002.

A2.4.2 River Flow $\delta^{18}O_R$

The $\delta^{18}O_R$ value probably is the key to reconstruction of variations in lake level. Results of direct measurements for water samples collected at Wabuska gauging station indicate that the $\delta^{18}O_R$ varies from –14.85 to –12.25 (‰, SMOW) with an average of 13.6 ‰, SMOW (see Figure 2-10). The $\delta^{18}O_R$ value observed may not be representative of that in prehistoric times since agricultural irrigation has the potential to increase the $\delta^{18}O_R$ value of stream water. Besides, the Walker River is fed by headwaters originating from the Sierra Nevada snowpack. Variations in the $\delta^{18}O$ value of the Sierra Nevada snowpack during the past few thousand years remain unknown. However, the ice $\delta^{18}O$ record from Kilimanjaro in tropical Africa (THOMPSON et al., 2002) reveals that the ice $\delta^{18}O$ at this location fluctuated within –10 ± 2 (‰) over the last two thousand years. The modern (1991-1992) ice $\delta^{18}O$ record from Guliya, China (THOMPSON, 1996) also indicates large variations (-20 to –8 ‰) in ice isotopic composition.

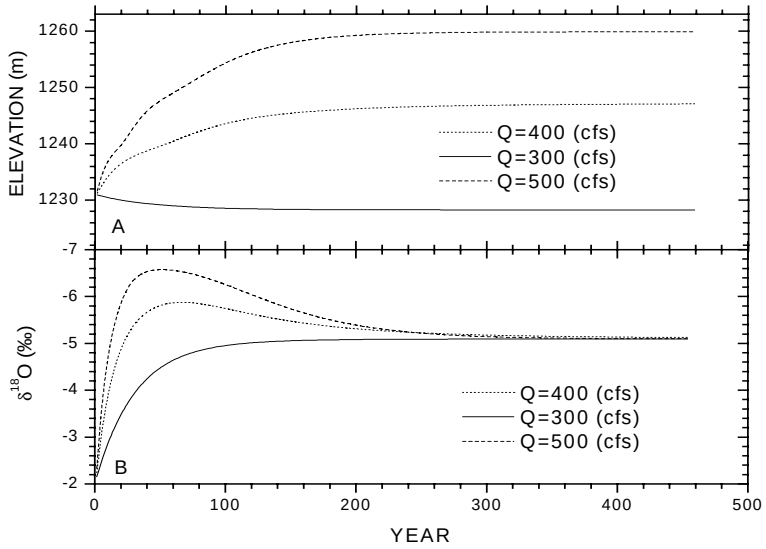

Figure A2-2. A) Response of lake level elevation to change in river discharge of the Walker River. B) Response of $\delta^{18}O_L$ to change in river discharge of the Walker River using a published hydrologic-isotopic model - HIBAL (BENSON and PAILLET, 2002). HIBAL simulations, using parameter values taken from the results of measurements in Pyramid Lake (BENSON et al., 2002), suggest that the steady-state $\delta^{18}O_L$ value is independent of the amount of river discharge of the Walker River.

To estimate the average $\delta^{18}O_R$ values of the past, the condition of steady-state is assumed. When stream discharge is held constant, a closed-basin lake level will ultimately reach a hydrologic steady state, a state without significant variations in lake level (Figure A2-2A). Moreover, when a lake maintains closed-basin conditions and stream flow is kept constant, it will achieve an isotopic steady state and its steady-state $\delta^{18}O_L$ value is independent of the amount of stream discharge (Figure A2-2B). In fact, the steady-state $\delta^{18}O_L$ value is positively correlated with the $\delta^{18}O_R$ value (Figure A2-3A) and negatively correlated with f_{ad} (Figure A2-3B). Further modeling experiments indicate that the steady-state $\delta^{18}O_L$ value is also independent of initial conditions (lake level and $\delta^{18}O_L$). However, the time to achieve a hydrologic-isotopic steady state is determined by the difference between initial and steady-state values of lake level and $\delta^{18}O_L$ as well as lake basin shape. Variations in both $\delta^{18}O_R$ and the amount of stream water affect the $\delta^{18}O_L$ value. Although detailed variations in $\delta^{18}O_R$ of the past remains largely

unknown, the $\delta^{18}O_C$ record preserved in down-core carbonate sediments may be used to determine a long-term average $\delta^{18}O_R$ value of the past.

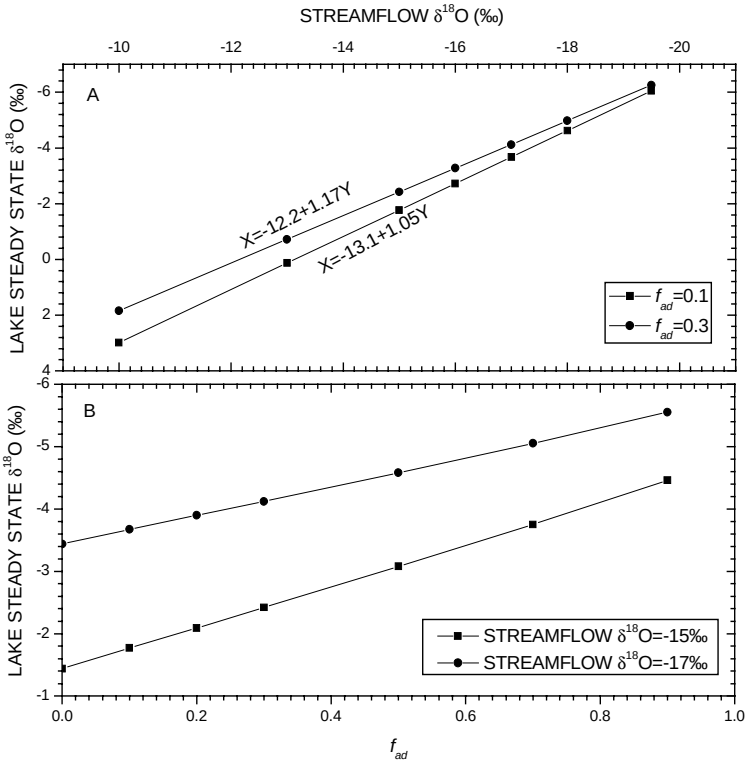

Figure A2-3. A) Linear correlation between steady-state $\delta^{18}O_L$ and $\delta^{18}O_R$. f_{ad} is the fraction of advected air in the thin boundary layer overlying the water surface of the lake. B) Correlation between steady-state $\delta^{18}O_L$ and f_{ad} based on HIBAL simulations.

A2.4.3 Model Parameters

A number of meteorological parameters (surface water temperature, on-lake precipitation, evaporation, relative humidity, f_{ad}, wind speed, etc) affect the oxygen and hydrogen isotopic distribution in an aquatic system. Most of these parameter values are taken from the measured data from Pyramid Lake obtained by Benson and Paillet (2002). The surface water temperature affects isotopic fractionation both between water vapor and surface water (T=14.2ºC) and between carbonate precipitates and host water (T=22ºC)[17]. Evaporation and on-lake precipitation rates are 135 and 12.5 cm yr^{-1}, respectively.

[17] Carbonate precipitation usually occurs in late summer and early fall while water evaporation occurs perennially. Annual mean temperature value is taken from measured data from Pyramid Lake [*Benson and Paillet*, 2002].

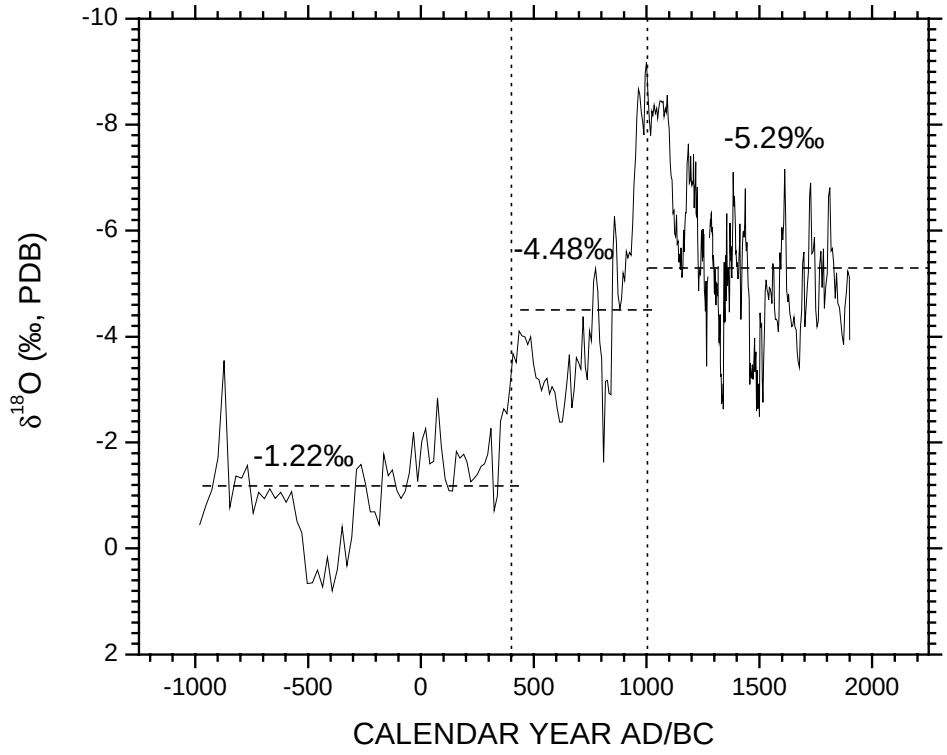

Figure A2-4. The TIC $\delta^{18}O_C$ record from Walker Lake divided into three stages with distinctive average $\delta^{18}O_C$ values. These isotopic values are used to infer $\delta^{18}O_R$ in corresponding stages.

Table A2-1 Input data and parameter values for reconstruction of the Walker Lake levels during the past 3,000 years

Input Data		Interval A (1000BC-400AD)	Interval B (400AD-1000AD)	Interval C (1000-1900AD)
$\delta^{18}O$	Carbonates[19] (‰, PDB)	-1.22	-4.48	-5.29
	Steam Water[20] (‰, SMOW)	-14.4	-17.8	-18.7
Parameters	f_{ad}	0.1	0.1	0.1
	RH (%)	53	53	53
	T (°C)	14.2	14.2	14.2
	E (cm yr^{-1})	135	135	135
	P (cm yr^{-1})	12.5	12.5	12.5

[19] Average $\delta^{18}O$ values indicated in Figure 5-4.

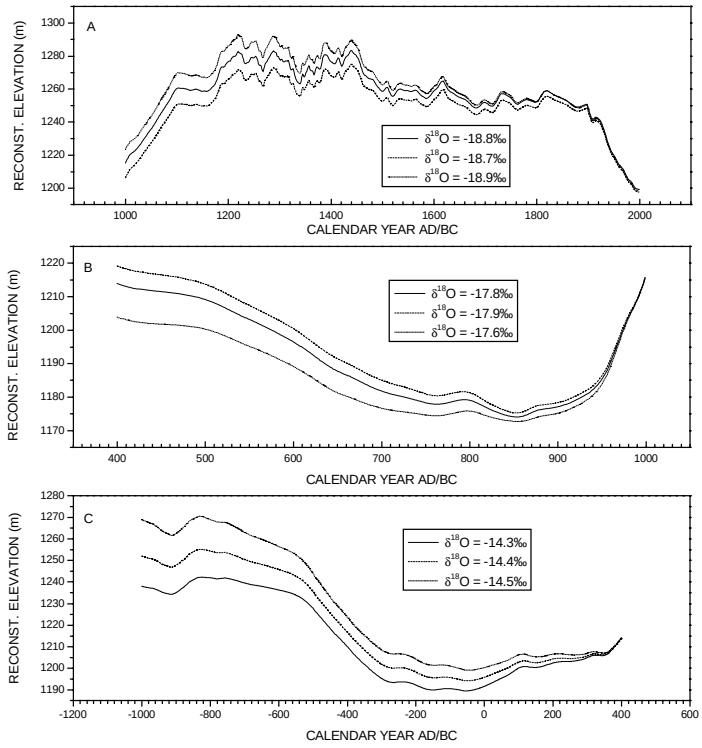

Figure A2-5. A) Reconstructed lake level elevation of Walker Lake for the period of 1000 to 2000AD using the reconstruction model and the inferred LTM value of $\delta^{18}O_R$. B) Reconstructed lake level elevation of Walker Lake for the period of 400 to 1000AD using the reconstruction model and the inferred LTM value of $\delta^{18}O_R$. C) Reconstructed lake level elevation of Walker Lake for the period of 1000BC to 400AD using the reconstruction model and the inferred LTM value of $\delta^{18}O_R$.

A2.6 Validation

A2.6.1 Walker River Discharge

Change in lake level of a closed-basin lake is a function of the amount of river discharge, evaporation, and on-lake precipitation. Change in lake level of Walker Lake can be simulated by assuming fixed mean annual values of evaporation (1.35 m) and on-lake precipitation (0.125 m). The Walker River discharge can also be estimated based on changes in lake elevation. On the basis of the reconstructed lake level record, continuous river discharge record for the Walker River is reconstructed (Figure A2-6A), assuming constant rates of on-lake precipitation and evaporation over the late Holocene. In Walker Lake, a continuous annual river flow record of the Walker River back to 1944 and a lake level record of Walker Lake back to 1861 have been documented (USGS). A 9-point-average historical river

flow[21] of the Walker River is consistent in general with that calculated from the reconstructed lake elevation record (Figure A2-6B).

The tree-ring based river flow record of the Sacramento River is compared with the $\delta^{18}O_C$-based river flow record of the Walker River (Figure A2-7). The intervals that show apparent correlation between these two reconstructed river flow records are not unexpected as historical stream flow records on both sides of the Sierra Nevada exhibit strong positive correlation (BENSON et al., 2002). However, the $\delta^{18}O_C$-based river flow record of the Walker River clearly indicates that the climate in this region was relatively wet during the MWE relative to the LIA. This feature is opposite to the tree-ring based river flow record of the Sacramento River.

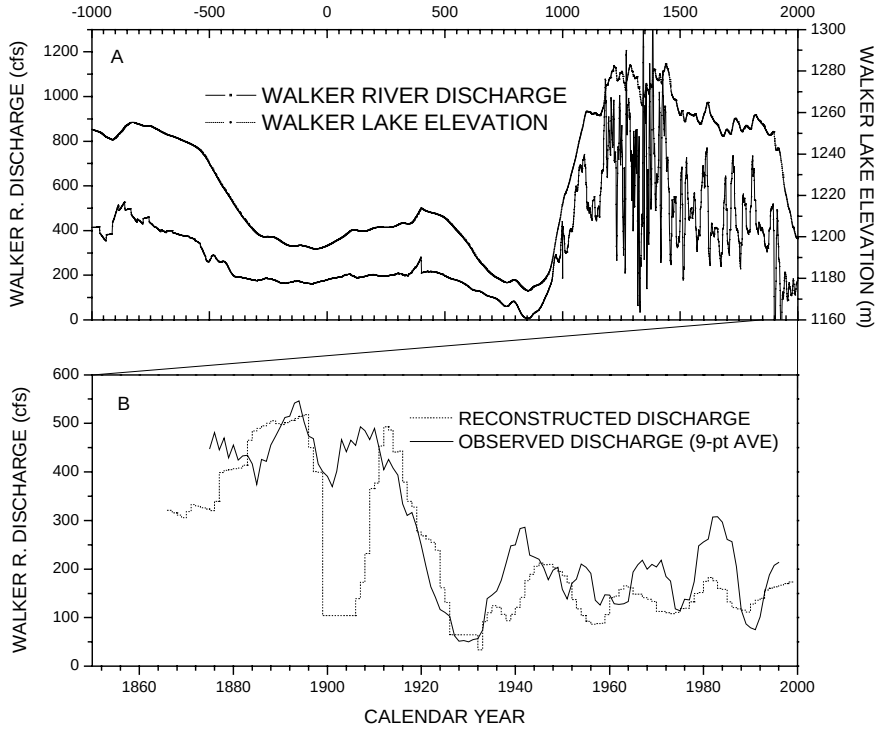

Figure A2-6. A) Reconstructed lake level elevation of Walker Lake and stream discharge of the Walker River during the late Holocene (3,000). B) Comparison of reconstructed and observed river discharge (USGS) records of the Walker River during the historic interval (1860-2000).

[21] River flow record was taken from Milne's (1987) for the interval of 1871 though 1920 and from USGS statistic data for the interval of 1921 through 2000.

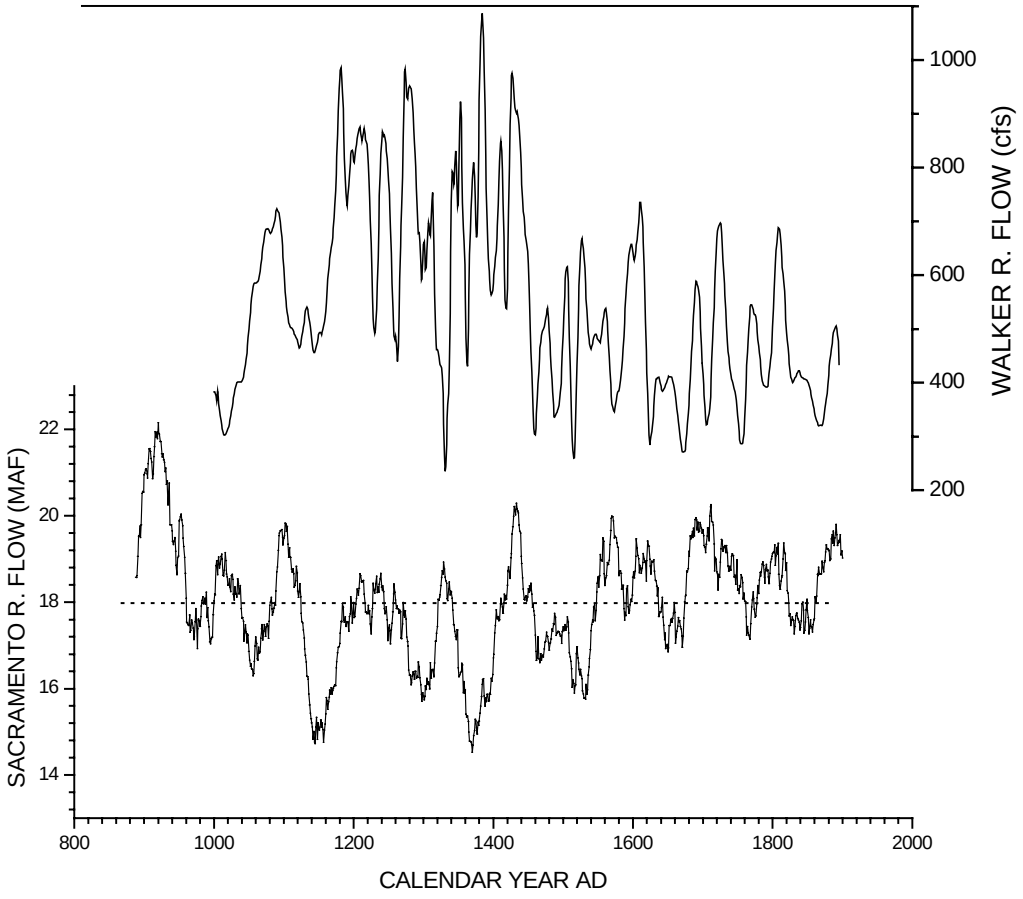

Figure A2-7. Comparing the reconstructed river flow record of the Walker River with the tree-ring based river flow record of the Sacramento River.

A2.6.2 Oxygen Isotopes

The reconstructed lake level record of Walker Lake is produced through the approach described in section A2.3, in which the model assumes that the lake is isotopically homogeneous. In fact, most closed-basin lakes, including Walker Lake, are limnologically stratified in summer and early fall and overturned in winter and early spring. However, isotopic modeling experiments indicate that the thermal-structure of the lake affects the $\delta^{18}O_L$ value only on yearly timescales (see Chapter 2). To validate the results produced by the reconstruction model, HIBAL is used to generate a $\delta^{18}O_M$ record of the lake carbonate using the reconstructed stream flow record of the Walker River.

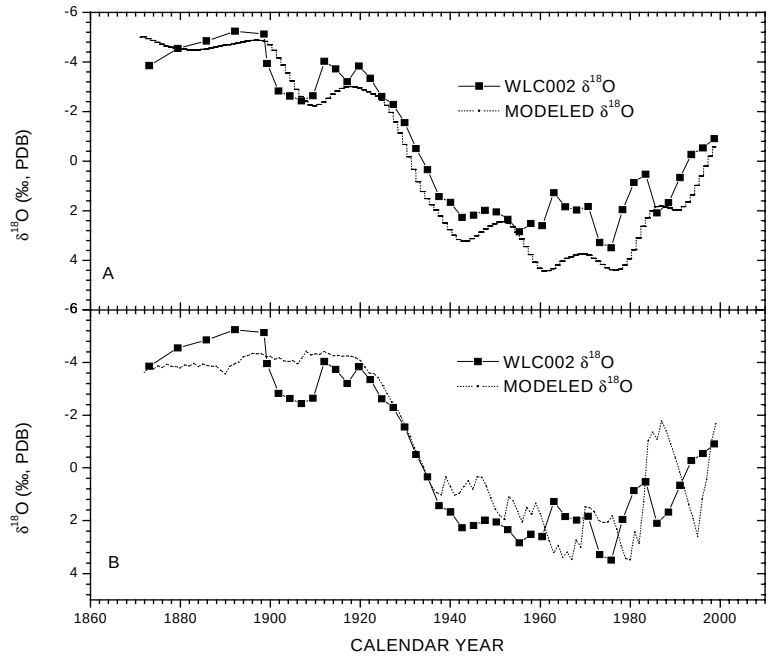

Figure A2-8. A) Comparing the HIBAL $\delta^{18}O_M$ record with the measured down-core TIC $\delta^{18}O_C$ record based on the reconstructed river flow of the Walker River. B) Comparing the HIBAL model-derived $\delta^{18}O$ record with the measured down-core TIC $\delta^{18}O_C$ record based on the measured river flow of the Walker River.

Because HIBAL requires lunar monthly meteorological and limnological parameter data, the results of measurements of these parameters from Pyramid Lake listed in Table 2-1 were used. The $\delta^{18}O_M$ record is generated separately due to substantial variations in LTM $\delta^{18}O_R$ values of the Walker River water, using fixed mean annual values of evaporation (1.35 m), on-lake precipitation (0.125 m), and f_{ad} (0.1). In the historical (1870-2000) interval, the Walker River probably experienced large changes in the $\delta^{18}O_R$ value. The mean value of $\delta^{18}O_R$ measured in a period of 1985 through 1994 is –13.6 ‰ (SMOW) and may be not representative of the historical $\delta^{18}O_R$ values of the Walker River since the results from running HIBAL suggest that the $\delta^{18}O_M$ values of the historical interval would reach ~10 ‰, (PDB) if a –13.6 (‰) value of $\delta^{18}O_R$ was assigned. Using the same $\delta^{18}O_R$ value (-18.7 ‰) of river flow that is assigned for lake level reconstruction for the last 1000 years, two $\delta^{18}O$ curves were generated using the reconstructed and actual river flow records (Figure A2-8A and Figure A2-8B). Both

$\delta^{18}O_M$ curves are in good agreement with the $\delta^{18}O_C$ record extracted from down-core (WLC-002) carbonate sediments. In addition, the HIBAL $\delta^{18}O_M$ results derived from the actual river flow data (USGS) captures two negative $\delta^{18}O$ excursions that occurred in the El Niño wet years of 1982/83 and 1997/98.

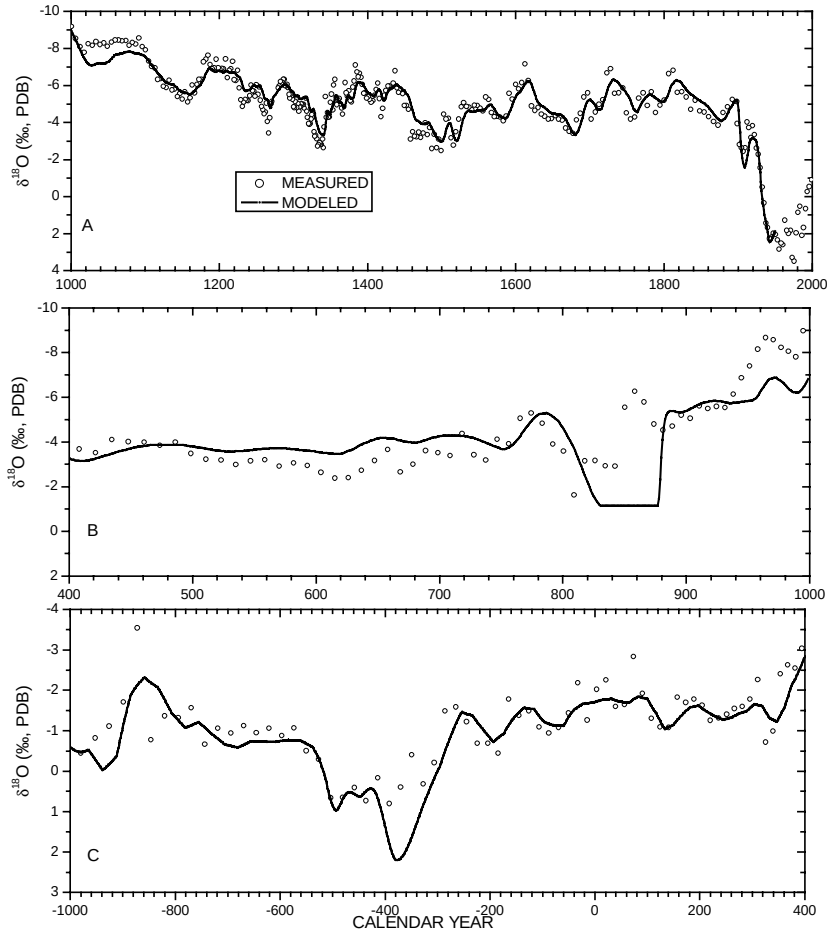

Figure A2-9. A) Comparing the HIBAL $\delta^{18}O_M$ record with the measured down-core TIC $\delta^{18}O_C$ record based on the reconstructed river flow of the Walker River spanning 1000 to 1900 AD. B) Comparing the HIBAL $\delta^{18}O_M$ record with the measured down-core TIC $\delta^{18}O_C$ record based on the reconstructed river flow of the Walker River spanning 400 to 1000 AD. C) Comparing the HIBAL $\delta^{18}O_M$ record with the measured down-core TIC $\delta^{18}O_C$ record based on the reconstructed river flow of the Walker River spanning 1000BC to 400 AD.

For the intervals from 1000 to 1900AD, from 400 to 1000AD, and from 1000BC to 400AD, the LTM $\delta^{18}O_R$ values of the Walker River are the same as those that are assigned for lake level reconstruction (-18.7, -17.8, and -14.4, respectively). HIBAL runs separately in these intervals, using the reconstructed river discharge data. The HIBAL $\delta^{18}O_M$ records are compared with the original $\delta^{18}O_C$ record (see Figure A2-9A, Figure A2-9B, and Figure A2-9C). The HIBAL $\delta^{18}O_C$ record closely matches the late Holocene $\delta^{18}O_C$ record of Walker Lake (Figure A2-10A). This demonstrates that fluctuations in the river flow record of the Walker River are the primary contributor to the variations in the $\delta^{18}O_C$ signal preserved in down-core carbonate sediments.

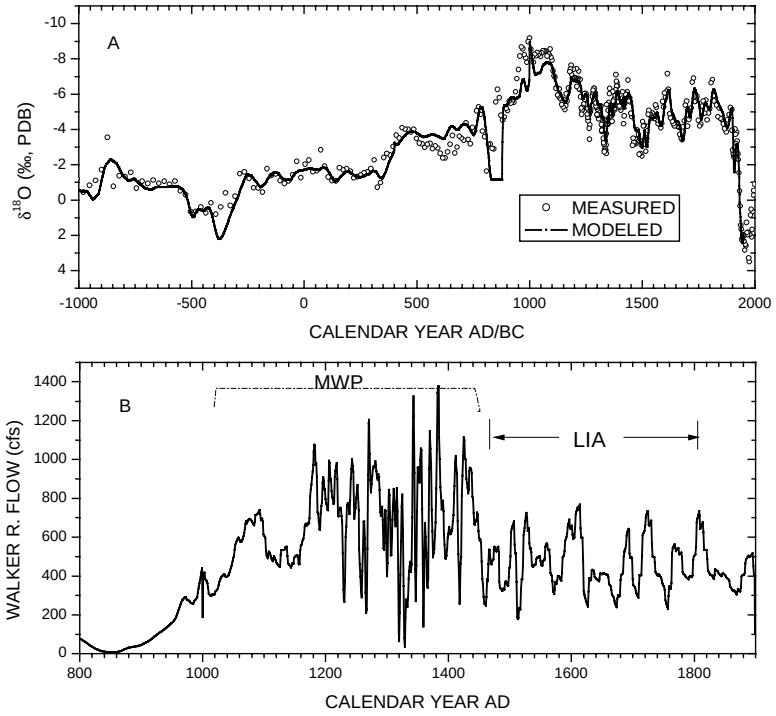

Figure A2-10. A) Comparing the HIBAL $\delta^{18}O_C$ record with the measured down-core TIC $\delta^{18}O_C$ record based on the reconstructed river flow of the Walker River spanning 1000BC to 2000 AD. B) Reconstructed Walker River discharge record spanning 800 to 1900.

A2.7 Discussion

I have presented an isotopic modeling approach to reconstruction of lake levels of Walker Lake and demonstrated the ability of the model to recover the history of lake level changes both in the historical

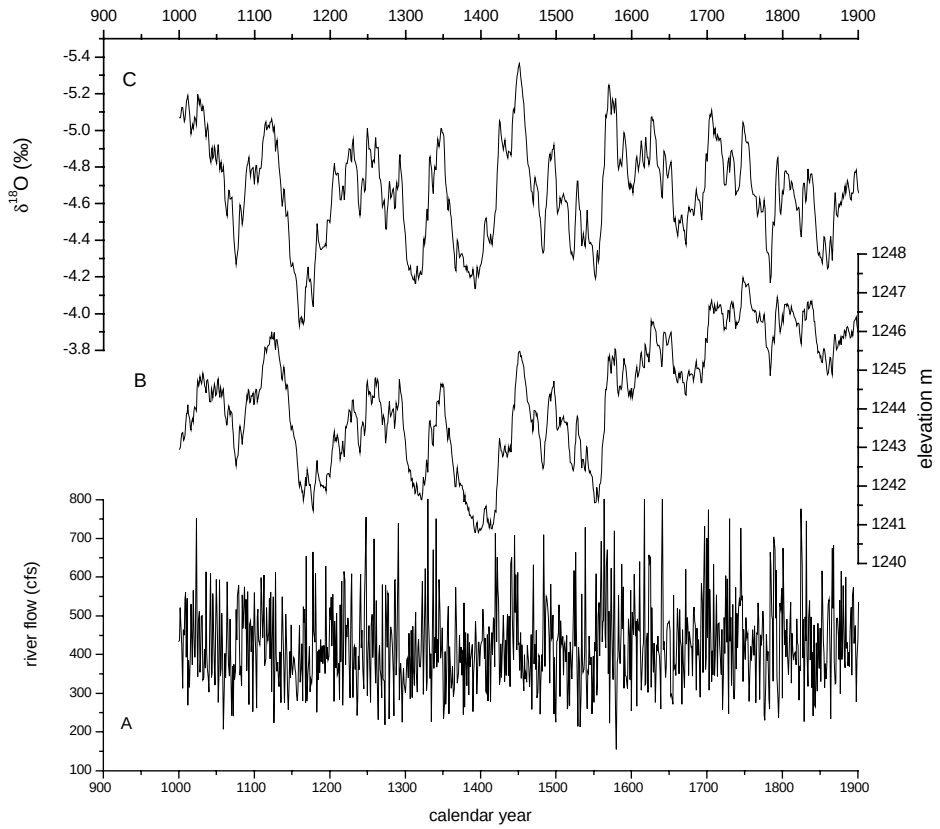

Figure A2-11. Modeled fluctuations in the Walker River discharge (panel A), Walker Lake level (panel B), and lake water $\delta^{18}O_L$ (panel C). Scaled annual Walker River discharge data (panel A) is based on the tree-ring-based Sacramento River flow (MEKO et al., 2001) and correlation of historic streamflow records (BENSON et al., 2002). Modeled Walker Lake elevations are inferred through a simple mass balance model (MILNE, 1987), assuming fixed rates of evaporation (135 cm per year) and on-lake precipitation (12.5 cm per year). The $\delta^{18}O_L$ data are modeled through HIBAL. Note that the magnitude of variations in $\delta^{18}O_L$ is within 2 ‰, which is far less than that of actual variations recorded and extracted.

Certainly, the isotopic reconstruction model is based on the assumption that the extracted downcore $\delta^{18}O_C$ signatures are representative to the $\delta^{18}O_L$ of host water when carbonates formed. Previous studies (SPENCER, 1977) suggested that monohydrocalcite is the dominant phase of carbonate precipitates today and subject to recrystallization (BENSON et al., 1991). More recent studies (JIMENEZ-LOPEZ et al., 2001) suggested that recrystallization of monhydrocalcite would create anomalously low $\delta^{18}O_L$ signatures on carbonates that have not had the opportunity for further exchange with the surrounding medium. The pseudo-isotopic signatures may be preserved or entirely erased depending on